Osaka University Knowledge Archive

| | |
|---|---|
| Title | OBSERVATION OF PRESSURE-INDUCED SUPERCONDUCTIVITY OF SnI4 |
| Author(s) | 竹下, 直 |
| Citation | 大阪大学, 1997, 博士論文 |
| Version Type | VoR |
| URL | https://doi.org/10.11501/3128789 |
| rights | |
| Note | |

*Osaka University Knowledge Archive : OUKA*

https://ir.library.osaka-u.ac.jp/

Osaka University

# OBSERVATION OF PRESSURE-INDUCED SUPERCONDUCTIVITY OF $SnI_4$

Nao TAKESHITA

Doctoral Thesis

**Faculty of Engineering Science**
**Department of Physics**
**Osaka University**
**Toyonaka, 560 Japan**
**1996**

# ABSTRACT

$SnI_4$ (tin tetra iodide) shows pressure- induced amorphization and recrystallization at high pressure, which are very characteristic physical properties of this compound. In the recrystallized phase at above 61GPa, the crystal structure of $SnI_4$ is considered to be fcc by X- ray diffraction study but the arrangement of tin and iodine atoms in the unit cell is still not clear. As the electrical resistivity rapidly decreases with amorphization, so $SnI_4$ is expected to have metallic resistivity at above 12GPa. It is interesting that the lattice constant and compressibility are almost the same to that of fcc iodine at the highest pressure phase in which iodine shows superconducting transition. Therefore the superconductivity is also expected in fcc recrystallized phase of $SnI_4$.

We have measured the electrical resistance and the magnetization of $SnI_4$ at pressure up to 95GPa and at temperature down to 60mK. At room temperature, we have observed the irreversible decrease of the electrical resistance at around 60GPa, which is consistent with previous reports on the lattice structure. At cryogenic temperature, we have observed clear superconducting transition both in the amorphous state and the recrystallized fcc state.

In amorphous state, the transition temperature $T_c$ was found to be around 1.3K at pressure $P$=30GPa but it became higher with increasing pressure. $T_c$ reached to 1.94K at 64GPa and the transition became very sharp in good agreement with the higher symmetry caused by recrystallization. The critical magnetic field $H_c$ was found to be about 1.7T which is considerably higher than that of fcc monatomic iodine. The transition temperature $T_c$ rapidly decreased at above 86GPa. The unknown phase at low temperature is expected at above this pressure. We have also observed the Meissner effect of $SnI_4$ by dc magnetizaton measurement at 40GPa. This is another strong evidence of the superconductivity of $SnI_4$.

# CONTENTS

§ 1. Introduction 1

§ 2. Experimentals

1. High Pressure Cell 6
2. Electrical Resistance Measurements 12
3. Magnetization Measurements 17
4. Low Temperature Cryostat 21

§ 3. Crystal Structures of $SnI_4$ 24

§ 4. Results

1. Electrical Resistance at Room Temperature 30
2. Electrical Resistance at Low Temperatures
   —Metallization and Superconductivity
   2-1. Amorphous Phase 32
   2-2. Recrystallized Phase 36
   2-3. At Low Pressures 49
   2-4. Reappearance of Superconductivity 52
3. Magnetization at Low Temperatures 55
   —Observation of Meissner Effects
4. Discussion 58

§ 5. Concluding Remarks 65

§ 6. Application to Heavy Fermion System

1. Introduction 66
2. $CeCu_2Ge_2$ 71
3. $CePd_2Si_2$, $CeRh_2Si_2$ 78

Acknowledgements 86

References 87

# § 1 Introduction

The tin tetra- iodide ($SnI_4$) is known for its unique physical properties of metallization and amorphization induced by applying pressure. $SnI_4$ is a brown molecular crystal and an insulator at ambient pressure and at room temperature. Several X- ray diffraction studies on $SnI_4$ have been performed and the structure is well- established at ambient pressure.[1] $SnI_4$ crystallizes into a cubic lattice as illustrated in Fig.1. Since there remains space among $SnI_4$ molecules, $SnI_4$ has unusually large compressibility. Lynch and Drickamer[2] reported that the volume changes up to $\Delta V/V=0.5$ at around 15GPa.

Fujii *et al.*[3] investigated the lattice structure of $SnI_4$ by X- ray diffraction measurement at high pressure. They reported broadening of the diffraction peaks above about 10GPa which may be concerned with amorphization.

Riggleman and Drickamer[4] reported that the electrical resistance of $SnI_4$ decreases rapidly above 10GPa and $SnI_4$ becomes metallic at 18.5GPa. Chen *et al.*[5] also studied the electrical resistance at high pressures and concluded that metallization pressure of $SnI_4$ is $12\pm1$GPa from the temperature dependence of the electrical resistance. We suppose that the amorphization is related closely with the metallization of $SnI_4$.

The amorphous state remains under high pressure. Surprisingly, Hamaya *et al.*[6] discovered a sudden recrystallization taking place at 61GPa. In this new crystal phase, iodine atoms forms fcc structure. The lattice constant is very similar to the value of fcc iodine (phase IV) at the same pressure.[7] It is very curious that both materials have nearly the same lattice constant at the same pressure. $SnI_4$ seems to be similar to fcc iodine.

On the other hand, solid iodine is typical example which has pressure induced insulator- metal transition and corresponding structural phase transitions.[7-9] At ambient pressure, iodine is a molecular solid which is an

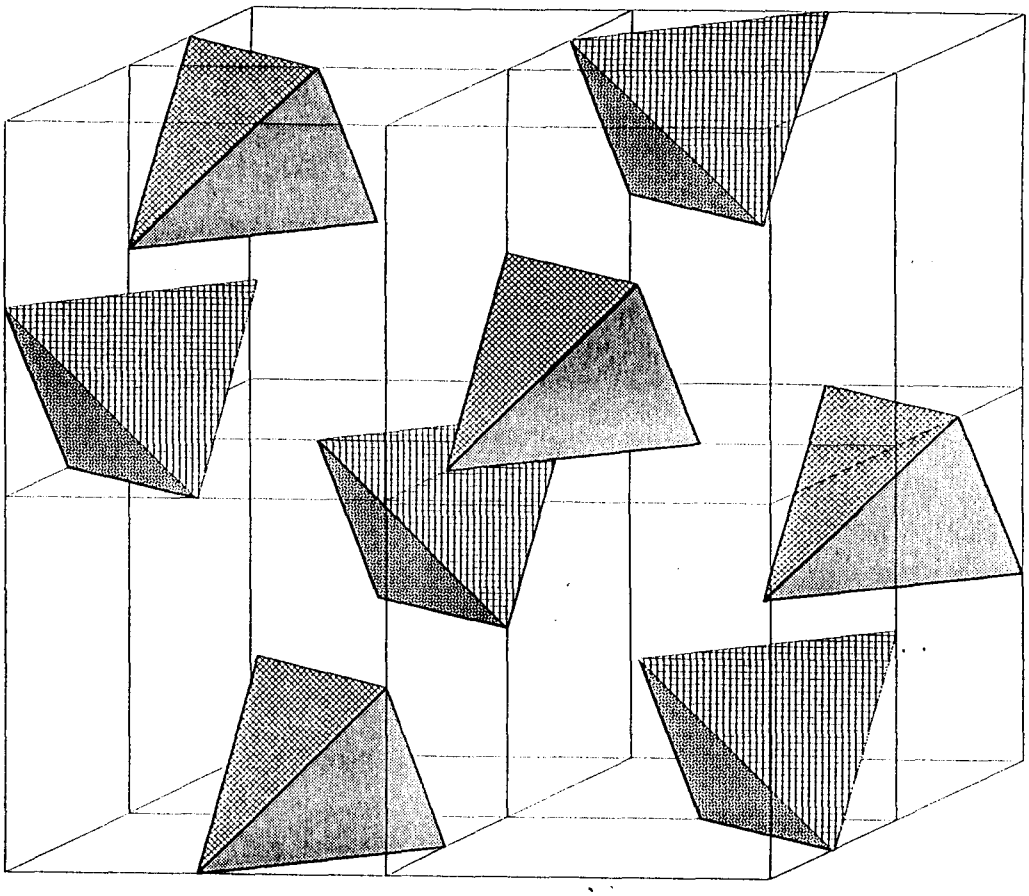

Fig. 1 The crystal structure of $SnI_4$ at ambient pressure. The unit cell contains eight $SnI_4$ molecules.

insulator. By applying pressure, the resistivity decreases rapidly, giving metallic resistivity as shown in Fig.2. Iodine is in the molecular phase at low pressure but it undergoes the molecular- dissociation under high pressure. Fujii's group found the molecular dissociation of iodine at 21GPa and iodine is in monatomic phase above this pressure. Fig.3 shows the crystal structure of iodine under pressures. There are two phase transitions in the monatomic phase, then iodine crystallizes in fcc structure above 55GPa[7] which is the highest pressure phase.

In the monatomic phase($P$>21GPa), iodine shows metallic resistivity. Shimizu *et al.*[10] discovered that iodine shows superconductivity at liquid He temperature in this phase. This transition to superconducting state does not appear in the metallic molecule phase. In fcc phase (phase IV), the transition temperature $T_c$ is about 0.7K at 60GPa.

The electrical resistance of $SnI_4$ at low temperatures had not been observed. Therefore, we observed the resistance of $SnI_4$ at very high pressures and at temperatures down to mK region to study the difference of physical properties between amorphous state and recrystallized state and the possibility of superconductivity of $SnI_4$.

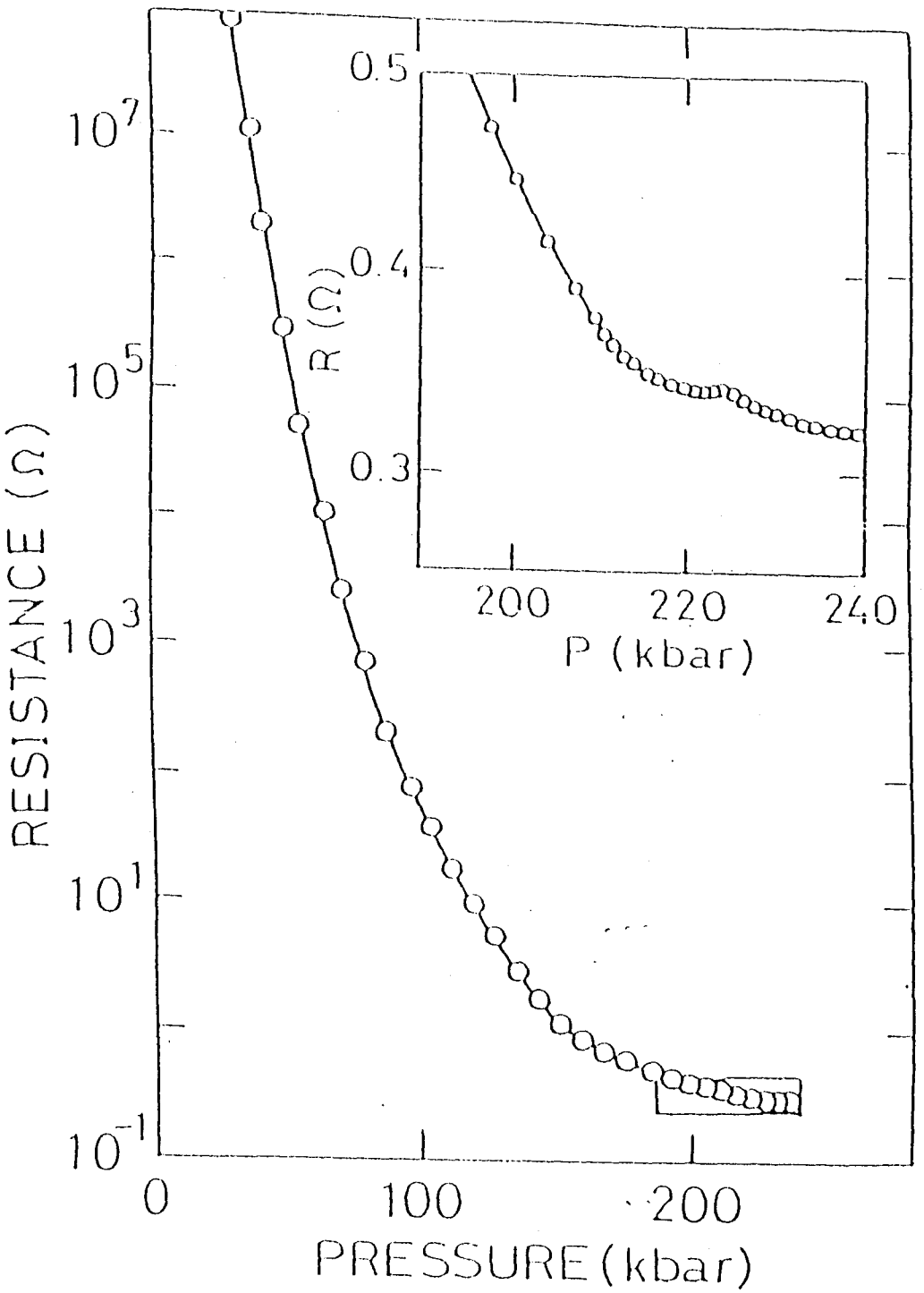


(10kbar=1GPa) N.Sakai *et al.*

Fig. 2 Resistance versus pressure for iodine at room temperature. The inset is a linear plot of resistance in enlarged scale near the molecular dissociating pressure.

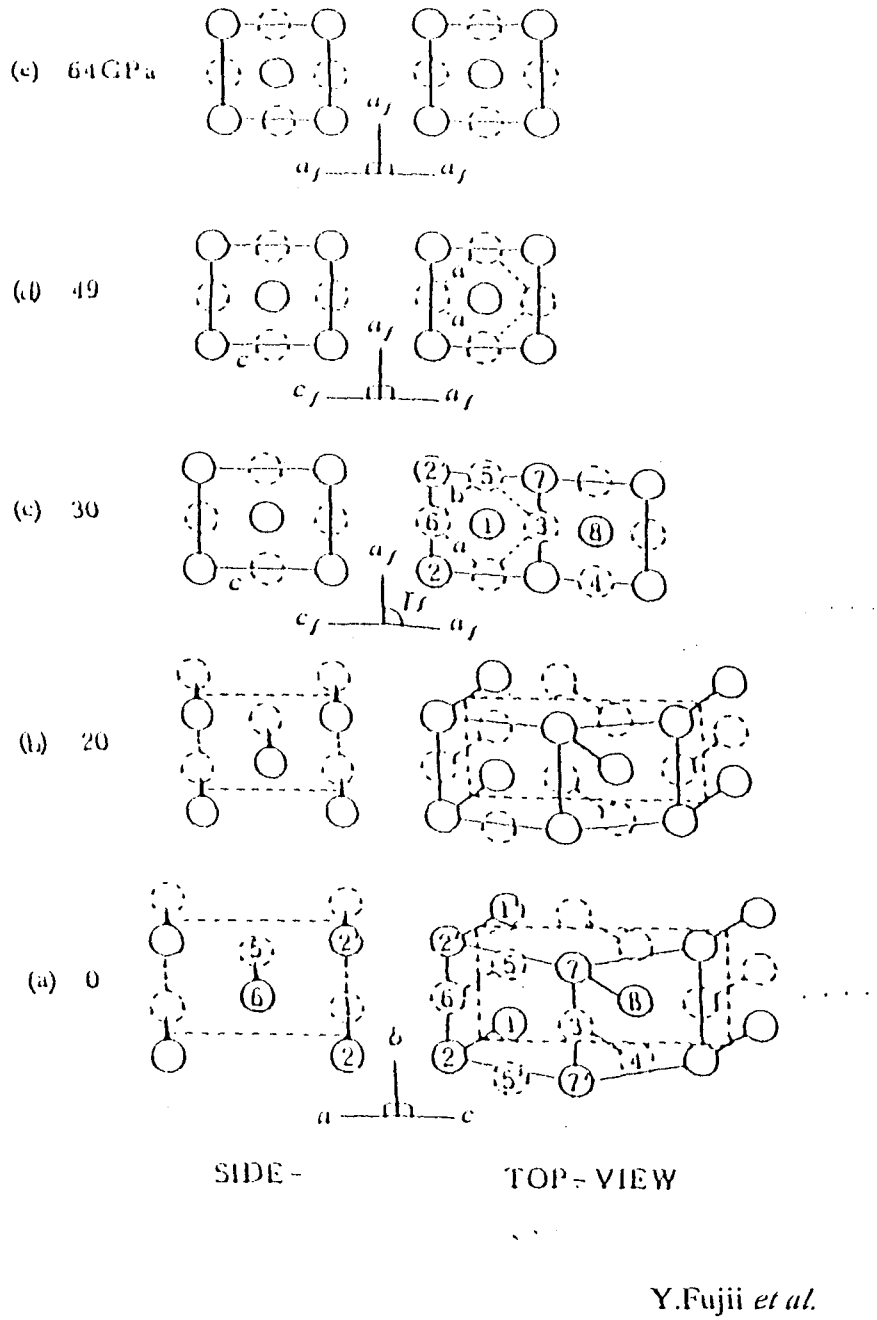


Fig. 3 Crystal structures of iodine under high pressures. The atoms drawn with the solid and dashed lines are located at the basal plane and the half- height plane perpendicular to the paper surface. The molecular dissociation occurs at 21GPa. At pressure above 55GPa, iodine crystallizes in fcc structure as shown in (e).

# § 2 Experimentals

## 1. High Pressure Cell

### Pressure apparatus

Experiments are performed under complex extreme conditions of high pressure and low temperature. The compact pressure apparatus made of good thermal conductor was newly developed in order to cool the system down to 0.1K. The clump- type Diamond Anvil Cell (DAC) is found to be the best apparatus for our purpose to produce the highest static pressure exceeding 200GPa.

Dr. Shimizu developed a DAC for cryogenic experiment and we used this DAC in our experiments. The schematic view of the DAC is illustrated in Fig.4. This DAC is made of cobalt- free Cu- Be alloy because of the best thermal conductivity and nonmagnetism as well among available hard materials. Another reason to employ this material is its low back ground signal in the case of magnetic measurements at the low temperature below 1K.

### Pressure determination

Ruby fluorescence method is used to determine pressure value. The block diagram of the measuring system is shown in Fig.5. There is an inevitable pressure change with temperature change. Fortunately, this change is reversible in most cases and we can calibrate the pressure value at low temperature. We perform ruby fluorescence measurement also at liquid $N_2$ temperature. Figure 6 shows the optical measuring system. The pressure value is measured before and after the experiment to check whether there is irreversible change of pressure or not.

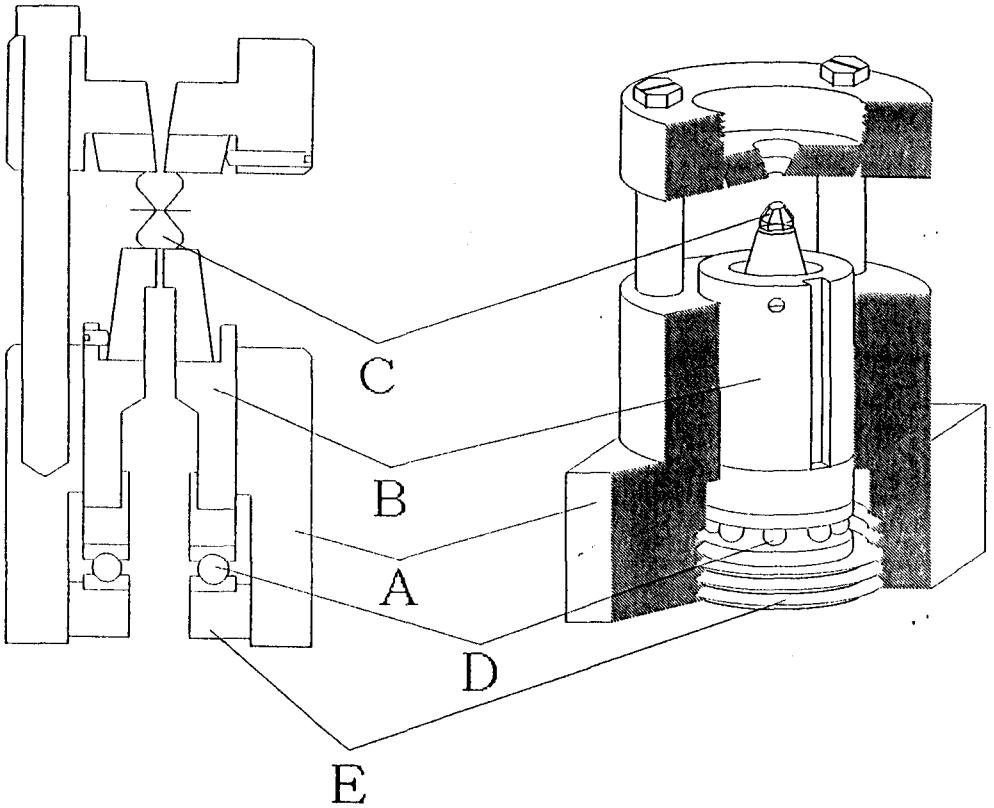


Fig. 4 The schematic view of our diamond anvil cell. A: Body. B: Piston. C: Diamond anvil. D: Ball bearings made of ceramics. E: Clamp nut.

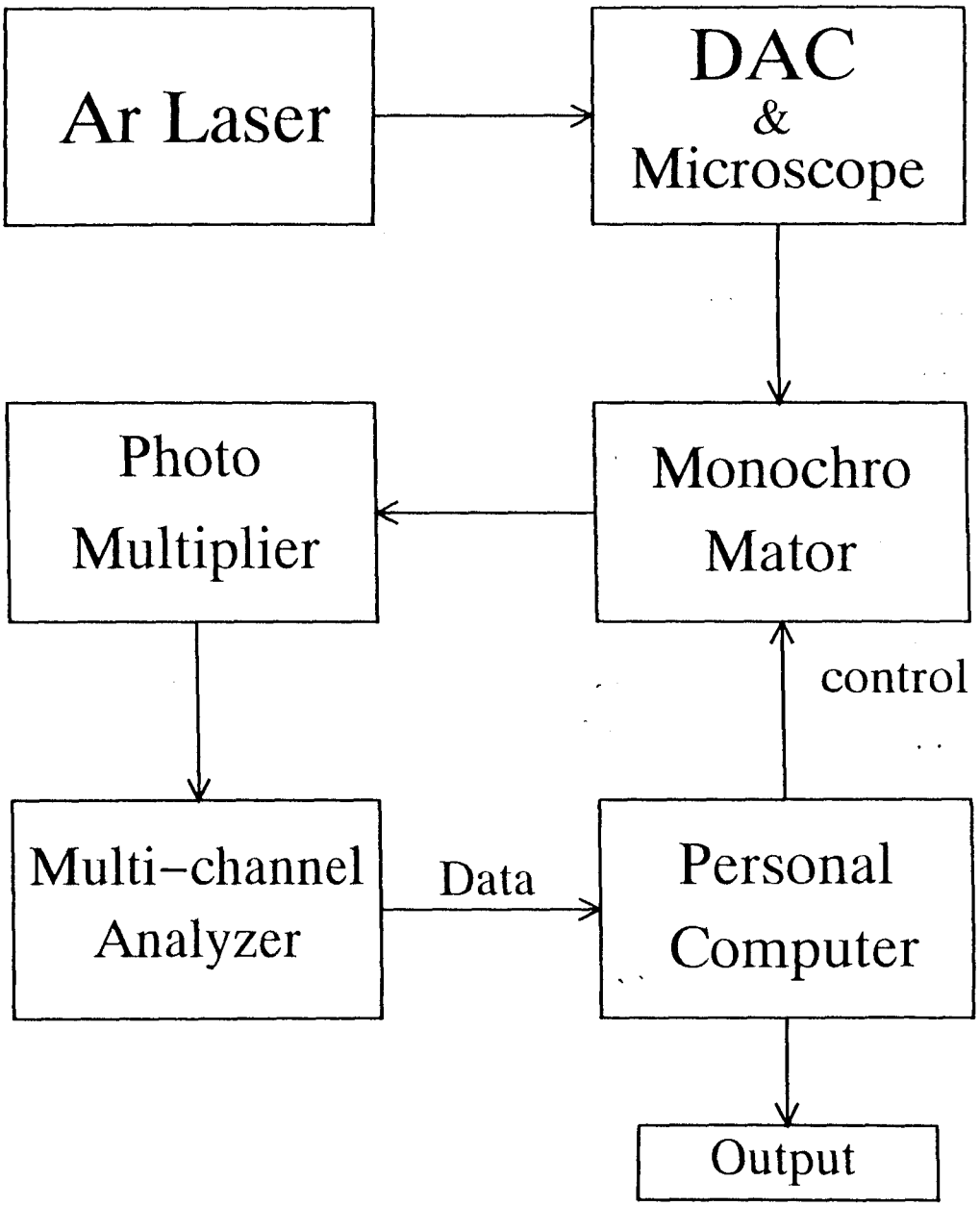


Fig. 5 The block diagram of the ruby fluorescence measuring system.

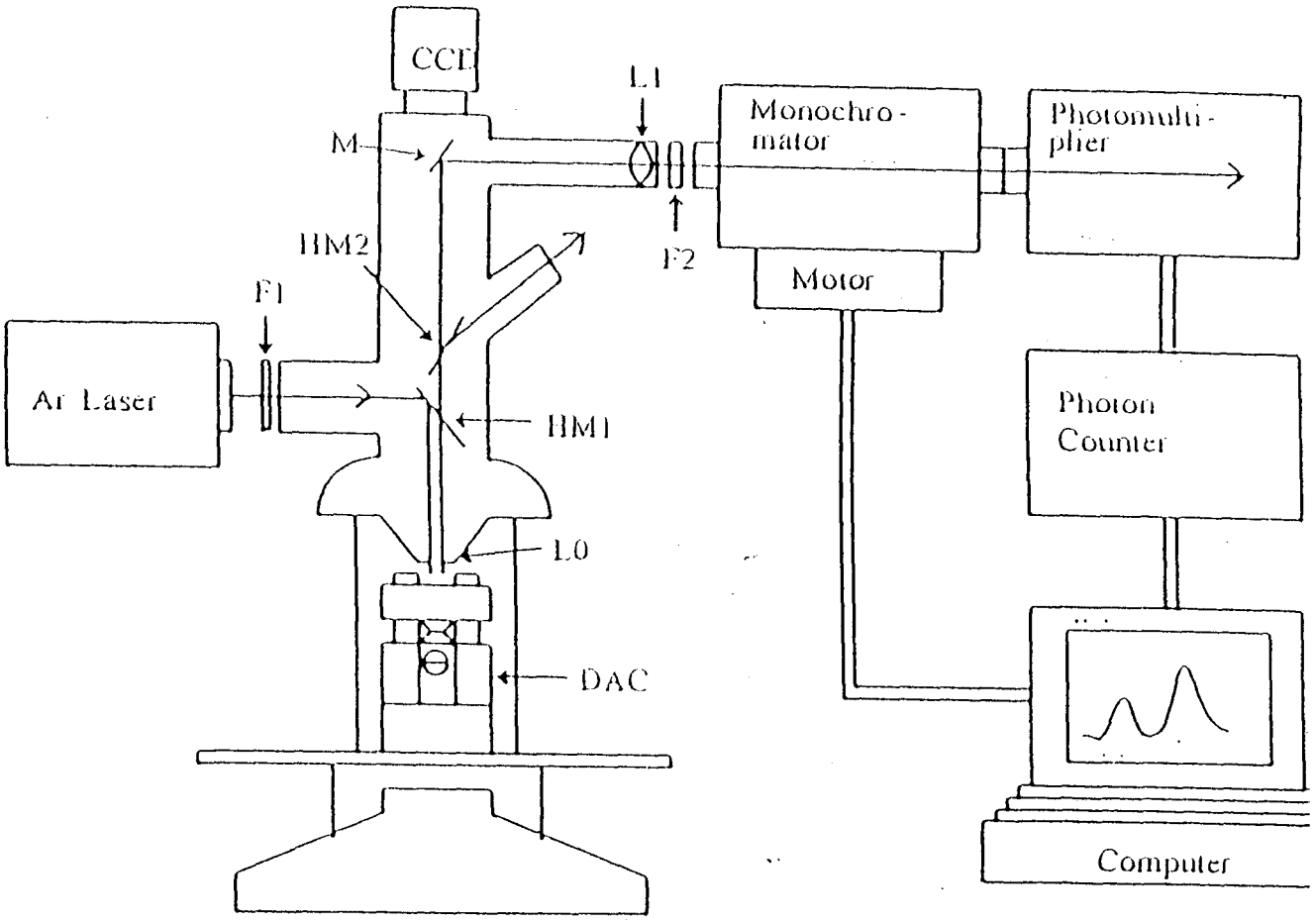


Fig. 6 The ruby fluorescence measuring system. The pressure can be determined at room temperature and liquid nitrogen temperature by this system.

**Pressure medium**

It is a serious problem that our DAC without any pressure medium normally supplies uniaxial pressure. The generation of hydrostatic pressure is very important to observe a physical properties in an isotropic experimental condition.

As DAC is one of the variation of opposite anvil type pressure apparatus, thus we are unable to avoid applying an uniaxial pressure to the sample. Pressure medium must be soft material and that transmit uniform and isotropic pressure to the sample. By using suitable pressure medium such as helium, the uniaxial pressures may be moderated even at cryogenic temperature.

The mixture of water and alcohol is often used as a pressure medium. Using this mixture, pressure around the sample is hydrostatic up to about 12GPa at room temperature. The mixture is also very easy to use in DAC. But sometimes this medium is not considered as the best choice because we perform an experiment at lower temperatures. In that case, rare gases are effective choice for substitution. If the sample reacts against water, inert gas medium is also effective.

However, it is difficult to use gases for pressure medium because it remains at gas state at room temperature. We must introduce rare gases into sample space in liquid or solid state. An apparatus for liquid confinement at cryogenic temperature is shown in Fig.7.

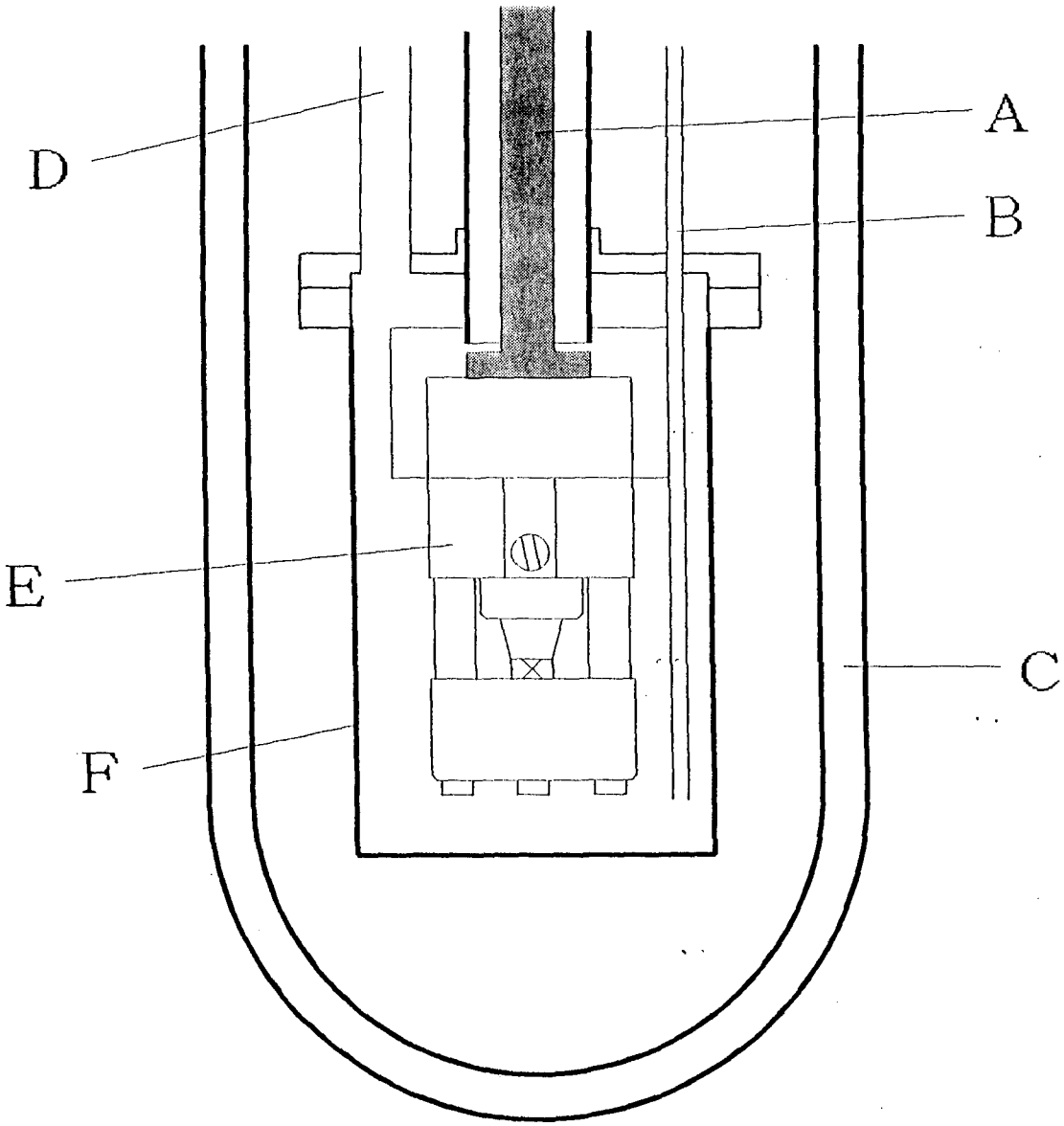


Fig. 7 Our handmade cryostat for liquid confinement into sample space in the DAC.

A: Pressurizing rod. B: Gas inlet line. C: Glass dewer.

D: Vacuum line. E: DAC F: Vacuum chamber.

## 2. Electrical Resistance Measurements

### Insulation of the electrodes

The resistance measurement seems to have several difficulties to be performed in DAC apparatus. We need electrodes to measure resistance, therefore it gives us an serious problem of insulating electrodes against the metal gasket. However, Dr. Shimizu solved this problem[10] by the use of $Al_2O_3$ insulation layer between the gasket and the electrodes. The arrangement around diamond anvil is shown in Fig.8. The insulation layer is very strong against the pressure, Shimizu has succeeded in resistance measurements above 150GPa. This is an only way at present to measure the electrical resistance above 10GPa in our experimental apparatus.

### Drickamer type anvil cell with natural diamond anvils

Another idea to maintain insulation is very simple. If the gasket is not metal, there is no problem. Figure 9 shows the schematic view of this cell. The anvil is made of natural diamond and the support is made of Cu-Be alloy. The anvils are cut conically and then cut so as to make a flat anvil surface. Then we put a pyrophyllite gasket, which is insulator, on the anvil. We can set a sample and 4 electrodes easily. Then, two anvils are set in a cylinder so as to face each other. The maximum pressure value using this apparatus is about 12GPa with anvil surface of 1mm in diameter. This upper limit of the pressure value is almost the same to that of conventional DAC with same diameter anvils. This arrangement is like a Drickamer type anvil cell replacing the anvil with natural diamond. By this replacement, we can measure a pressure value by ruby fluorescence method even at liquid $N_2$ temperature.

There is a big difficulty to perform resistance measurements in uniaxial

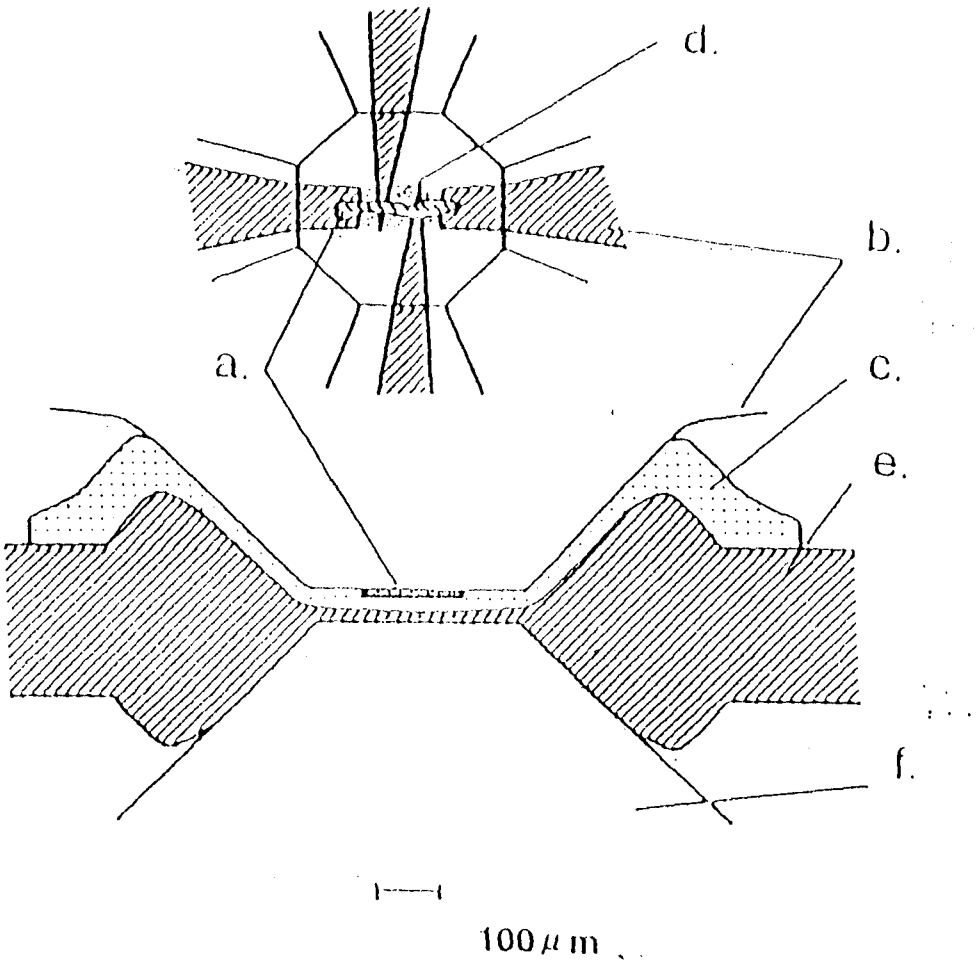




Fig. 8 The arrangement of the sample and the electrodes on the diamond anvil. a: Sample. b: Electrodes. c: $Al_2O_3$ powder. d: Ruby chips. e: Metal gasket. f: Diamond anvil.

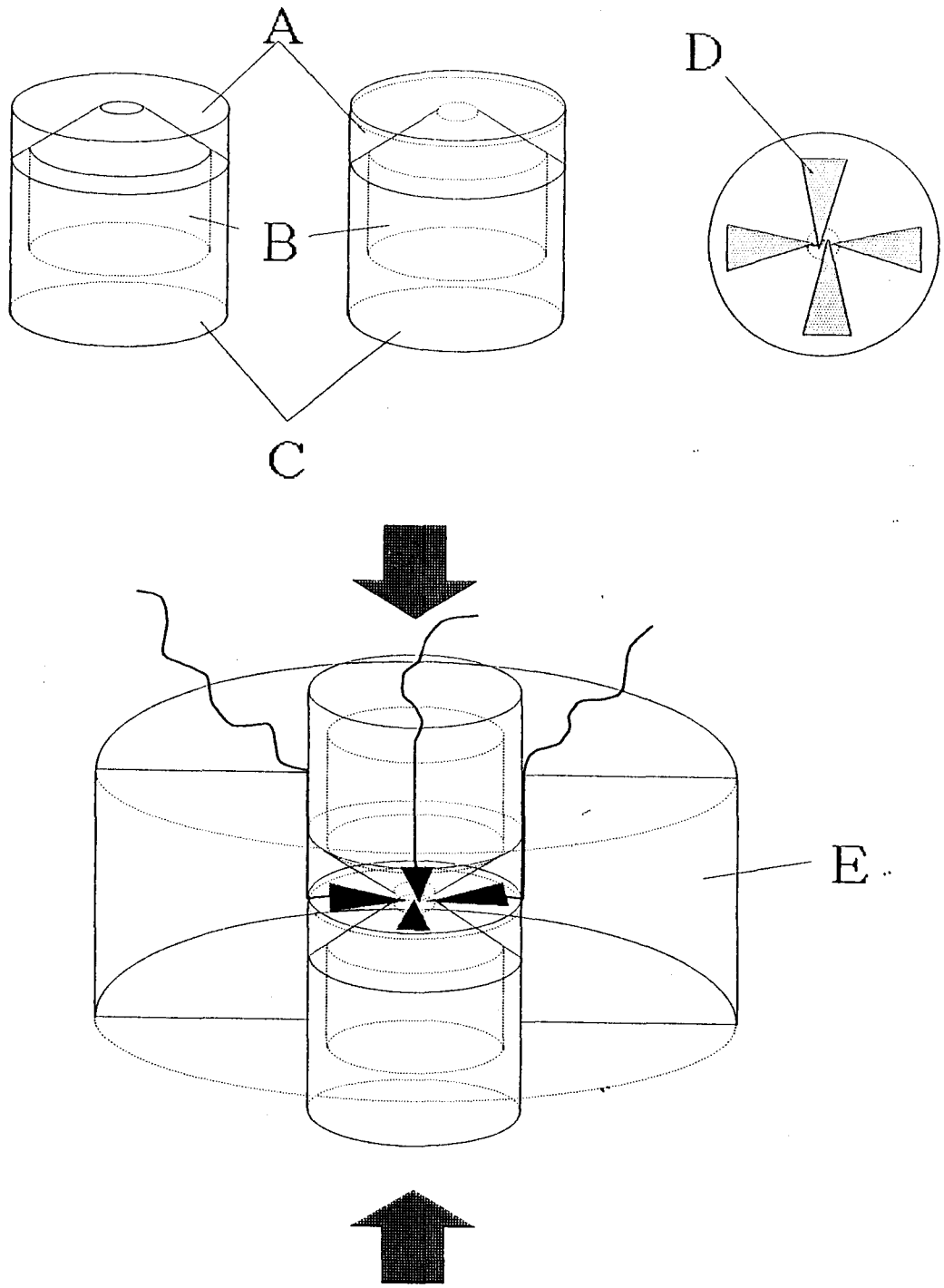


Fig. 9 The schematic view of the Drickamer type cell using pyrophyllite gasket and natural diamond anvils.
A: Pyrophyllite gasket. B: Natural diamond anvil. C: Anvil support made of Cu-Be alloy. D: Electrodes. E: Anvil guide.

pressure. Basically as we can not use pressure medium in resistance measurements, the uniaxial pressure may cause extrinsic effects on superconductivity such as broadening of transition.

### Electronics

The resistance of a sample in a DAC is measured by AC 4-terminal method. The circuit diagram is shown in Fig.10. We can adjust the measuring current value corresponding to the magnitude of the resistance. Too much current may heat the DAC or destroy weak superconductivity of the sample, so we should select current values as small as we can. The signal voltage is amplified by lock- in amplifier. We can also amplify the signal by 100 times with low noise input- transformer if necessary. We can observe a signal voltage less than 10nV with this system.

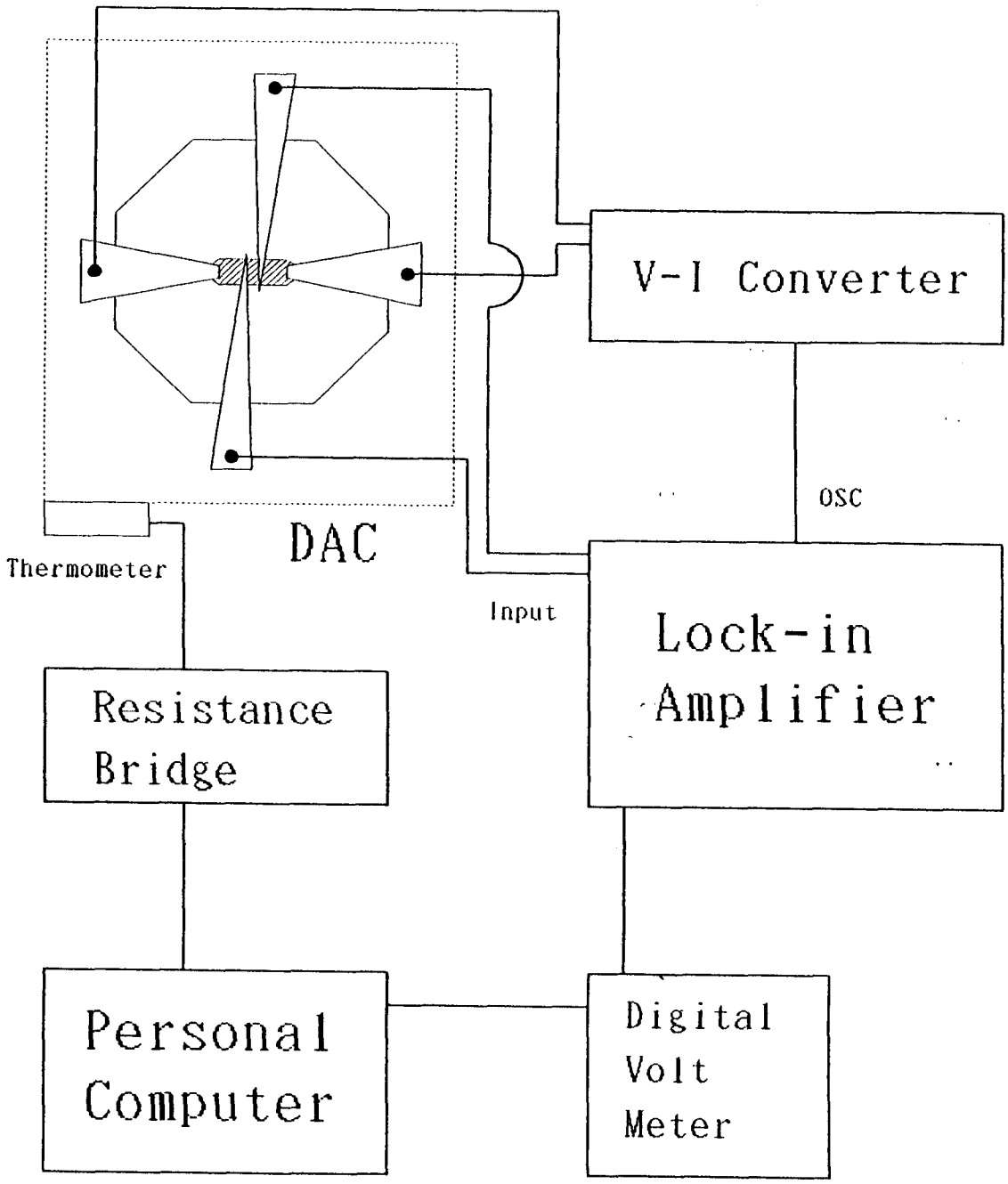


Fig. 10 The block diagram of the resistance measurement system.

# 3. Magnetization Measurements

### Magnetization measurement

It is very difficult to perform magnetic measurements of the sample in a DAC. As the sample volume is inevitably very small in a DAC, so we must employ a very high sensitive magnetometer to detect a signal. Then, we use a SQUID magnetometer. Fortunately, we can detect a Meissner signal of the sample in a DAC because it is extremely big. Further, the magnetization measurement has advantages over the resistance measurement. There is no effective pressure medium in the resistance measurement, but we can use pressure medium in magnetization measurement easily. Also, measurements are performed by pick- up coil outside the anvil, without worrying about the breaking of electrode during the pressurizing process as in the case of resistance measurements.

Figure 11 and 12 shows the magnetization measuring system we use. The pick- up coil is made of Nb-Ti fine wire ( $\sim 70\,\mu$ m $\phi$ ). It is wound around diamond anvil every time we make sampling. The SQUID magnetometer detects a persistent current induced on pick-up coil which is proportional to the change of the magnetic flux. At the constant magnetic field, the change of the magnetic flux is considered to be proportional to the change of the magnitude of magnetization. There is no compensation mechanism in the detection system.

Mainly, there are mainly two sources to produce magnetization, sample and gasket. Of course the gasket has a giant volume in comparison with the sample. So we request the gasket to be nonmagnetic and to have high yield strength. Cu- Ti alloy is the best material for the gasket at present. The gasket is cut in small shape ($\sim$4mm $\times$ 4mm) in order to decrease the back ground signal from it.

Figure 11 shows the primary coil system to produce the magnetic field.

The primary coil is constructed as small as we can, so as to apply the magnetic field just around the sample. The most important point is to stabilize the magnetic field inside the pick- up coil. If we drive the primary coil by DC constant current source with poor stability, we can not carry out the measurement. The best solution of this problem is to drive the primary coil by persistent current which has an extreme stability. We must prepare an persistent switch for that reason. Figure 11 shows the schematic view of the primary coil and the persistent switch. There is a heater around the switch to change current value.

A pipe made of Nb was placed around the primary coil.(Fig.12) This superconducting pipe plays a role of field stabilizer and shields the pick-up coil system against magnetic noise coming from outside the system.

The magnetic field is changeable while the cell is at the lowest temperature. This is an another advantage of this system. If the sample is non-ideal type- II superconductor, the Meissner signal becomes small in general. Sometimes we can not identify the signal. The magnetic flux may penetrate into the sample even in its superconducting state and the pick-up coil senses signal little.

Under magnetic field, some magnetic flux may be trapped in a sample below transition temperature in the cooling process. Even if the magnetic field goes to zero, the magnetic flux is still trapped in sample. Then, we try to warm up the sample. It should be no signal from the background because there is no magnetic field. So we can detect only the signal from trapped magnetic flux in the sample. It is found that S/N ratio is improved considerably on magnetization measurements in this way.

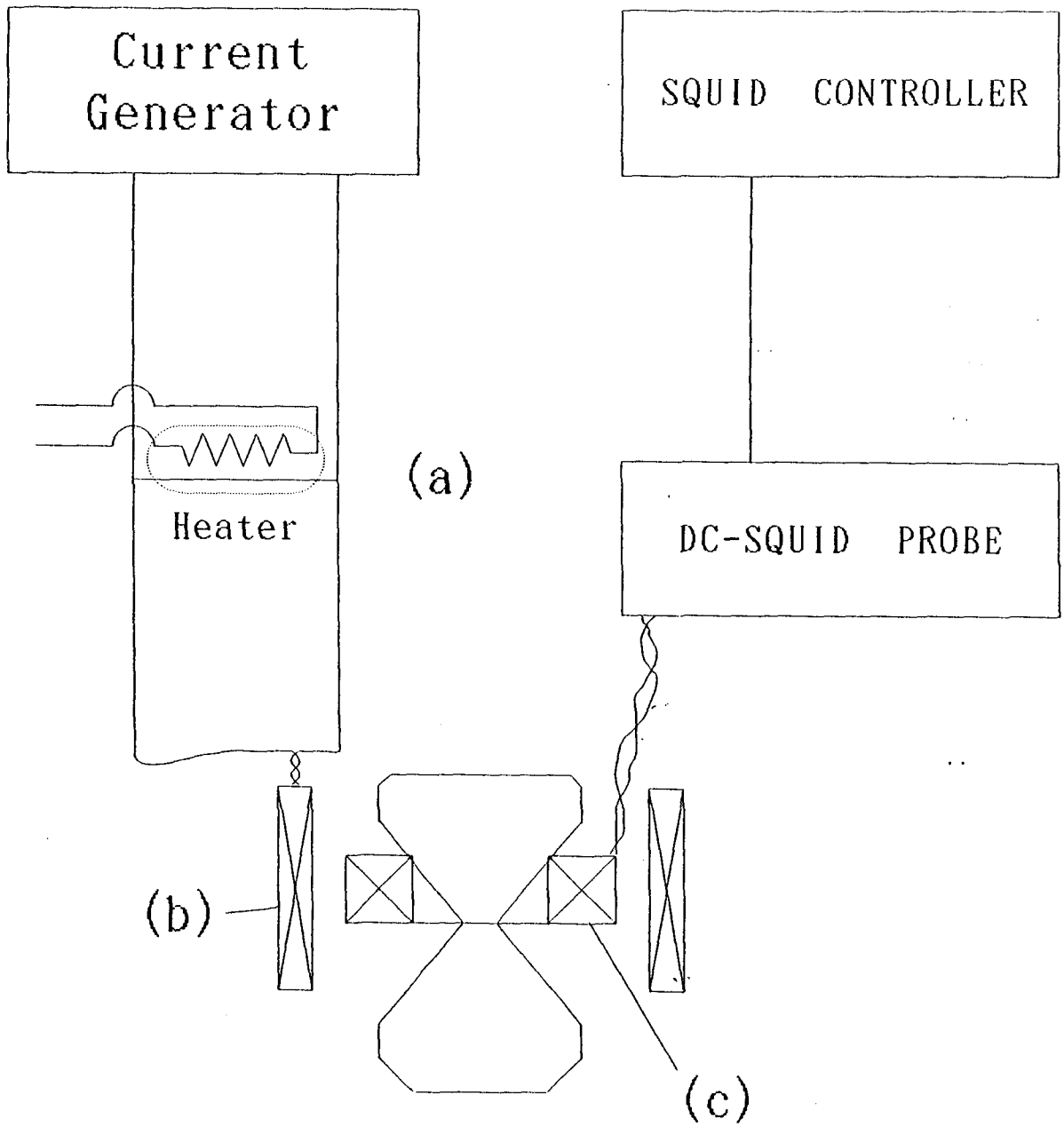


Fig. 11 The schematic view of the magnetization measuring system. (a): Persistent switch. (b): Primary coil. (c): pick-up coil.

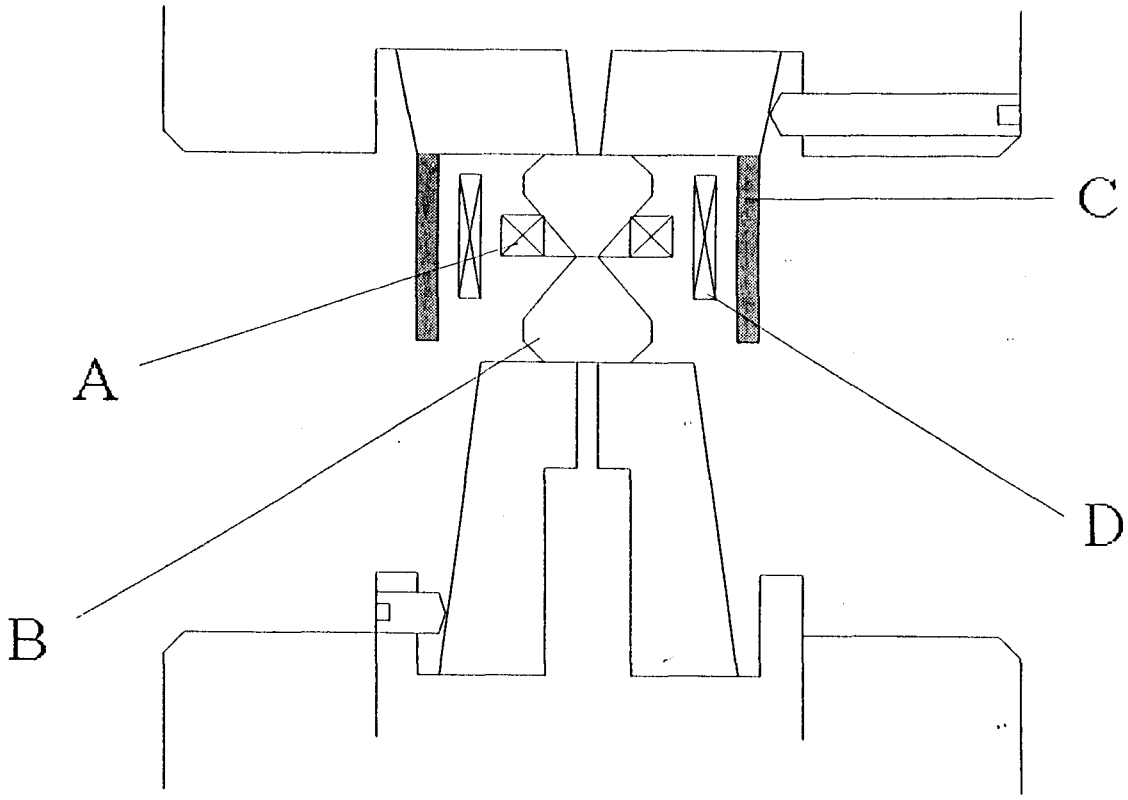


Fig. 12 The illustration of the coil system for magnetization measurement in DAC. A: Pick-up coil. B: Diamond anvil. C: Niobium tube for magnetic shield. D: Primary coil.

# 4. Low Temperature Cryostat

### Refrigerator and temperature control

Two kinds of refrigerator are used in our experiments in order to cool a DAC . We used liquid $^3$He or $^3$He/$^4$He dilution refrigerator that covers the temperature range which we need. There is no problem to cool DAC down to 100mK but we must pay attention for heating the refrigerator by measuring the thermometer and the electrical resistance of samples.

The temperature is determined by a calibrated resistance thermometer. We used platinum ($T$>77K), germanium ($T$>4.2K) and carbon ($T$<4.2K) resistance thermometer. The resistance is measured by AC resistance bridge (AVS-46). The block diagram of the measuring system is shown in Fig.13.

The temperature of the DAC is controlled by an electrical heater which is fixed on the DAC or the mixer in the case of the $^3$He/$^4$He dilution refrigerator. The heater is driven by a DC current generator. The values of constant current are determined by personal computer to warm up DAC at indicated ratio.

### Magnet

We can confirm decrease of superconducting transition temperature $T_c$ under the magnetic field through resistance measurements. Sets of observed $T_c$ and the corresponding $H_c$ are enables us to determine a $T_c$- $H_c$ phase diagram characteristic of the sample. The value of $H_c$ is very important for discussions of the type or origin of the superconductivity which is observed in the experiment. We constructed a superconducting magnet for our dilution refrigerator shown in Fig.14. It is very compact and easy to operate. The highest magnetic field is about $H$=1.8T for a driving current of $I$=40A, which is enough to suppress the superconductivity of $SnI_4$. The magnet is made of 0.38 $\phi$ NbTi wire wound up to 20 layers.

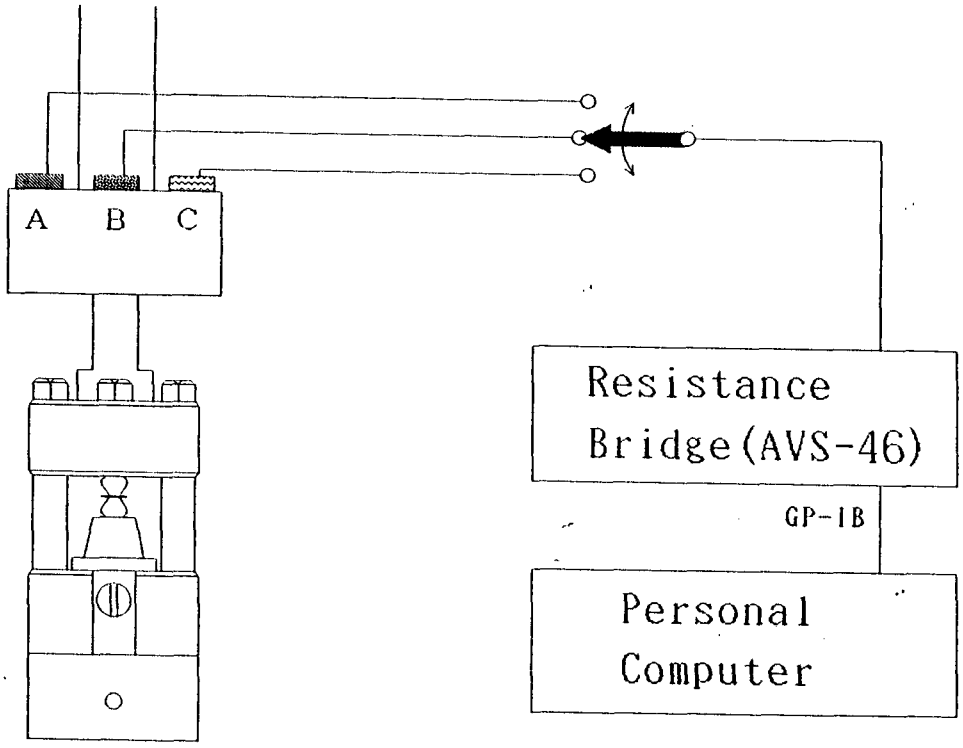


Fig. 13 The block diagram of the temperature measuring system. There are three different resistance thermometer (A, B and C) on the mixer of dilution refrigerator. The resistance is measured by AC- resistance bridge and the value of the temperature is calculated by personal computer. A: Platinum resistance thermometer. B: Germanium resistance thermometer. C: Carbon resistance thermometer.

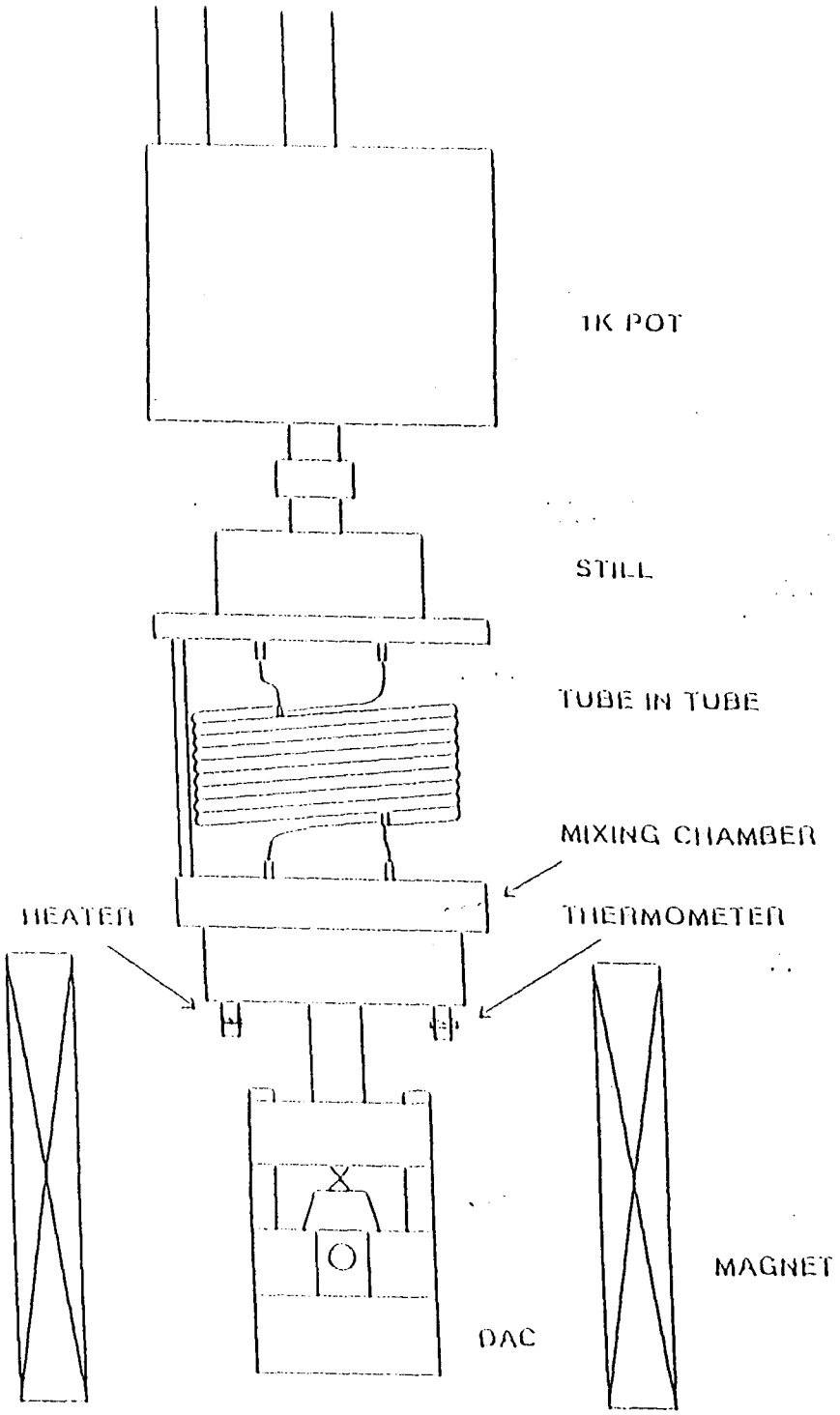


Fig. 14 Schematic view of the dilution refrigerator and the superconducting magnet. The magnet is placed in the Helium bath outside of the vaccum chamber.

## § 3 Crystal structure of $SnI_4$

At atmospheric pressure, the tin tetra iodide ($SnI_4$) crystallizes into a cubic lattice (Phase I)[1] which contains eight molecules in a unit cell. (T6h- *Pa3*) The eight $SnI_4$ molecules are packed loosely in the unit cell (a=12.273Å), so $SnI_4$ has large compressibility. Fig.1 shows the structure of $SnI_4$ at ambient pressure. Fujii *et al.*[3] studied about the structure of $SnI_4$ at pressures up to 33GPa, they discovered the halo pattern gradually developed between 10 and 20GPa, which suggests an amorphization of $SnI_4$.

Since then, the mechanism of amorphization have been studied extensively. Sugai[11] reported by Raman study that $(SnI_4)_2$ dimmer is formed in the amorphous state. Pasternak and Taylor[12] suggested the formation of randomly oriented poly- tin- tetraiodide conducting chains from their M study. From recent XAFS study by Wang and Ingalls,[13] a model structure of distorted $SnI_4$ molecules linked with tetrahedral units of iodine atoms is proposed. Fig.15 shows these models of amorphization of $SnI_4$. Although there are some suggestions of amorphization, its mechanism is still not clear.

Recently, Hamaya *et al.*[6] studied about structure of $SnI_4$ by synchrotron X- ray diffraction experiment at pressures up to 153GPa. This careful study gave us many information about pressure sequence of structure. They discovered a phase transition at pressure $P$=7.2GPa. It is very clear that a new and sharp diffraction peaks appeared above $P$=7.2GPa, as shown in Fig.16. The crystal structure above $P$=7.2GPa (PhaseII) is not determined yet. $SnI_4$ would undergo the metallization gradually in this new phase, because the drastic decrease of the electrical resistance begins at around 7GPa.[3,4] They also observed the broadening of the diffraction peaks and the halo scattering pattern, above 15GPa (Fig.17) which is caused by amorphization.

This amorphous phase is stable up to 60GPa but at 61GPa the amorphous state transformed into a crystal phase (PhaseIII)[6] showing a simple

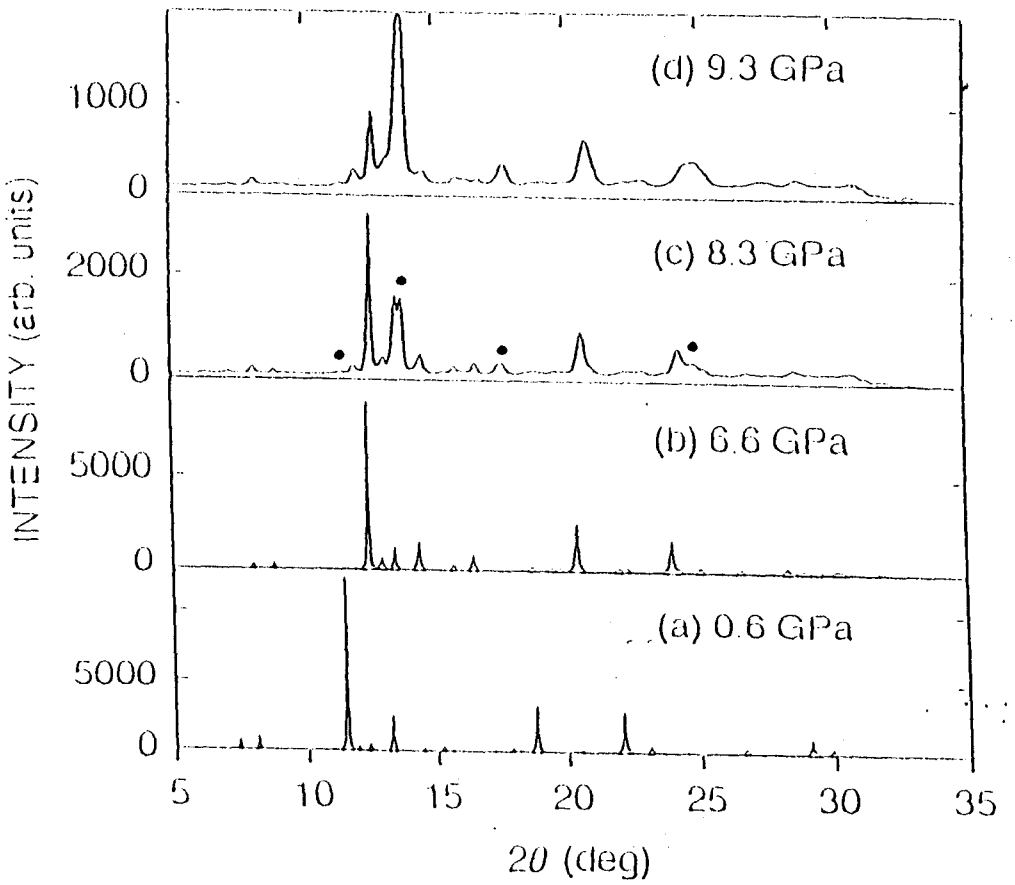


N. Hamaya *et al.*

Fig. 15 X- ray diffraction patterns of $SnI_4$ with increasing pressure. At above 7.2GPa, new peaks appear and two phases are coexistent in (c) and (d).

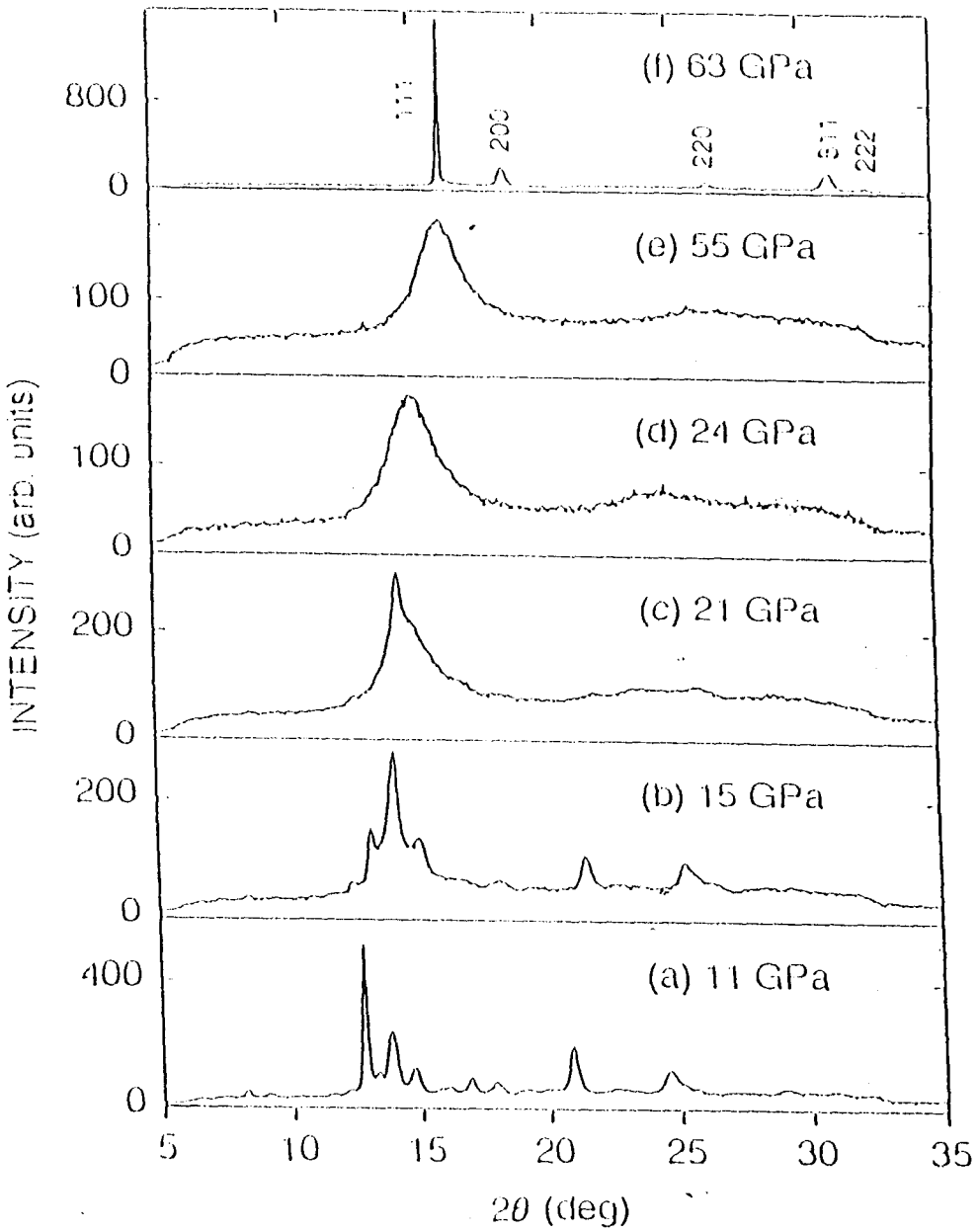


N. Hamaya *et al.*

Fig. 16 X- ray diffraction patterns of $SnI_4$ with increasing pressure up to 63GPa. Amorphization starts at above 11GPa, so diffraction peaks become broad as increasing pressure. At 61GPa, recrystallization occurs and sharp peaks appear which explained by the fcc lattice.

diffraction pattern as seen in Fig.18. This clear peaks can be explained by fcc lattice with a lattice constant of 4.248±0.002Å. The nearest-neighbor distance is calculated to be 3.003±0.001Å. It is very interesting that this value is exactly the same as that of 3.00±0.02Å measured in iodine having the monatomic fcc structure (PhaseIV) at $P$=64GPa.[7] This new recrystallized phase is reported to be stable up to 153GPa at room temperature and its P- V relation curve coincides with that of fcc iodine[14] within experimental error.

Hamaya *et al.* propose two models for this recrystallized phase. One is a partially disordered structure and the iodine atoms form fcc structure while tin atoms randomly occupy one of interstitial sites. Only tin atoms are distributed at random in the crystal. Another model is a fully disordered structure in which both tin and iodine atoms are randomly placed at the fcc sites. It seems that former structure has small compressibility than fcc iodine. On the other hand, the unit cell volume of fully disordered model is five forth of the former structure, so it may have large influence on some physical property. The structure of recrystallized phase will be made clear in near-future.

The amorphization is characterized by large pressure hysteresis. The amorphization occurs around $P$=15GPa in applying pressure process but the amorphous state survives near 1GPa in decreasing pressure process.

Hamaya *et al.* pressurized again the amorphous specimen quenched in this way, and then discovered two discrete jumps of the halo peak at $P$=5.8GPa and 13GPa as seen in Fig.17. They distinguished three amorphous state(AS); AS-I at $P$<6GPa, AS-II at 6-13GPa and AS-III at $P$>13GPa. AS-III exhibits the identical compression behavior to that of initially compressed specimen, whose first halo obviously turns into the 111 reflection of recrystallized phase. This result implies that AS- III has closer structural relation to recrystallized phase (phaseIII) at pressure above $P$=61GPa.

These studies are carried out at room temperature. There is no information about phase boundaries of $SnI_4$ at low temperatures. But we

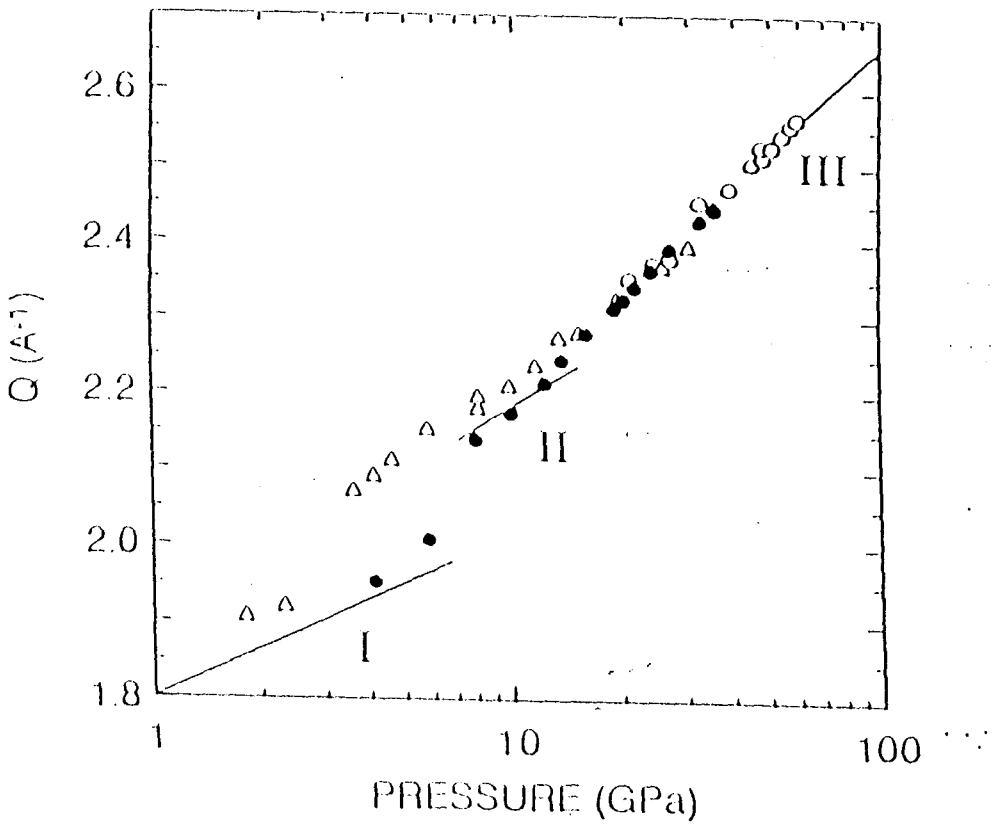


N. Hamaya *et al.*

Fig. 17 The pressure dependence of the wave number, Q, of the first halo peak of $SnI_4$. Solid circle denotes Q measured in the second compression. In this sequence, the halo peak position changes discontinuously and three different states can be distinguished, which suggests the occurrence of structural changes in the amorphous state.

performed experiments, expecting similar amorphization and recrystallization at experimental cryogenic temperatures.

# § 4 Results

## 1. Electrical Resistance at Room Temperature

Since it is necessary to generate above 60GPa and to measure electrical resistance in the experiment, $Al_2O_3$ insulating layer on the gasket between DAC and then electrodes also were arranged with great care. At first, the pressure dependence of the resistance at room temperature was measured. The result is shown in Fig.18. At pressure range between 10 and 20GPa, there is a drastic decrease of the resistance due to the metallization which is consistent with the previous work.[3,4] As applying pressure further, the resistance decreases gradually and shows a small drop at around 60GPa as shown in the inset. This drop may concern with recrystallization of $SnI_4$. The lattice scattering of conduction electron becomes small when $SnI_4$ recrystallizes from the amorphous state. The magnitude of the drop is about one third of the resistance value.

This anomaly is not able to be observed with decreasing pressure. This hysteretic behavior is consistent with that of the pressure dependence of the crystal structure reported by Hamaya *et al.* .[6] As decreasing pressure, the resistance increases rapidly below 20GPa. This increase is reflection of the metal-insulator transition.

It is very difficult to estimate the exact value of the electrical resistivity of the sample in DAC because the accurate thickness and effective length of the sample in DAC cannot be measured directly. But if we adopt reasonable values for the cross sectional area of $1\times10^{-2}cm^2$ and for the thickness of $5\times10^{-3}$ cm, we can estimate the resistivity of $\rho=2\times10^{-2}\Omega\cdot$cm at P=20GPa which is consistent with a previous work.[3,4]

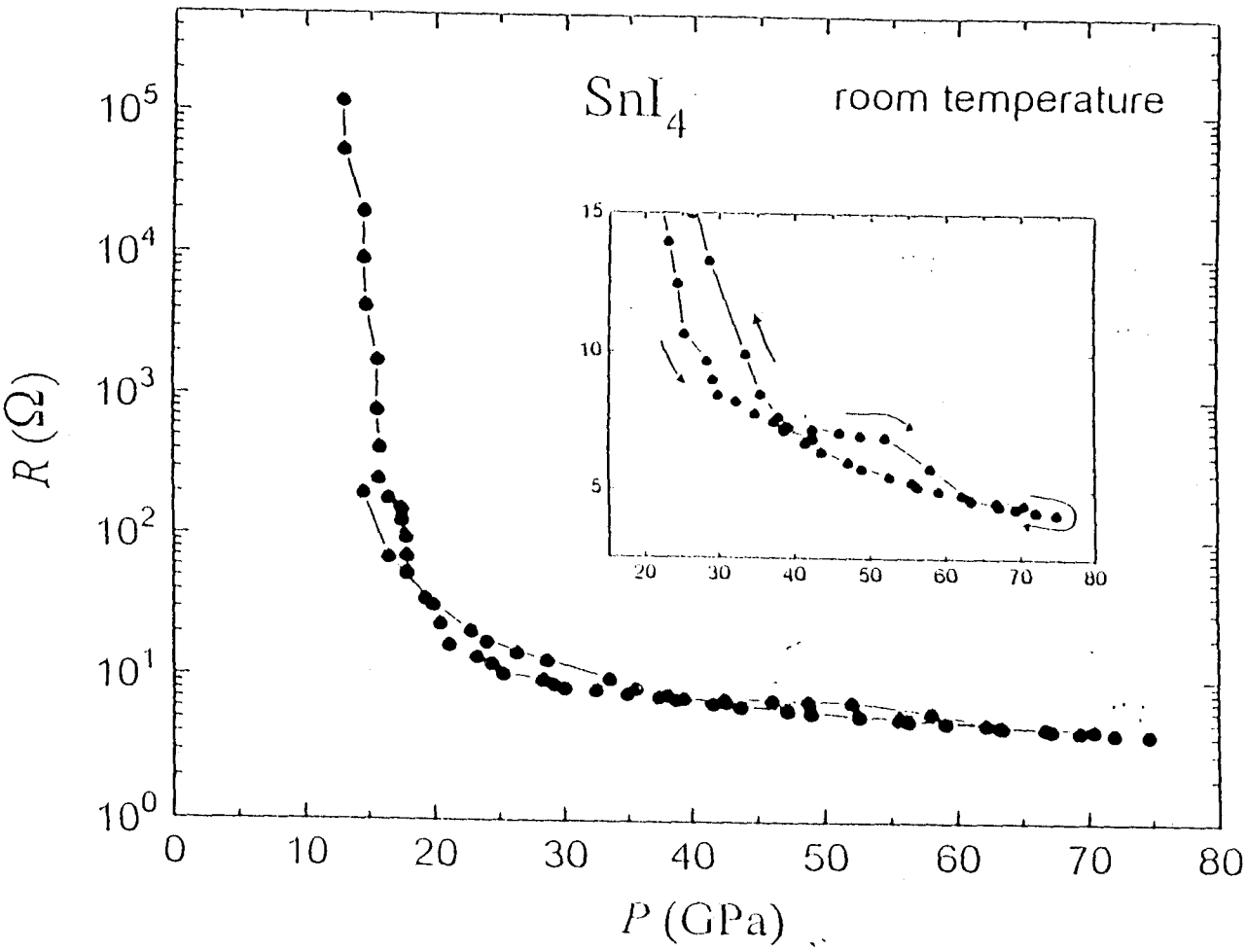


Fig. 18 The pressure dependence of the electrical resistance of $SnI_4$ at room temperature.

## 2. Electrical Resistance at Low Temperatures

### 2-1. Amorphous phase

After the experiment at room temperature, we measured temperature dependence of the electrical resistance of $SnI_4$ with the same arrangement. At first, the pressure value was determined to be 35GPa at liq. $N_2$ temperature. Figure 19 shows the electrical resistance of $SnI_4$ at $P$=35GPa.

At temperature around 1.3K, a sudden drop of resistance is observed and electrical resistance became to zero below this temperature. This anomaly is expected to be a superconducting transition of $SnI_4$. The transition temperature $T_c$ is estimated to be 1.34K from the midpoint of the transition. Figure 20 shows the electrical resistance under magnetic fields at the same pressure. The transition is suppressed by applying magnetic field and almost disappears at $H$=1.2T.

Then, we applied pressure up to 42GPa at liq. $N_2$ temperature, the specimen is supposed to be still in an amorphous state. The electrical resistance at low temperatures are shown in Fig.21. We were able to observe the superconducting transition again. The critical temperature $T_c$ increased slightly to 1.36K. The pressure dependence of $T_c$ is very small in the amorphous phase.

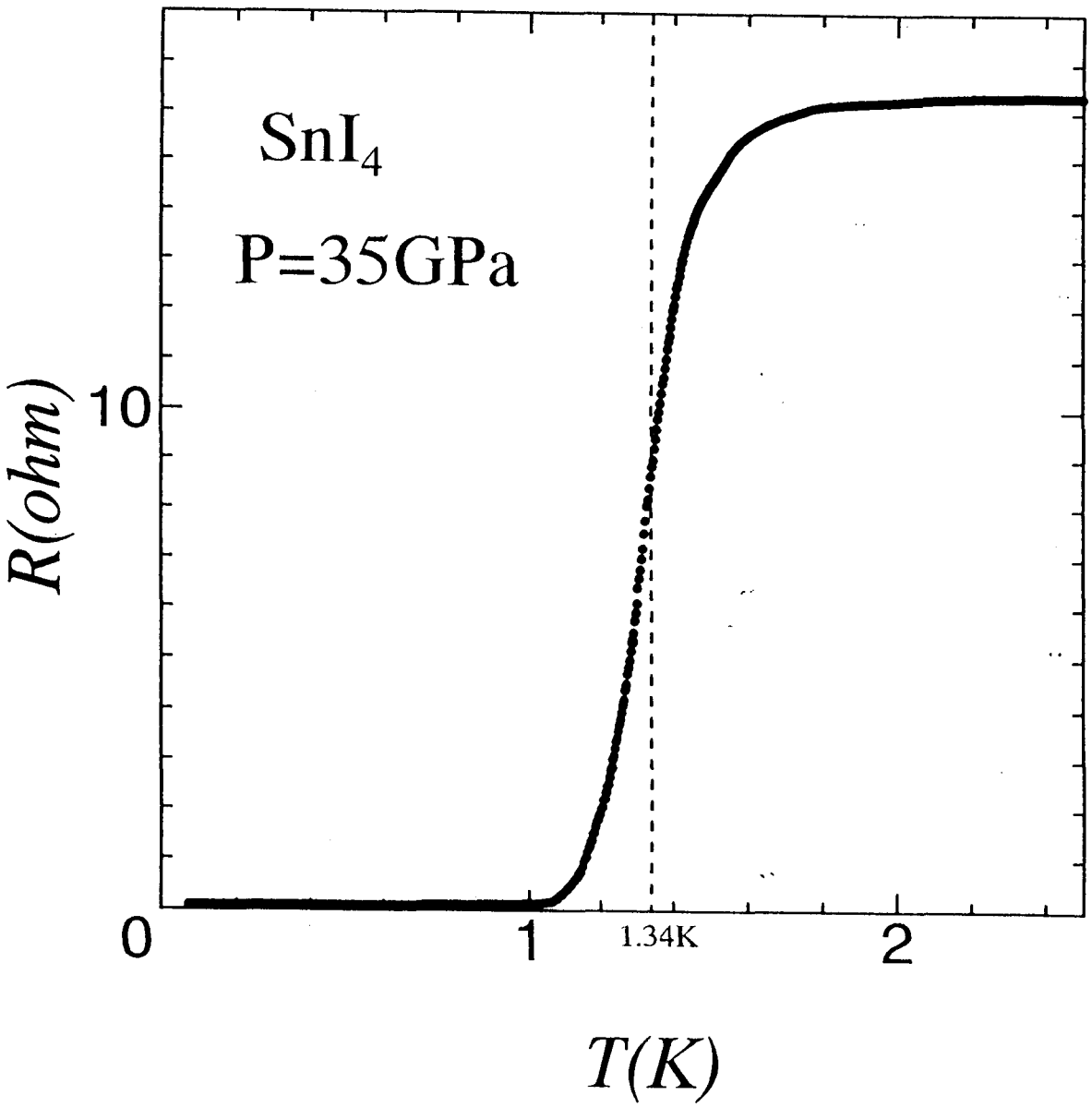


Fig. 19 The superconducting transition of $SnI_4$ at 35GPa

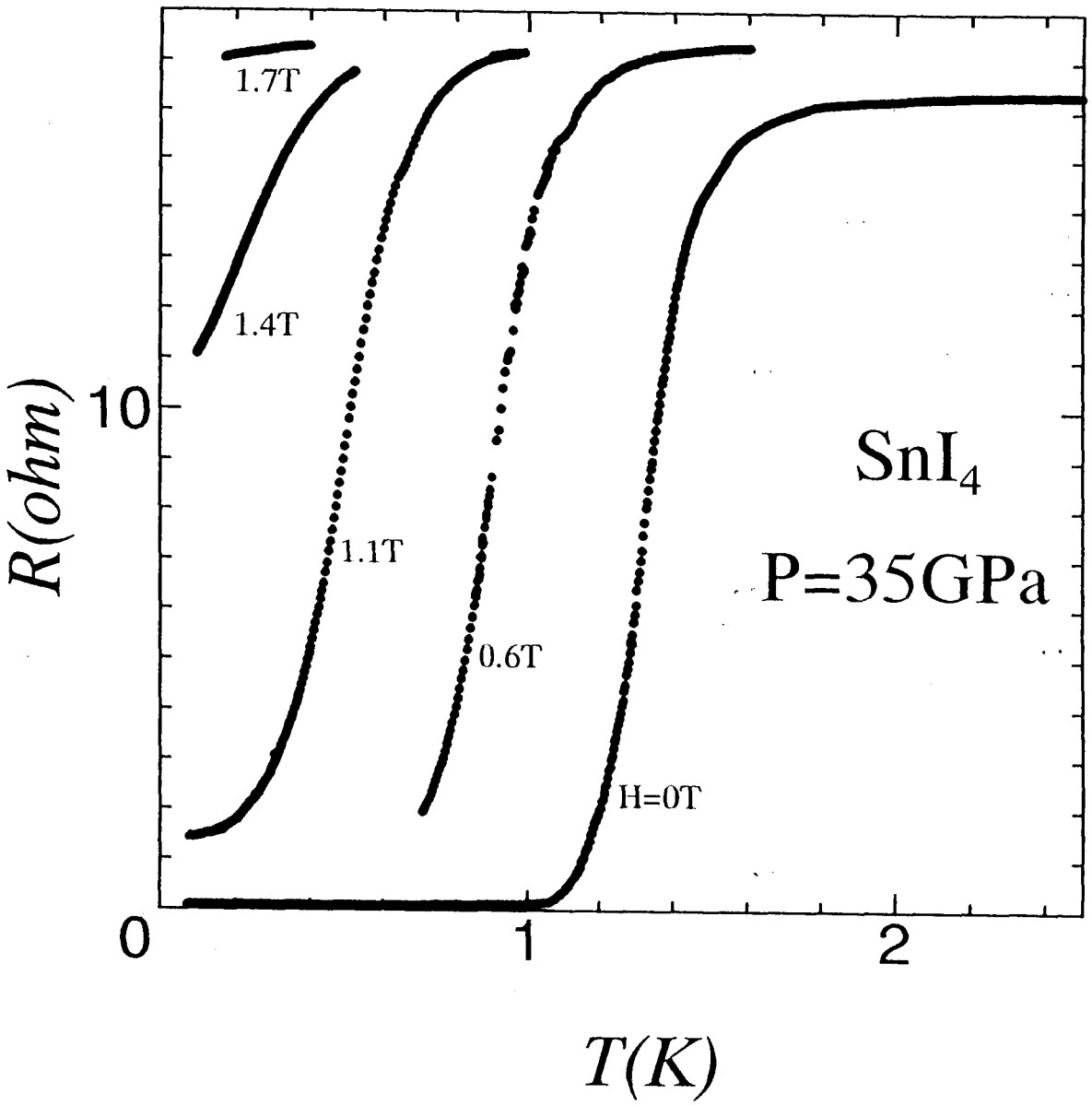


Fig. 20 The superconducting transition of $SnI_4$ at 35GPa under various magnetic fields.

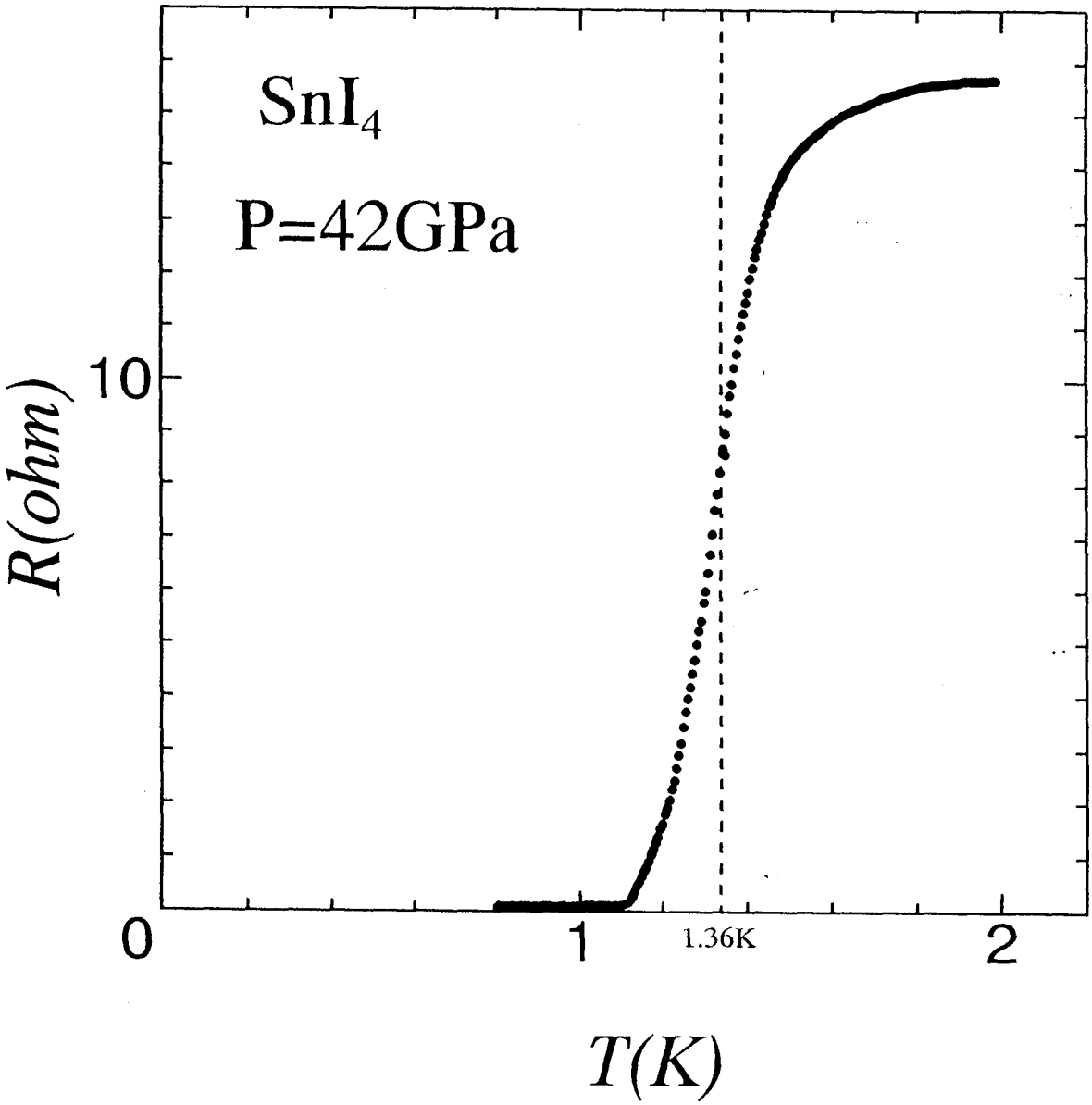


Fig. 21 The superconducting transition of $SnI_4$ at 42GPa.

## 2-2. Recrystallized phase

We increased pressure up to 64GPa in the following experiment. The specimen is supposed to be in the recrystallized phase. We show the temperature dependence of the electrical resistance in Fig.22. The superconducting transition is observed again but the characteristics of the transition looks quite changed. The transition becomes very sharp and the temperature range of the transition jumped up to near by 2K. The critical magnetic field also becomes higher in consistent with the increase enhancement of $T_c$. This behavior may concern with the recrystallization of $SnI_4$.

The temperature dependence of the electrical resistance at various magnetic fields is shown in Fig.23. It is very clear that the superconducting transition is suppressed by the magnetic field. We can estimate the critical magnetic field $H_c$ by midpoint of the transition. Figure 24 shows the temperature dependence of the critical magnetic field. The point at the lowest temperature is determined by resistance measurements under the magnetic field up to 1.7T at the lowest temperature of 60mK where we can reach using our dilution refrigerator. This obtained $H_c$- $T_c$ phase diagram is displayed in Fig.25.

We increased pressure up to 72GPa at low temperature in the following run. The electrical resistance at low temperature is shown in Fig.26. We could also observe the superconducting transition in this run. There is little change of the superconducting transition temperature $T_c$, comparing with the experimental result at $P$=64GPa.

In the subsequent run, we set $P$=78GPa as the pressure value. We could confirm the superconducting transition with almost the same $T_c$. The temperature dependence of the electrical resistance is shown in Fig.27. The pressure derivative of the superconducting transition temperature $dT_c/dP$ is supposed to be small in the recrystallized phase.

The pressure determination by ruby fluorescence becomes difficult in

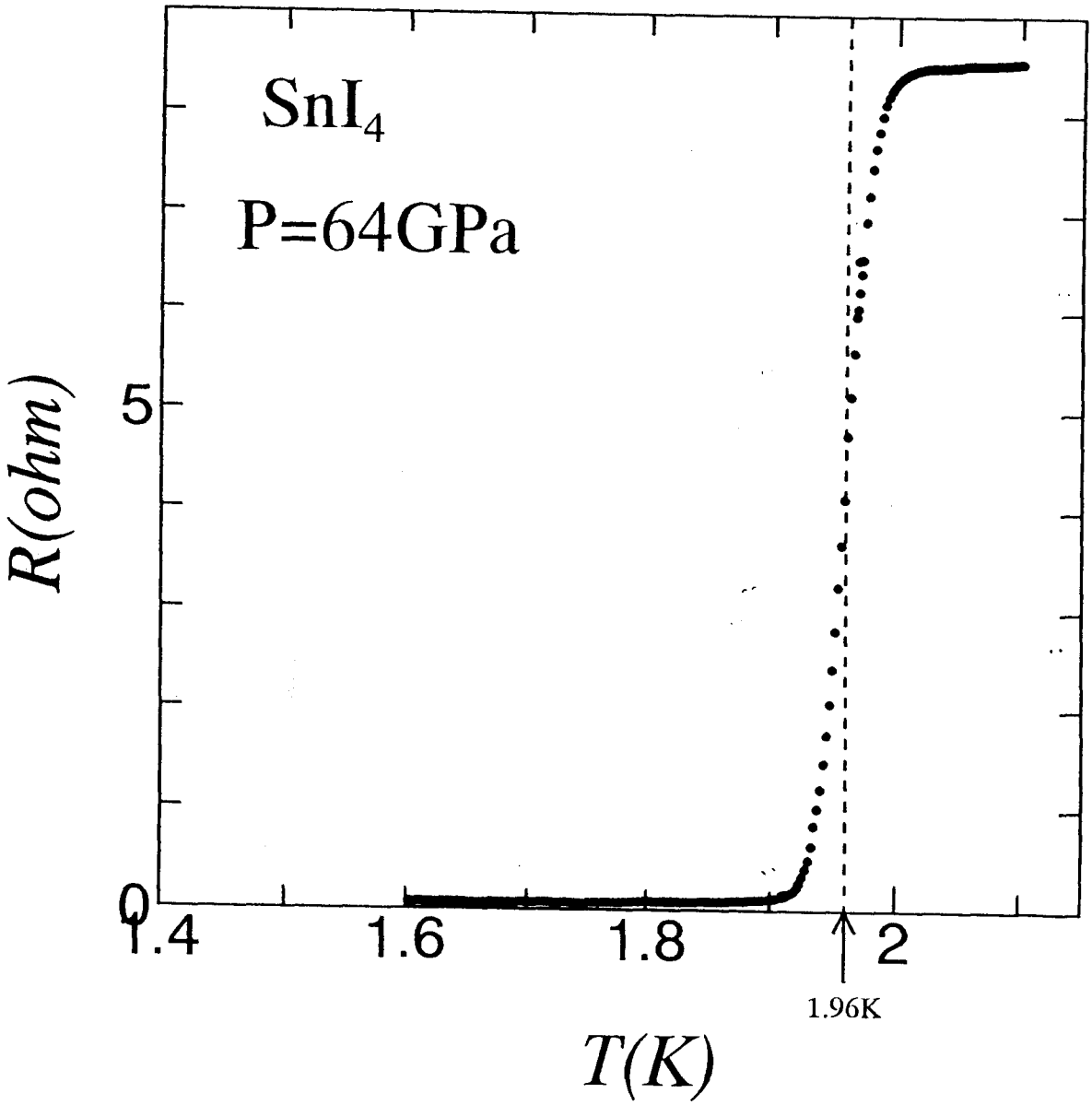


Fig. 22 The superconducting transition of $SnI_4$ at 64GPa.

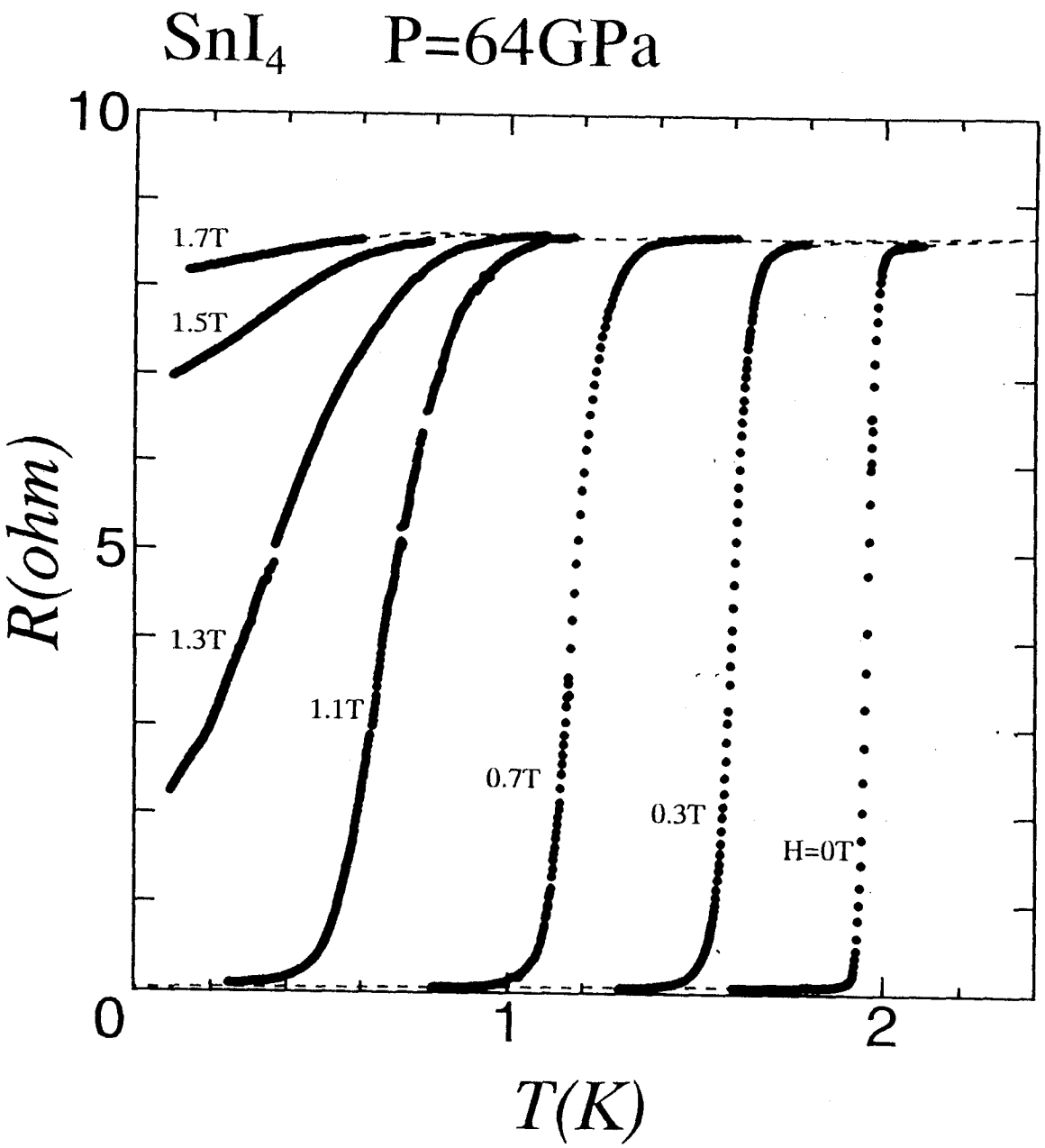


Fig. 23 The superconducting transition of $SnI_4$ at 64GPa under various magnetic fields.

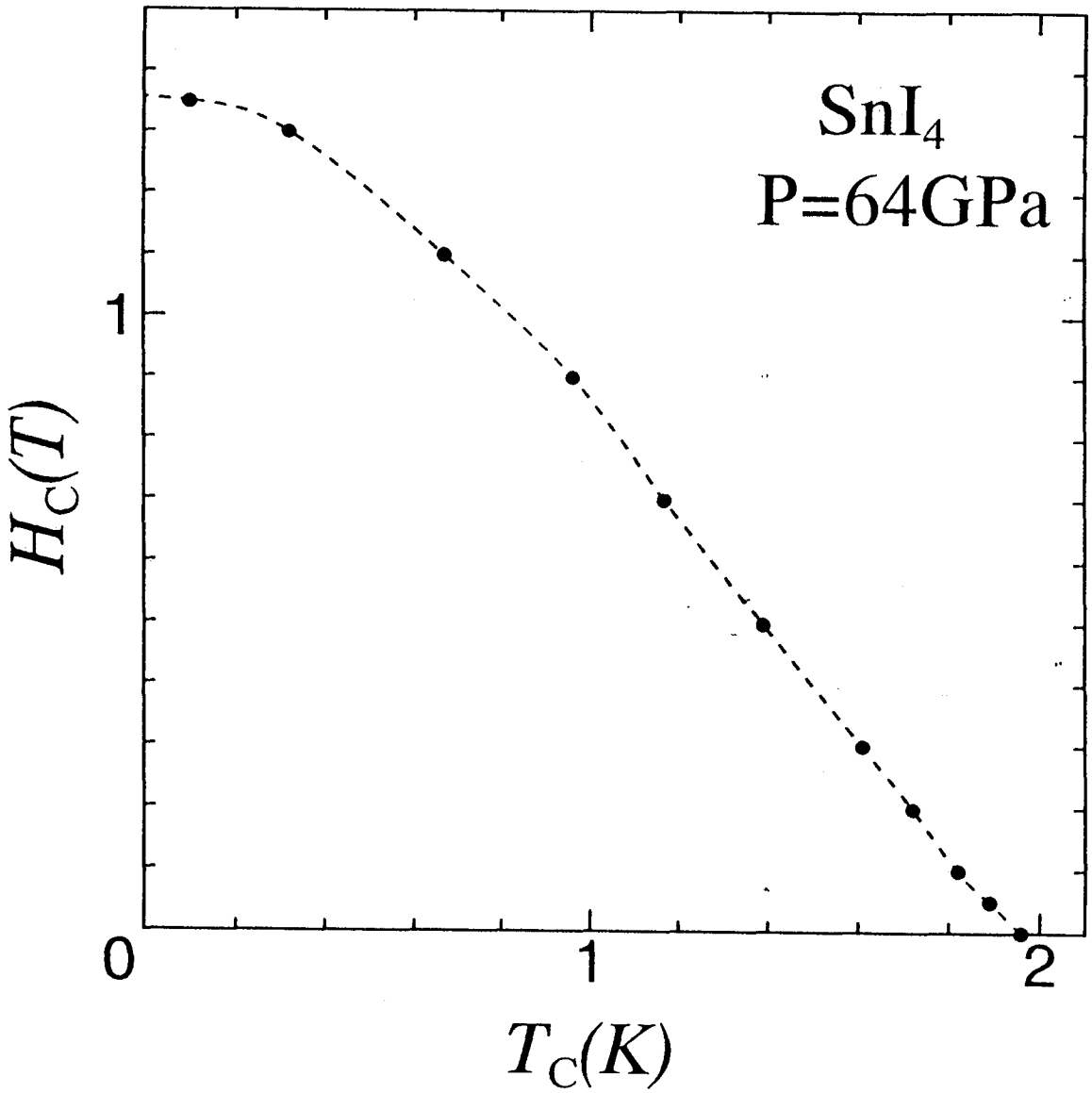


Fig. 24 The temperature dependence of the critical magnetic field $H_C$ estimated by midpoint of the transition at 64GPa.

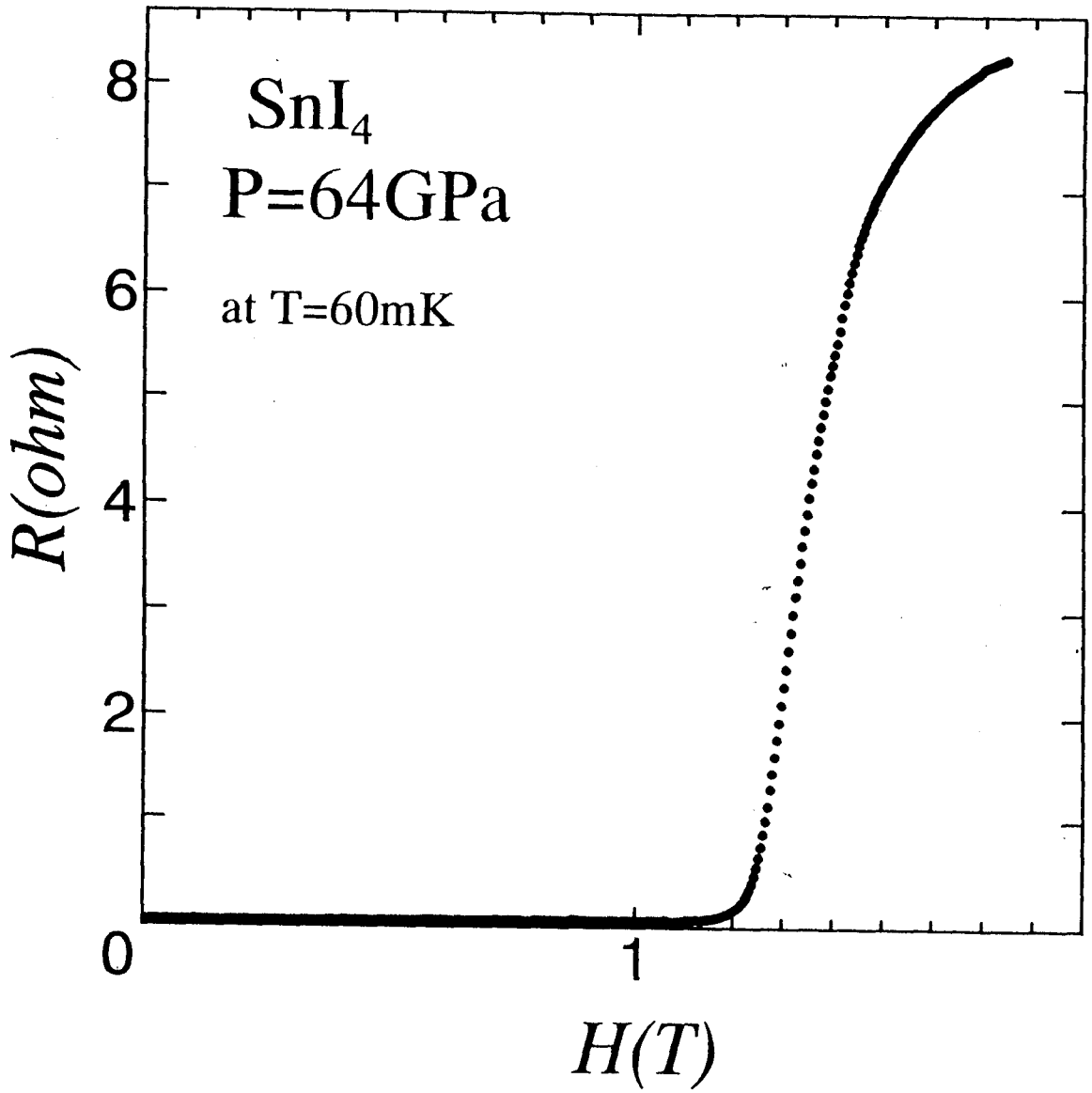


Fig. 25 The electrical resistance of $SnI_4$ under the magnetic field at the lowest temperature of $T$=60mK.

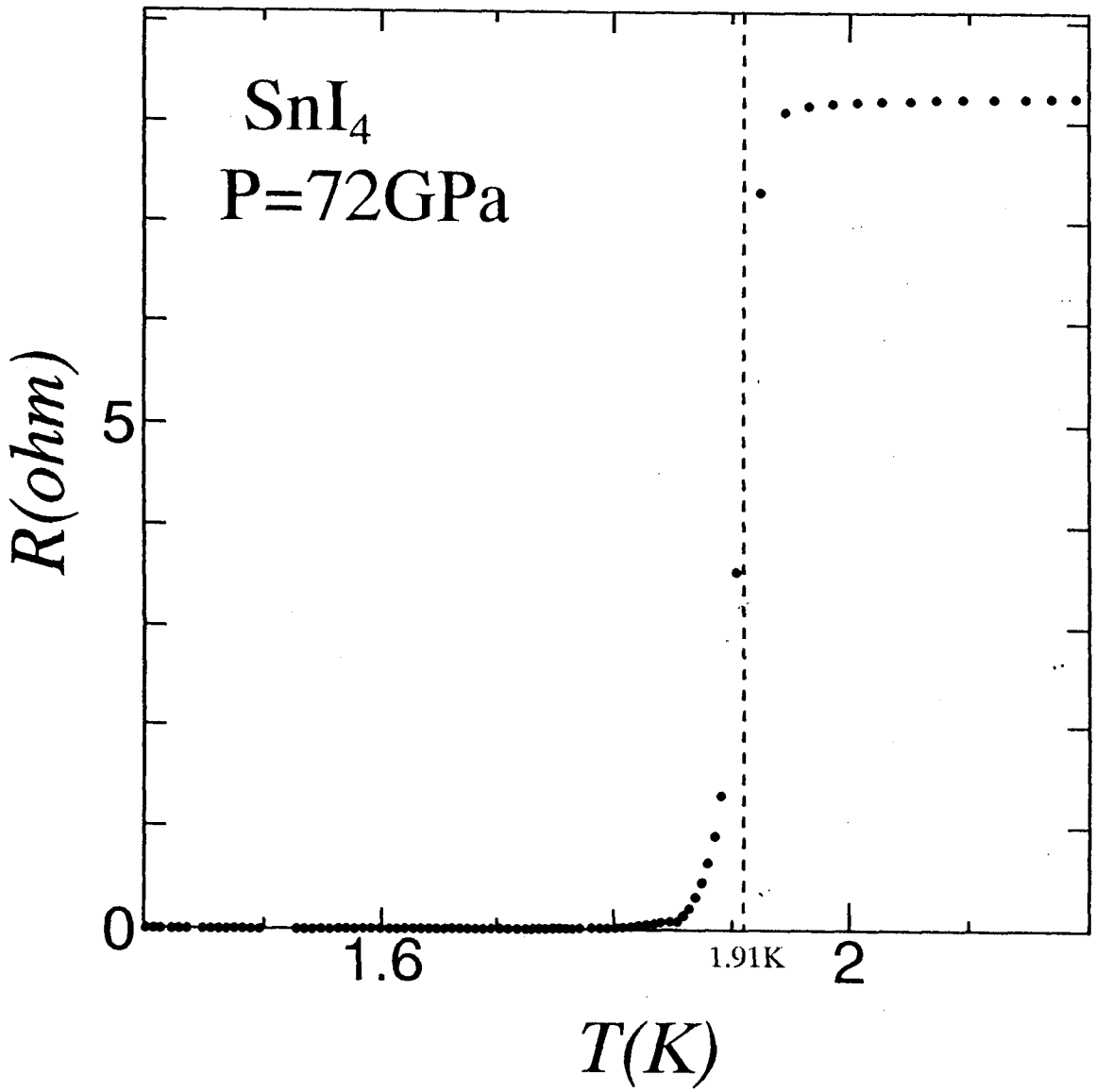


Fig. 26 The superconducting transition of $SnI_4$ at 72GPa.

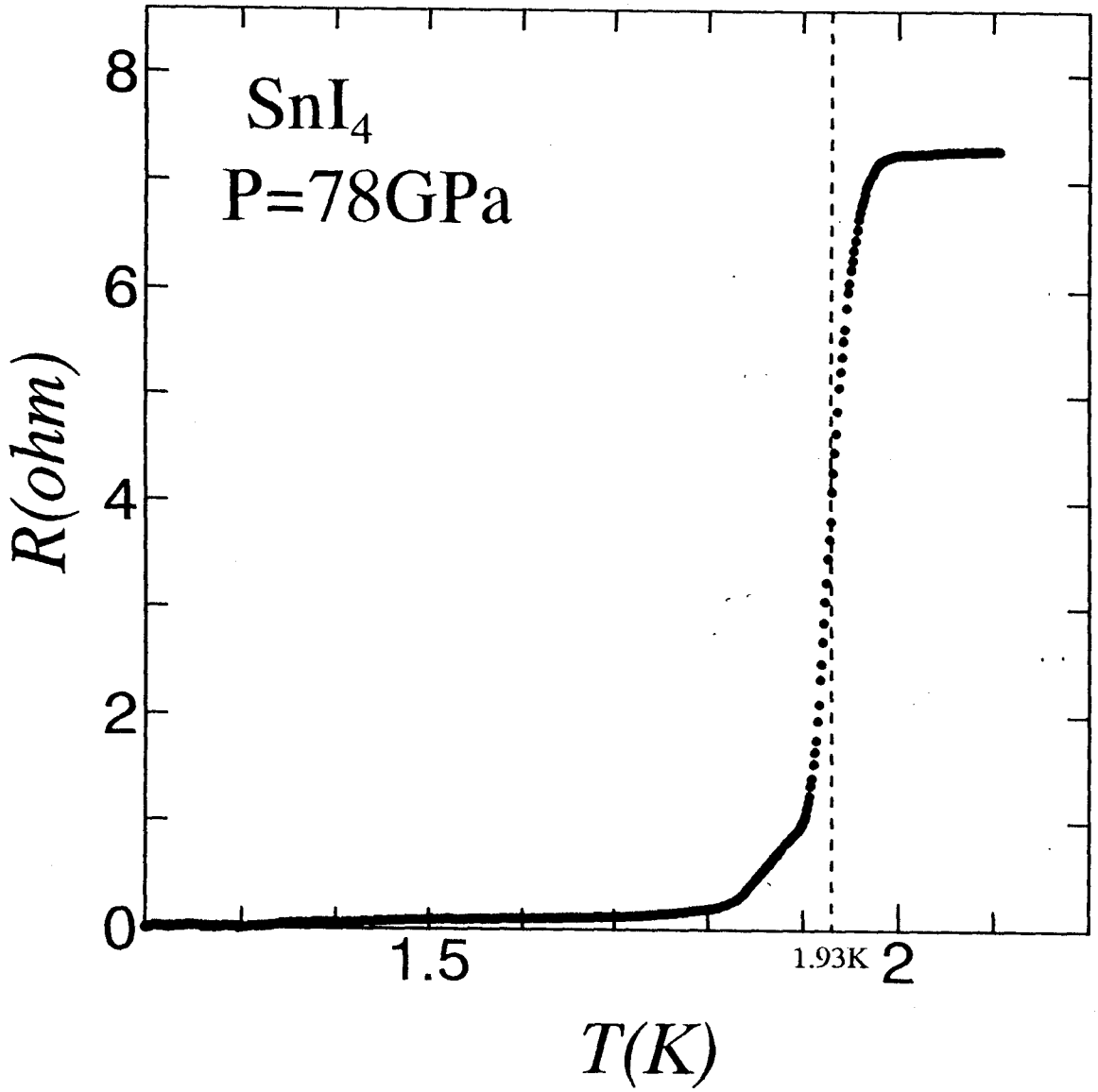


Fig. 27 The superconducting transition of $SnI_4$ at 78GPa.

general towards higher pressure because the fluorescence intensity becomes weaker with increasing pressure. The intensity also becomes at low temperature. We increased pressure value after the experiment at $P$=78GPa, but we could not determine at liquid $N_2$ temperature because the intensity of ruby fluorescence was too weak to observe. However, the pressure value at $N_2$ temperature is expected to be higher than 80GPa because the pressure at room temperature is higher than that of the former run. We estimate the pressure for 86GPa according to the pressure value at room temperature and increasing ratio of former run.

The superconducting transition was observed again but there was big difference in its behavior. Figure 28 shows the superconducting transition at $P$=86GPa. The transition looks like a combination of two superconducting transitions. One is the transition around $T_c$=1.8K, and the other around $T_c$=1.2K. These two transitions have different critical magnetic fields. The resistance curve under high magnetic field is shown in Fig.29. The transition of low temperature side is suppressed at $H$=0.8T but another transition does not disappear yet. The transition is completely suppressed at $H$=1.7T which is almost the same value as those in the recrystallized phase. So, there seems to be an unknown phase boundary at low temperature around 80GPa. There must be a coexistent phase of $SnI_4$ accidentally.

In further run, the ruby fluorescence is also too weak to determine a pressure value at liquid $N_2$ temperature. Fortunately, we can determine the pressure value at room temperature, so we estimate the pressure value for 95GPa at liquid $N_2$ temperature as in former run. The temperature dependence of the electrical resistance at low temperature is shown in Fig.30. The superconducting transition could be observe in this experiment too. The superconducting temperature $T_c$ becomes lower. The specimen was supposed to be in an unknown phase completely.

There is an possibility that we have performed our resistance measurements with too much current. Excess current would destroy a

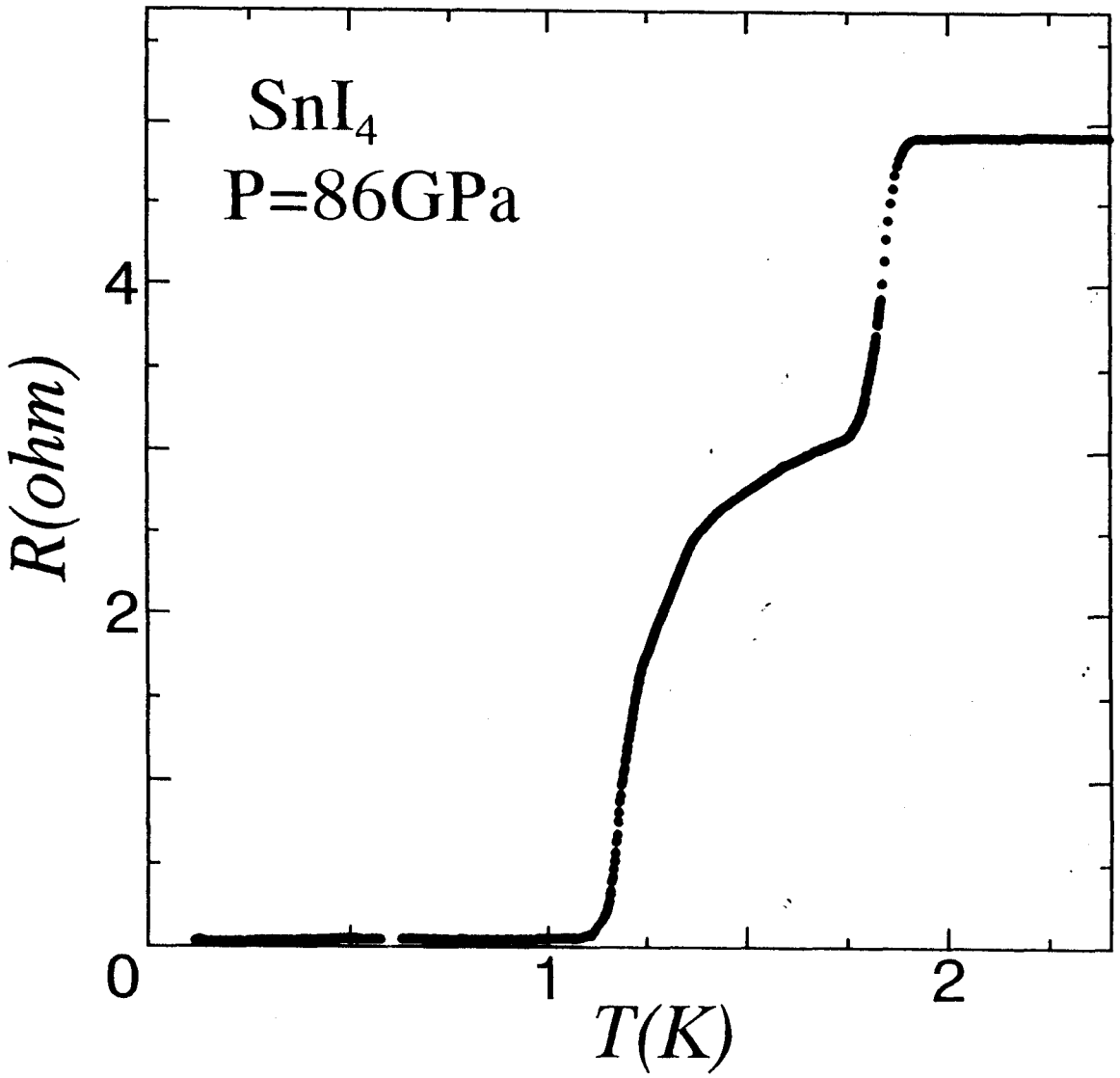


Fig. 28 The superconducting transition of $SnI_4$ at 86GPa

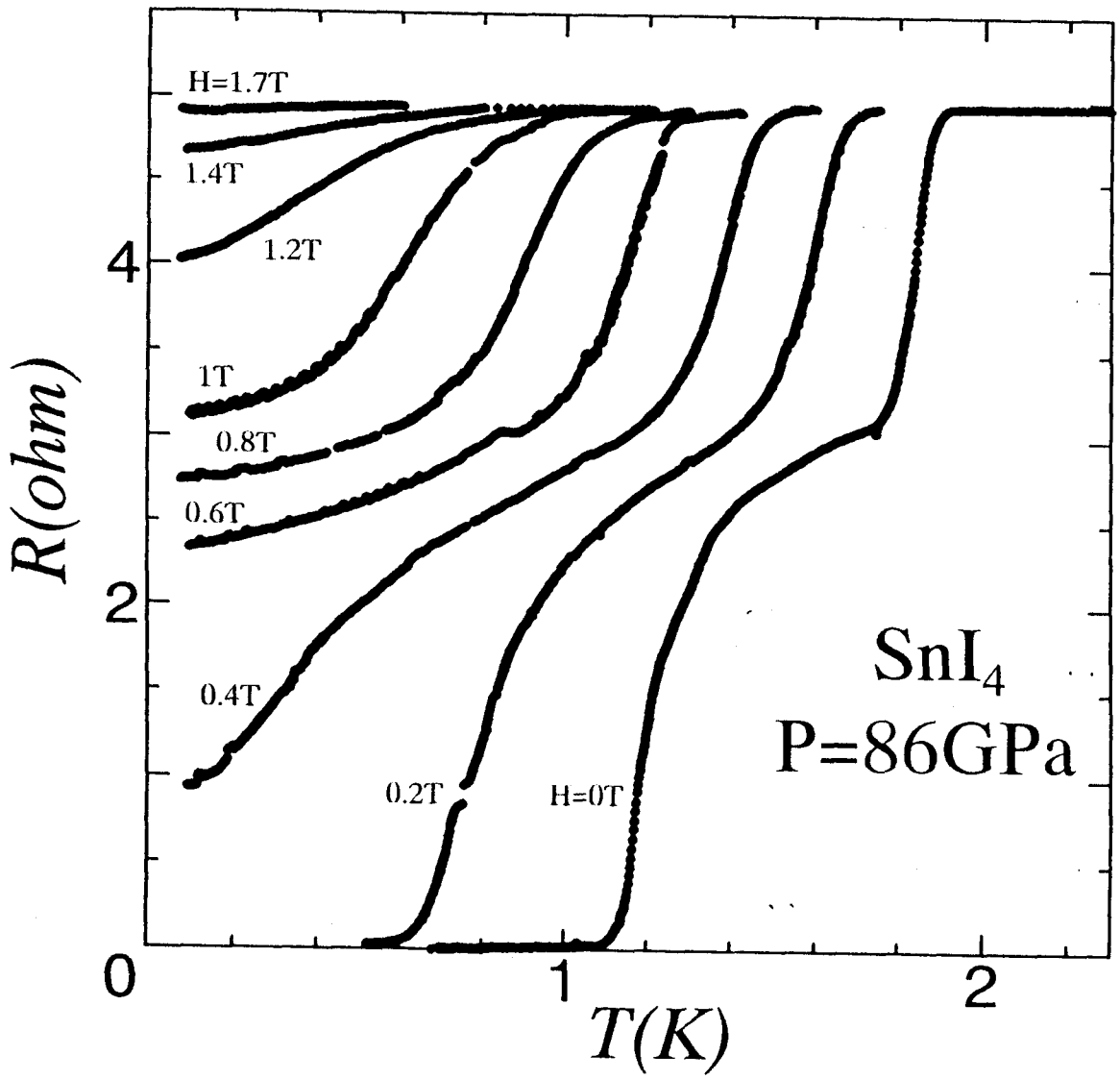


Fig. 29 The electrical resistance of $SnI_4$ at 86GPa under various magnetic fields.

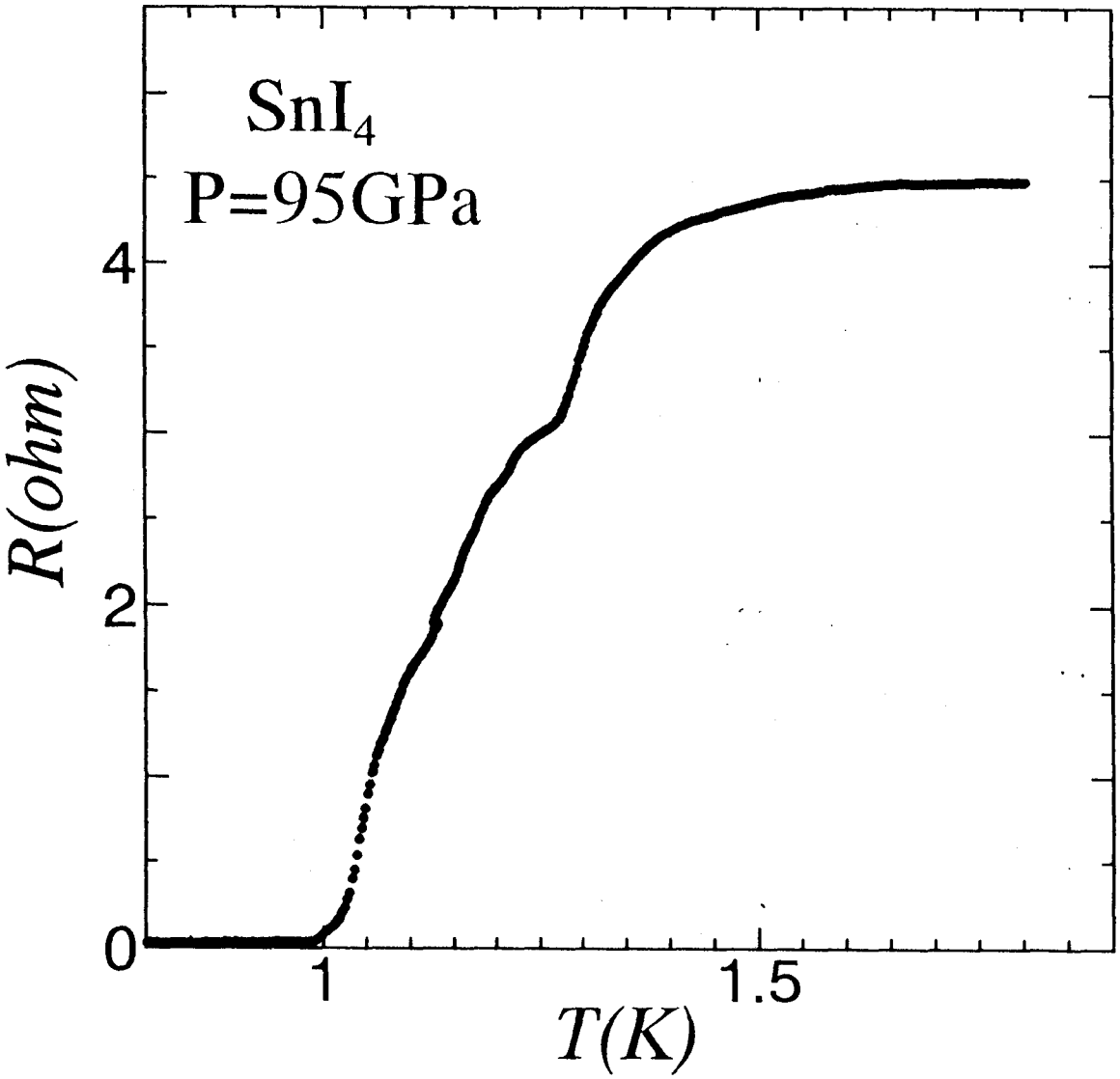


Fig. 30 The superconducting transition of $SnI_4$ at 95GPa

superconductivity and cause disappearance of $T_c$. So, we measured resistance also at very small current in this experiment to deny this possibility. Figure 31 shows the superconducting transition with measuring current of $i$=1$\mu$A and 10nA. There is no definite difference between each curve in spite of the worse S/N ratio. All resistance measurements had been performed at measuring current of $i$=1$\mu$A so there is no problem of errors by excess measuring current in our data. This run is obtained at the highest pressure because the diamond anvil had a possibility of destruction.

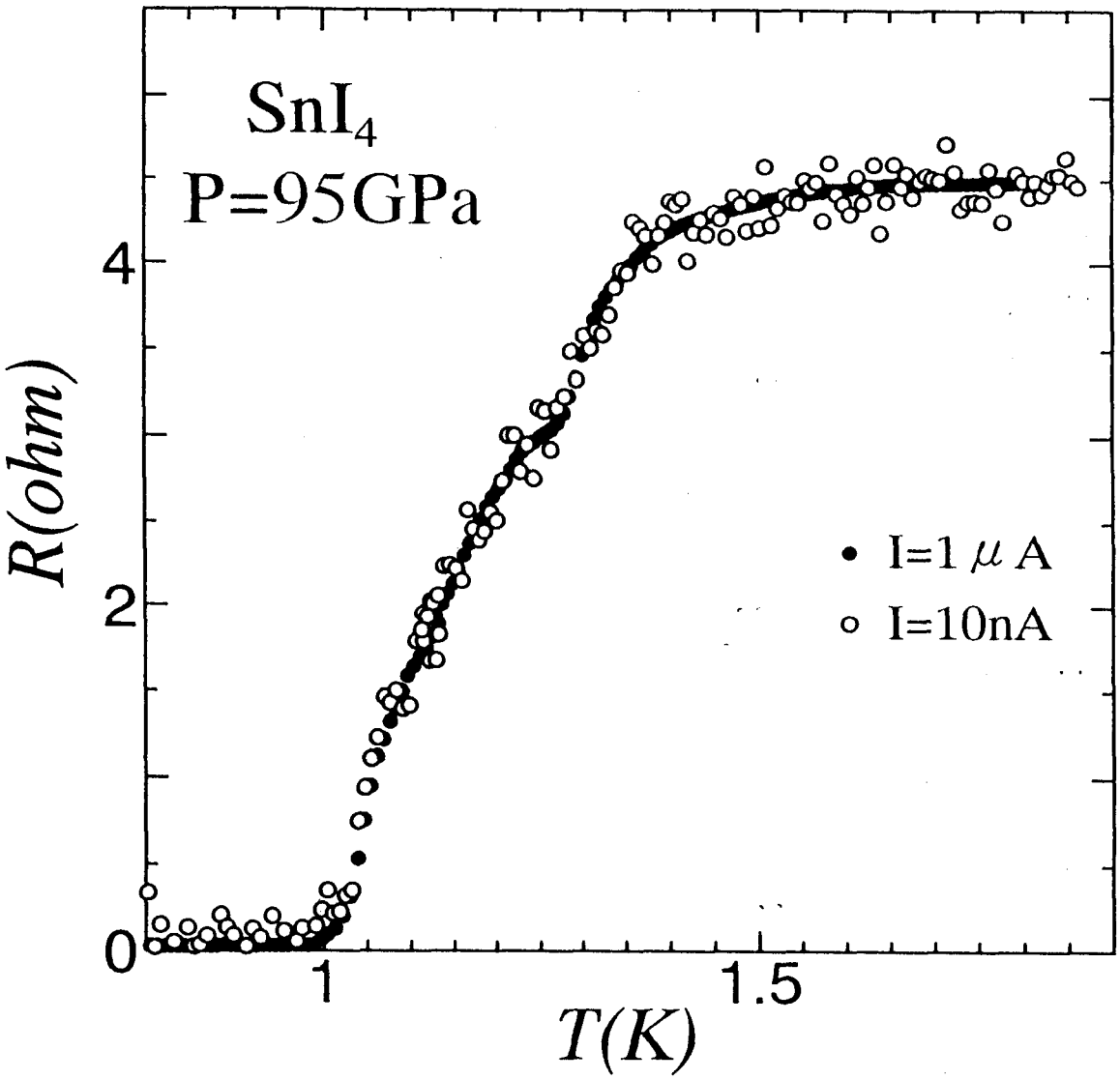


Fig. 31 The electrical resistance of $SnI_4$ measured with different currents of $i$=1$\mu$A and 10nA at 95GPa.

## 2-3. At low pressures

We made newly a setting of a sample to observe the electrical resistance at low temperature with the purpose to see how much pressure we need to bring about the metallization and the superconductivity. At first, we performed an experiment at $P$=6.6GPa. The lattice is supposed to be cubic (phaseI) and $SnI_4$ is semiconductive. Figure 32 shows the electrical resistance down to liquid $N_2$ temperature. We measure the resistance at temperature down to 60mK but no superconducting transition was observed. Then we increased pressure up to $P$=9.2GPa. The superconductivity did not appear at the pressure.

Chen *et al.* suggest that $SnI_4$ metallizes at pressure of $P$=12$\pm$1GPa. As we were interested in metallization and appearance of superconductivity, so we measured the temperature dependence of the resistance from room temperature to liq. $N_2$ temperature for several times at pressure range between 10GPa and 25GPa. Figure 33 shows the results of the experiments. The value of pressure is changed by thermal expansion of DAC body, so the value at room and liq. $N_2$ temperature is presented in this figure. Below 12GPa, the resistance increases with cooling down, which suggests that $SnI_4$ is semiconductive in this pressure region. Above this pressure, the resistance also increases but an anomaly appears around $T$=200K. This anomaly may be caused by phase transition. Hamaya *et al.* reported that there is a jump of halo peak position at pressure $P$=13GPa. This change of amorphous state may cause the anomaly of the resistance, but it is not clear now. Further X- ray diffraction experiments below at room temperature are required. The metallization pressure is considered to be above 20GPa.

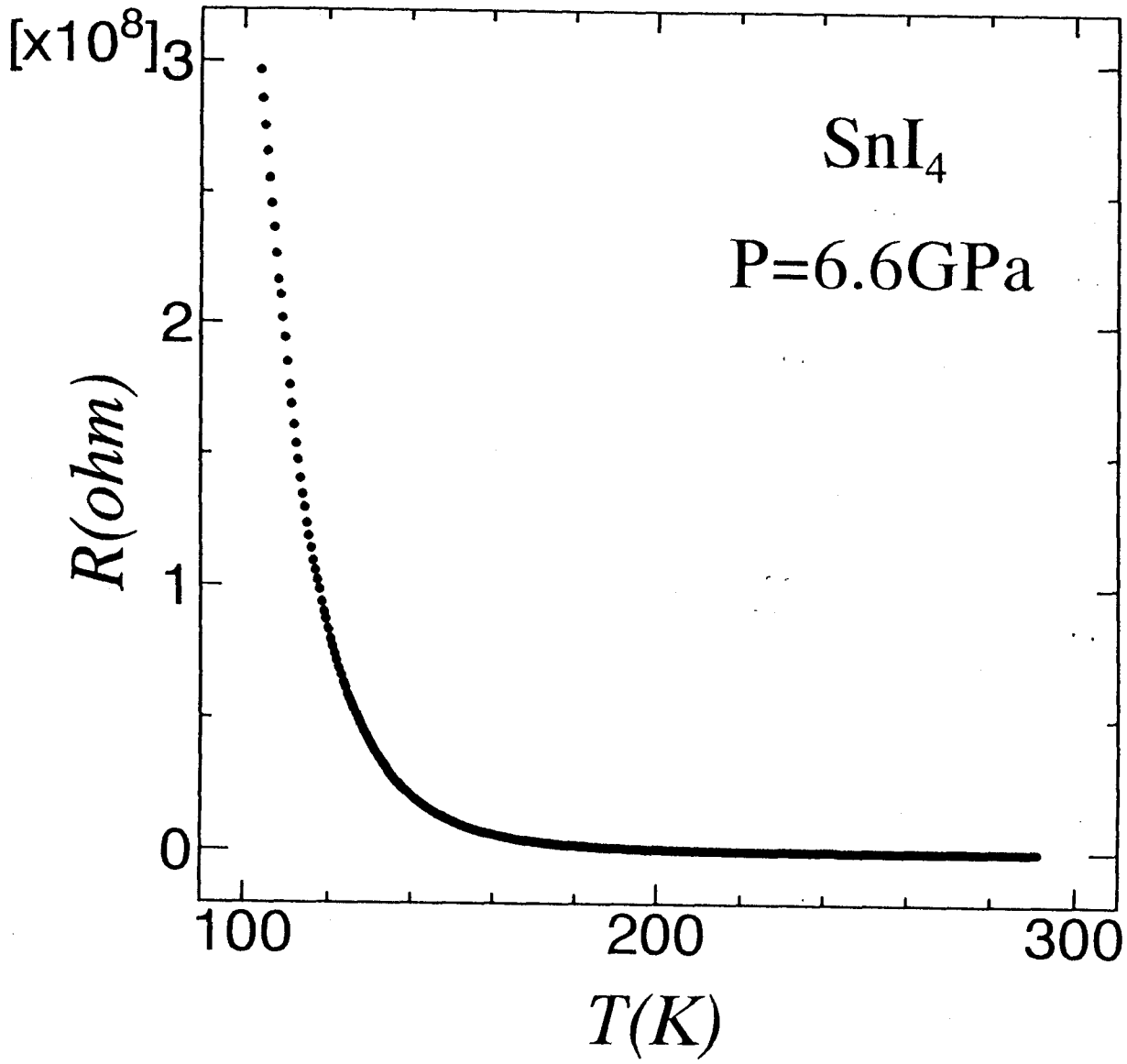


Fig. 32 The electrical resistance of $SnI_4$ at 6.6GPa. The resistance increases rapidly with cooling down.

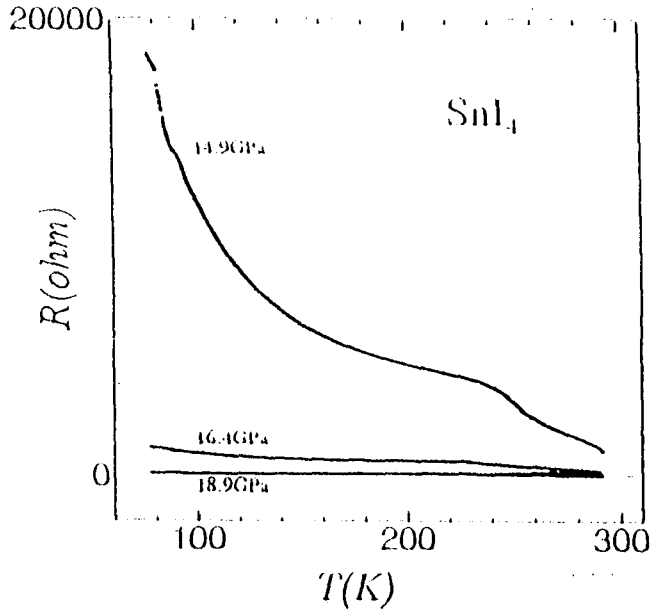


(a)

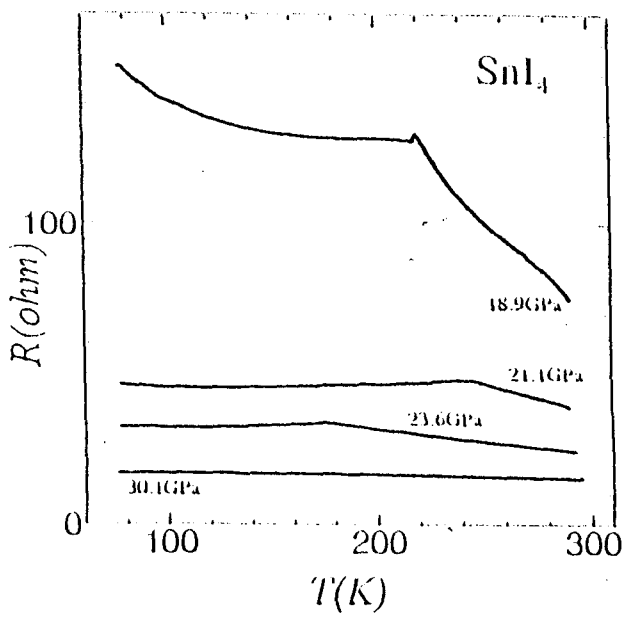


(b)

Fig. 33 The temperature dependence of the electrical resistance of $SnI_4$ at various pressure. Rapid increase of the resistance in cooling process is suppressed as applying pressure (a), but an anomaly appears at above 14.9GPa.((a),(b)) At 30.1GPa, anomaly disappears and superconducting transition is observed at liquid Helium temperature.

## 2-4. Reappearance of Superconductivity

We increased pressure up to 25GPa but no superconductivity is observed at temperatures down to 60mK. Then, we increased pressure up to 36GPa and the superconducting transition is also observed as shown in Fig.34. We confirm the appearance of the superconductivity of $SnI_4$ in different sampling. Finally, we confirm the superconducting transitions in this series of the experiments at pressures $P$=36, 47 and 54GPa. The transition temperature $T_c$ is smoothly going up with increasing pressure, and is considered to be connected with $T_c$ in recrystallized phase at around 60GPa.

On the other hand, we arranged another sampling by using different type of DAC which designed by Dr. M.Eremets. We also confirmed a superconductivity with $T_c$=1.25K in this experiment at pressure $P$=30GPa, this is the lowest pressure which we confirmed the superconductivity. Figure 35 shows the pressure dependence of the transition temperature $T_c$ from all experiments we performed.

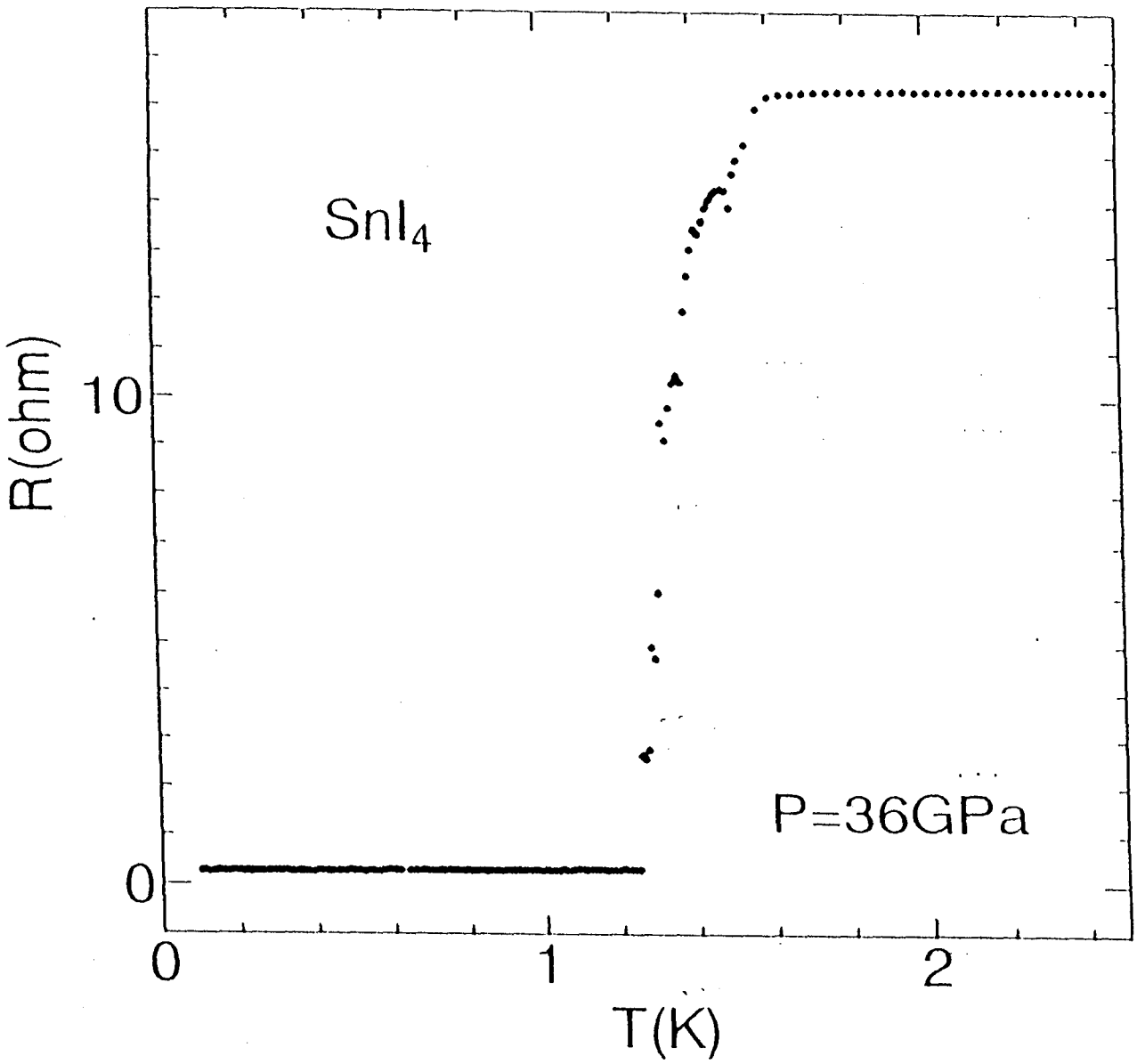


Fig. 34 The superconducting transition of $SnI_4$ at 36GPa with different sampling.

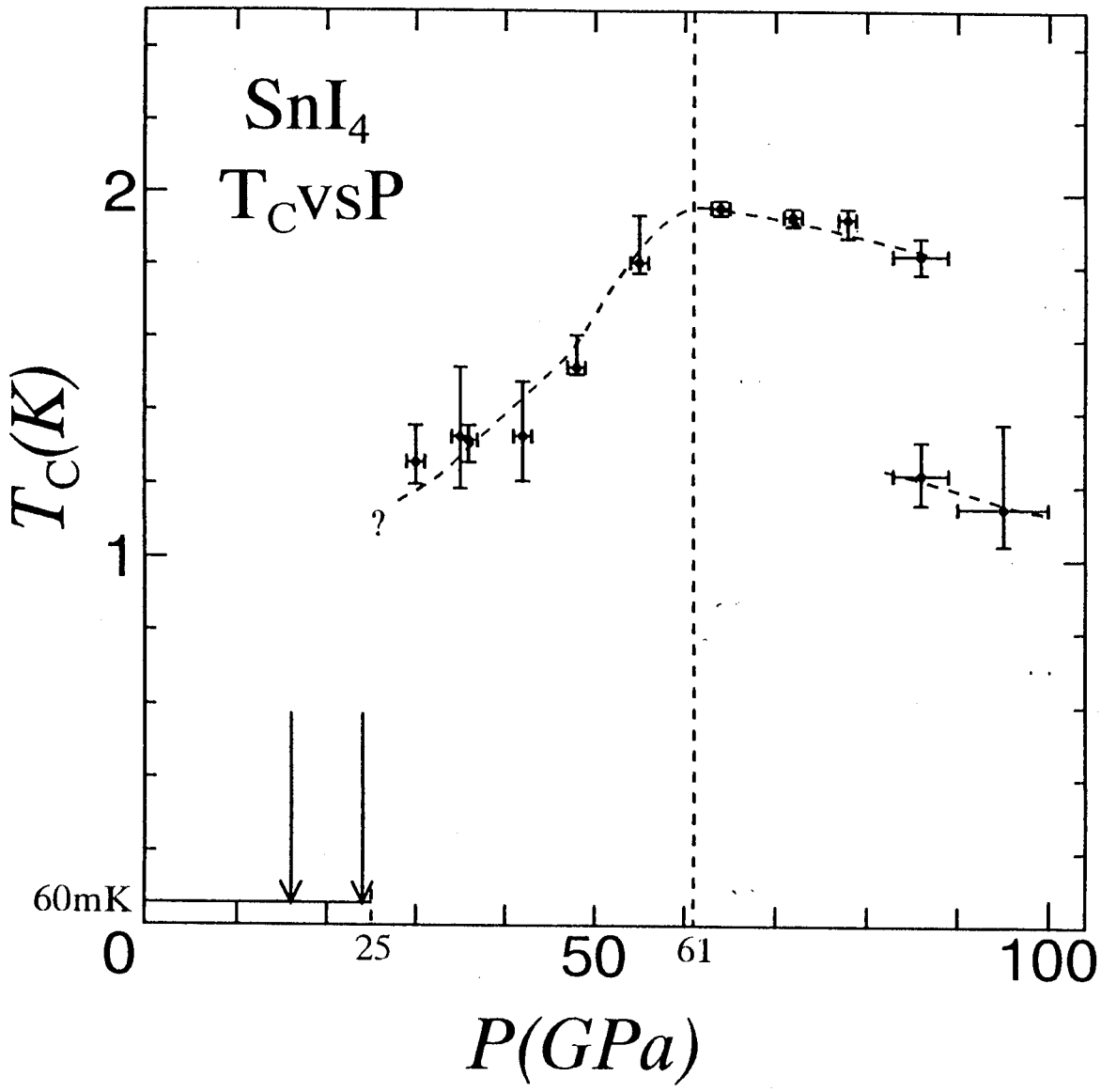


Fig. 35 The $T_C$ vs $P$ phase diagram of $SnI_4$.

## 3. Magnetization at low temperatures

If we can observe a Meissner effect from $SnI_4$ under high pressure, it will give us another strong evidence of superconductivity. It is very difficult to measure magnetization in a DAC because of its extremely small sample. But, as the diamagnetic signal due to superconducting transition (Meissner effect) is huge, we can observe it by using SQUID magnetometer.

We set the pressure $P$=40GPa at which we might observe a superconductivity, judging from the results of resistance measurements. Figure36 shows the magnetization at low temperature. The unit of magnetization is arbitrary. There is a signal increasing with low temperature. It is considered to be the background signal from almost CuTi arroy gasket. At around 2K, there is an anomaly which may be from huge and rapid decreasing magnetization signal from specimen. We have measured already a background signal, so we can subtract it from the total signal and obtain Meissner signal only. The subtracted signal of magnetization is shown in Fig.37. We can see the decreasing (diamagnetism) of magnetization between $T$=1K and 2K. This signal is considered to be a Meissner signal of $SnI_4$.

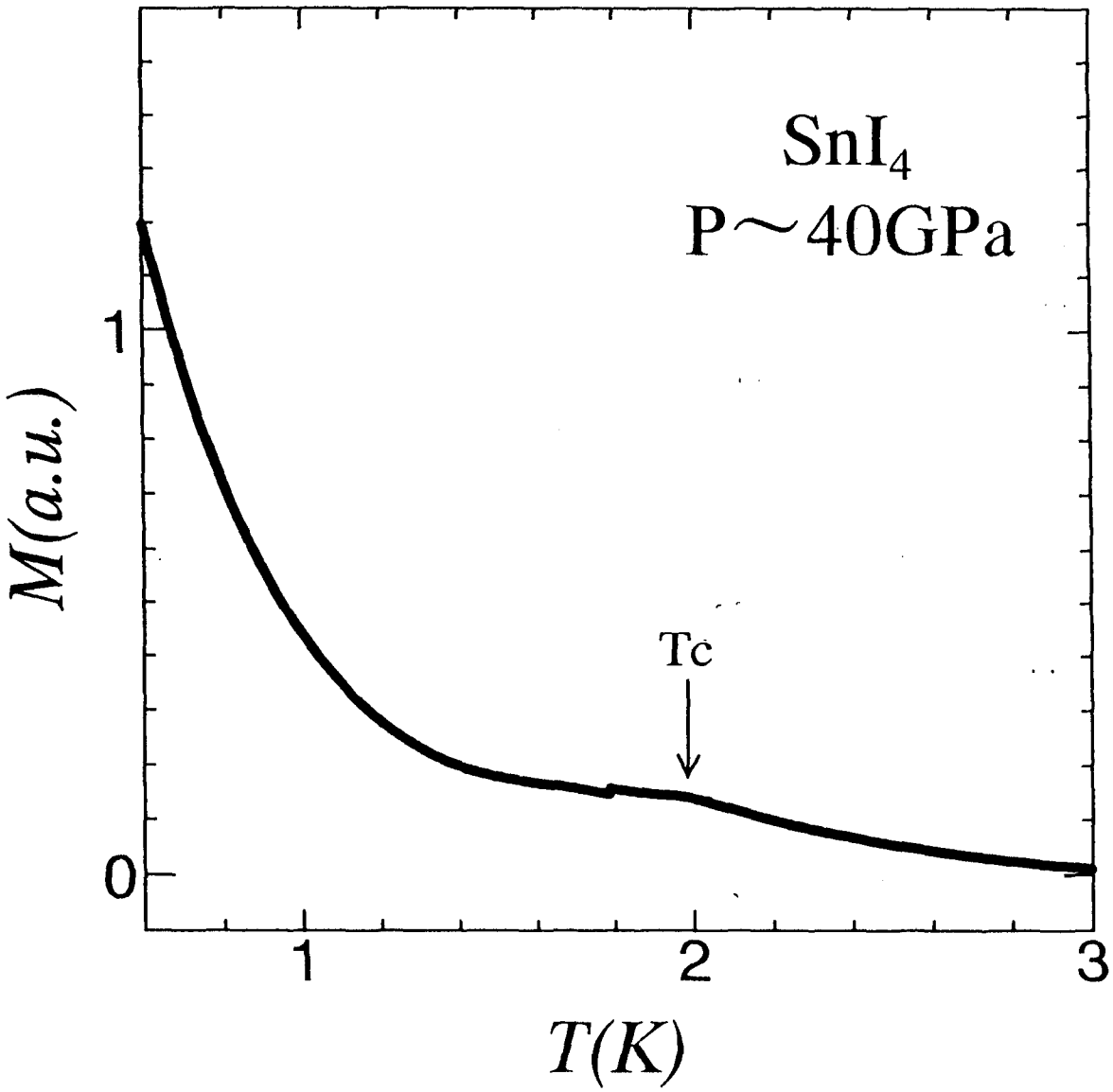


Fig. 36 The total magnetization of $SnI_4$ and the background signal at 40GPa.

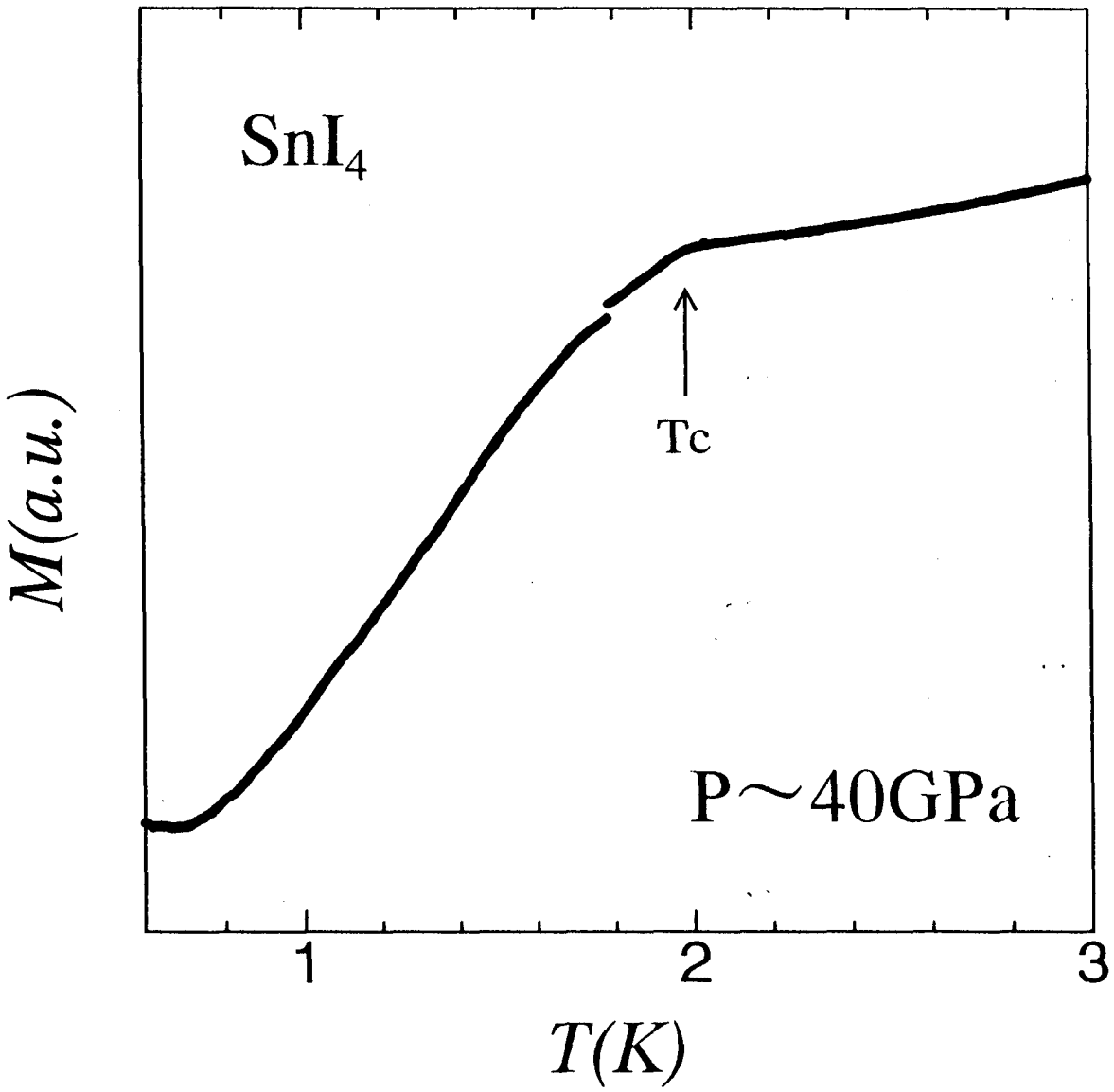


Fig. 37 The Meissner signal of $SnI_4$ at the superconducting transition obtained by subtracting the background signal.

# 4. Discussion

### Phase boundaries at low temperatures

Hamaya *et al.* reported[6] that $SnI_4$ has three phases at room temperature. But we suppose there is another phase boundary at pressure around $P$=80GPa at temperature $T$~1K. Figure 35 shows the pressure dependence of the superconducting transition temperature $T_c$. There is an drastic change of $T_c$ at around $P$=80GPa, so it is natural that there is an unknown phase boundary of $SnI_4$. We call this new phase as phase IV.

Hamaya *et al.* also suggests that amorphization and metallization of $SnI_4$ gradually occurs in phase II ($P$>7.2GPa). Figure 38 shows the crystal phase diagram of $SnI_4$ with respect to pressure. As the lattice scattering is dominant in electrical resistance at high temperature, so there may be a drastic change in resistance for structural phase transition. We arrange our resistance data at various pressures with normalization by the value at liquid $N_2$ temperature ($T$=77K). Figure 39 shows these data.

The resistance curves can be divided into three groups(A, B and C) and each group is supposed to correspond to the crystal phases(phase II,III and IV) at low temperature. The decreasing ratio at low temperature limit of Group A(amorphous state, phase II) is about 0.98. In the recrystallized fcc phase(Group B, recrystallized into fcc, phase III), it is about 0.95, and there is an obvious difference between two phases.

If there are many lattice defects, the residual resistance ratio should become large. The amorphous state is supposed to be a kind of a lattice including many defects, so we can understand the difference of residual resistance ratio.

In phase IV (probably in crystallized phase), the residual resistance ratio becomes smaller than that of phase III. This results may support that there is an unknown phase boundary around $P$=80GPa. We discuss about this in the

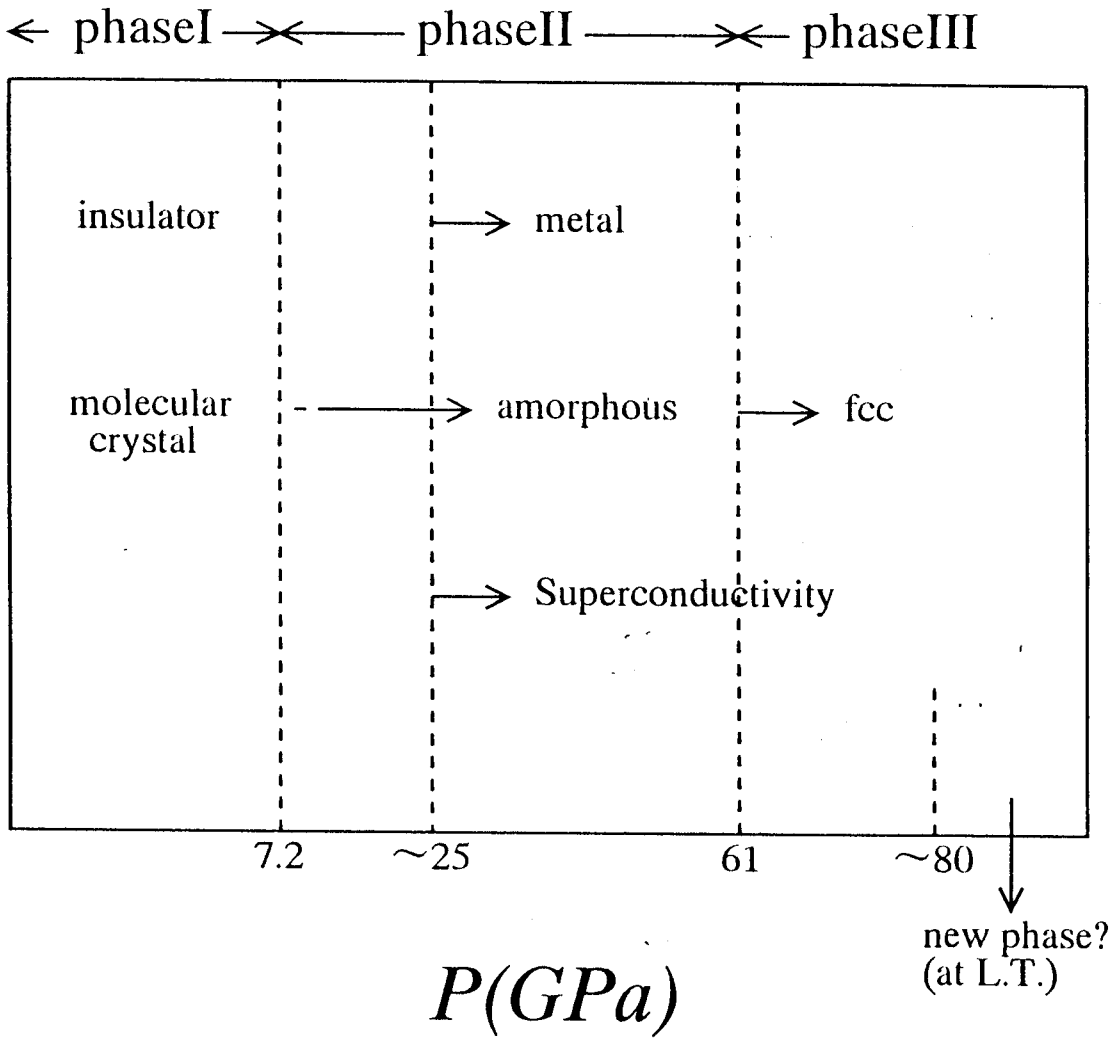


Fig. 38 The phase diagram of $SnI_4$ with respect to pressure.

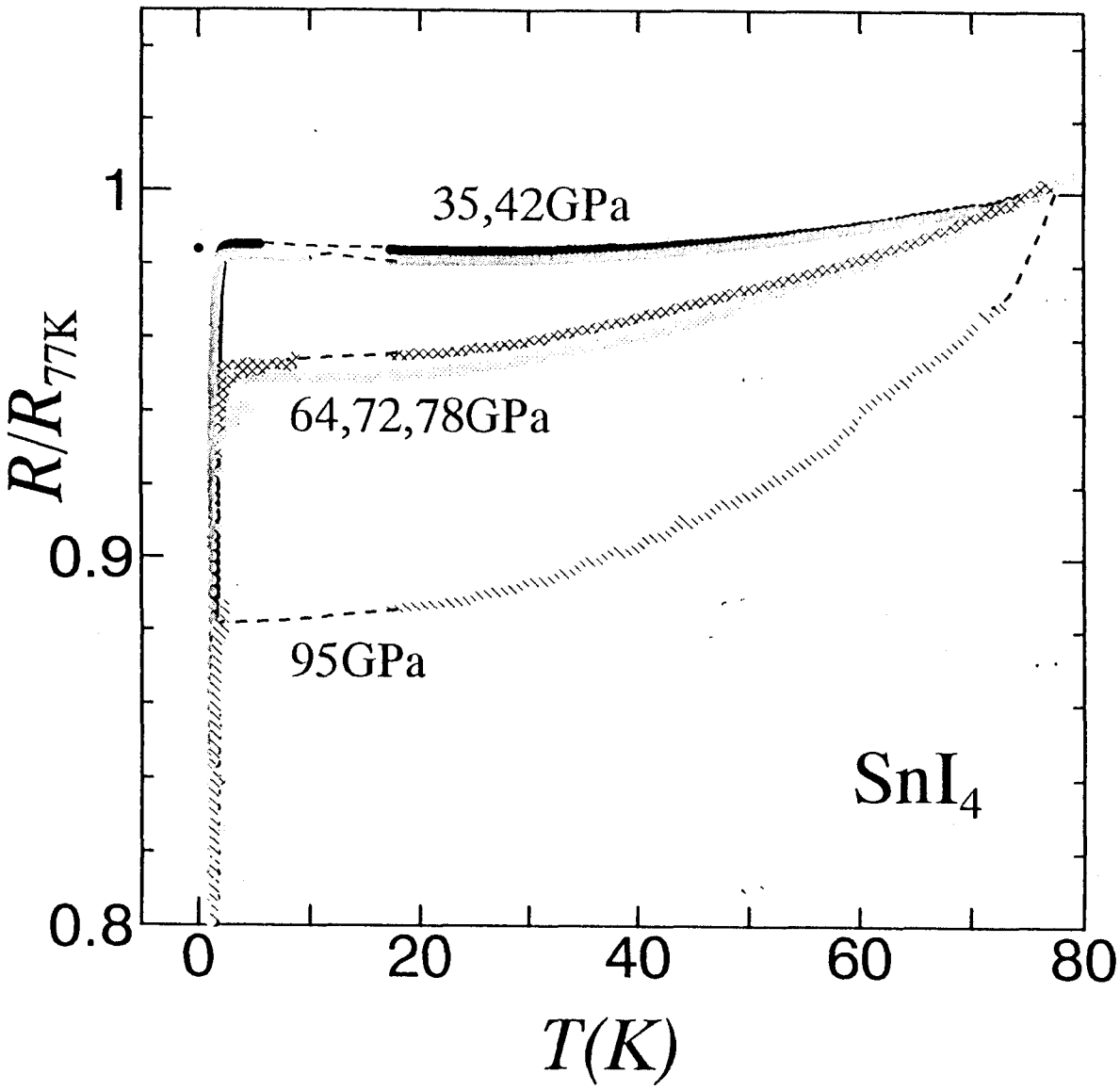


Fig. 39 The electrical resistance of $SnI_4$ normalized by the value at liquid nitrogen temperature.

following section.

### Pressure induced superconductivity of $SnI_4$

We could observe the superconductivity of $SnI_4$ in every experiment above 35GPa. We also observed the Meissner signal at $P$=40 and 50GPa. Therefore, we are sure that $SnI_4$ shows superconductivity at pressures above $P$=30GPa. Figure 35 shows the pressure dependence of superconducting transition temperature $T_c$ which changes dramatically under pressures.

This change of $T_c$ is expected to be caused by structural phase transition. In phase II (amorphous state), $T_c$ is around 1.3K and the transition is somewhat broad. In phase III, the superconducting temperature $T_c$ were observed at around 2K, which is the highest mark in our series of experiments. Above 80GPa, $SnI_4$ may enter into another phase (phase IV) and $T_c$ goes down rapidly.

### Recrystallization of $SnI_4$

The mechanism of amorphization is not clear but there are some proposals. Recently Hamaya *et al.*[6] propose the model of a crystal which has molecular dissociated micro crystal (like phase III,fcc) inside. From this point of view, the above model seems to explain the fact that superconducting transition temperature $T_c$ is low and broad in contrast to that in recrystallized phase (phase III). The fact is also consistent with the higher symmetry caused by recrystallization. So the recrystallization may happen at about 62GPa even at low temperature.

It is very curious that $T_c$ in the phase III is about three times higher than that of fcc monatomic iodine with the same lattice constant at the same pressure. Similarly, the critical magnetic field $H_c$ is about ten times bigger than that of iodine. The tin atoms in $SnI_4$ is considered as an impurity in fcc iodine.

Shimizu *et al.* reported[10] that the pressure dependence of $T_c$, $dT_c/dP$ in fcc iodine is positive. If the tin atom plays a role to generate a chemical pressure to the lattice, this enhancement of $T_c$ may be understandable. But Sakamoto *et al.*[15] calculated the negative value of $dT_c/dP$ in fcc iodine. Determination of the structure, the position of tin atoms, is very important to clear up these mysteries.

**New phase at above P=80GPa**

The $T_c$ of $SnI_4$ is decreasing rapidly with pressure above 80GPa. No phase boundary has been reported until now at around 80GPa in the experiment performed at room temperature, and there is no experiment at low temperatures. It is clear that there is some change in the crystal lattice at around 80GPa according to the results of residual resistance ratio shown in Fig.39. From this figure, the defects of lattice seem to decrease because the ratio becomes lower above 80GPa. But if the lattice becomes complete, the $T_c$ might be higher. To explain the detail of this transition, a supplementary experiment of resistance measurement and structural studies at low temperature are required.

**Magnetization measurement**

The Meissner signals are observed in our experiment at 40GPa. There are some problems in these results; 1. The onset of the transition was around 2K but $T_c$ is estimated as about 1.3K from the resistance measurements. 2. The transition is very broad as compared with resistance measurements.

If we stand on the model of dissociated fcc micro crystal in amorphous phase, the onset of the superconducting transition may looks like around 2K which is the $T_c$ in the recrystallized phase III. So, let us verify the results of resistance measurements in the phase III again. The detail of resistance around 2K at 42GPa is shown in Fig.40. We can confirm the onset of a little drop of the resistance at around 2K. This may be a sign from the superconducting transition

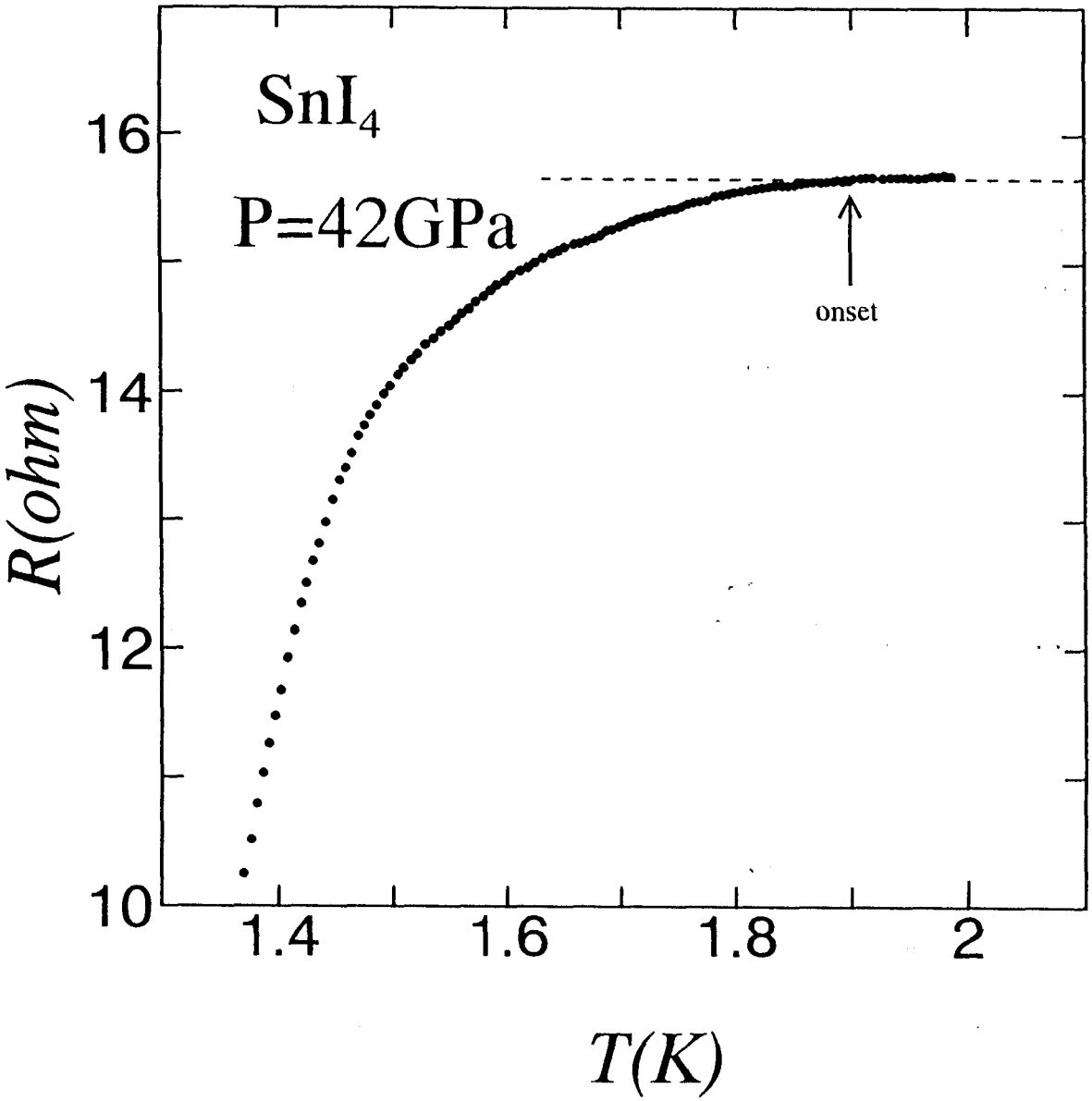


Fig. 40 The onset of the superconducting transition of $SnI_4$ at 42GPa.

of fcc micro crystal in the amorphous state. The pressure dependence of $T_c$ in the fcc recrystallized phase of $SnI_4$ is considered to be small from the resistance measurements. It would be reasonable that $T_c$ in the fcc micro crystal phase is around 2K.

## § 5 Concluding Remarks

### Observation of superconductivity of $SnI_4$

We observed superconductivity of $SnI_4$ at high pressure and low temperature. We performed resistance and magnetization measurements at high pressure and the transition could be detected by both methods.

### $T_c$ of $SnI_4$

We can not observe superconducting transition of $SnI_4$ below $P$=30GPa. There may be three phases in superconducting state with increasing pressure.(Fig.35) The $T_c$ and the pressure dependence of $T_c$, $dT_c/dP$ are summarized as follows.

| | | |
|---|---|---|
| phase I | ($P$<7.2GPa, crystal) | :No superconductivity is observed. |
| phase II | ($P$>7.2GPa, amorphous) | :No superconductivity is observed. |
| | ($P$=35GPa, amorphous) | :$T_c$=1.35K, $dT_c/dP>0$. |
| phase III | ($P$>65GPa, recrystallized) | :$T_c$=1.95K, $dT_c/dP\sim 0$. |
| phase IV | ($P$>80GPa, recrystallized?) | :$T_c$=1.2K($P$=95GPa), $dT_c/dP<0$. |

# § 6 Application to Heavy-Electron System

## 1. Introduction

Investigation of heavy-electron systems under high pressure is currently of extensive interest because their physical properties which are caused by the hybridization between f- and conduction electrons are systematically controlled by an application of pressure. Much interest is especially drawn to the interplay between magnetic phenomena and superconductivity.

Steglich *et al.*[16] discovered the first heavy-electron superconductor $CeCu_2Si_2$ in 1979. All the compounds of $CeM_2X_2$(M=Cu,Ru,Pd,Ag,Au,Rh・・・X=Si,Ge) have heavy-electrons and the same structure ($ThCr_2Si_2$ type) but the ground state of this compounds are variegated. Some compound shows magnetic order and the other shows superconductivity at low temperature. We are interested in the superconductivity of these compounds and try to discover possible universality and characteristic physical properties in these compounds through the experiments under high pressures.

In heavy-electron compounds, the conduction electrons strongly correlate to the f- electrons(4f- electron in $CeM_2X_2$). If we cool down this system, f- electrons are combined to conduction electrons below $T_K$ (Kondo-temperature) and has some advantage of energy, then the specific heat of conduction electrons becomes very large. In this case the magnetic moment of f- electrons becomes small, so the scattering of the conduction electrons become small and the decreasing of the electrical resistivity can be observed. The $T^2$-dependence of resistance also appears at low temperatures caused by scattering of heavy-electrons which cannot be observed in normal metals.

The ground states of these heavy-electron compounds can be classified according to the strength of the correlation between f- electrons and conduction electrons. $T_K$ becomes high and no magnetic order appears in low temperatures in the strong correlation and $T_K$ becomes low and a magnetic order

(mostly orders antiferromagnetically) appears in the case of weak correlation. The application of the pressure causes the lattice constant short and the correlation between f-electrons and conduction electrons becomes large. Then the magnetic ordering temperature $T_M$ drops and $T_K$ increases. If we applies pressure further, the magnetic ordering is completely suppressed and the heavy-electrons with no magnetic order is realized below $T_K$. But some compounds has superconductivity in this critical region. However, this superconductivity is quite unconventional. The physical properties in conventional BCS superconductor depends on temperature as $e^{(-\Delta/T)}$ below transition temperature $T_c$, but there appears $T^n$ dependence in heavy- electron superconductors. It is so fascinating that great efforts have been devoted to make clear the mechanism of superconductivity in heavy-electron systems.

On the other hand, only one Ce- based compound, $CeCu_2Si_2$, has been discovered which shows superconductivity at ambient pressure. But the following three compounds of $CeCu_2Ge_2$, $CePd_2Si_2$ and $CeRh_2Si_2$ have been also discovered in these five years to show superconductivity under pressure. Loidl *et al.*[17] arranges $T_K$ and $T_M$ of this group of compounds, $CeM_2X_2$, as a function of its unit cell volume as shown in Fig.41. Roughly speaking, $T_K$ increases and $T_M$ decreases as decreasing the volume of the unit cell. Applying pressure is considered to be equivalent to decreasing of unit cell volume, so the superconductivity may appear if we applied pressure and reduce unit cell volume to be identical with $CeCu_2Si_2$.

$CeCu_2Ge_2$ is a typical case of this sequence. Jaccard *et al.* measured the electrical resistance under pressure.[18] $CeCu_2Ge_2$ orders antiferromagnetically at temperature $T_N$=4.2K at ambient pressure. As applying pressure, $T_N$ decreases and magnetic order becomes completely suppressed and superconductivity appears at the pressure of $P$=7.5GPa. The phase diagram of $CeCu_2Ge_2$ under pressure is shown in Fig.42. In a normal BCS superconductor, cooper pairs are constructed through electron- phonon interaction. Spin fluctuation may play a

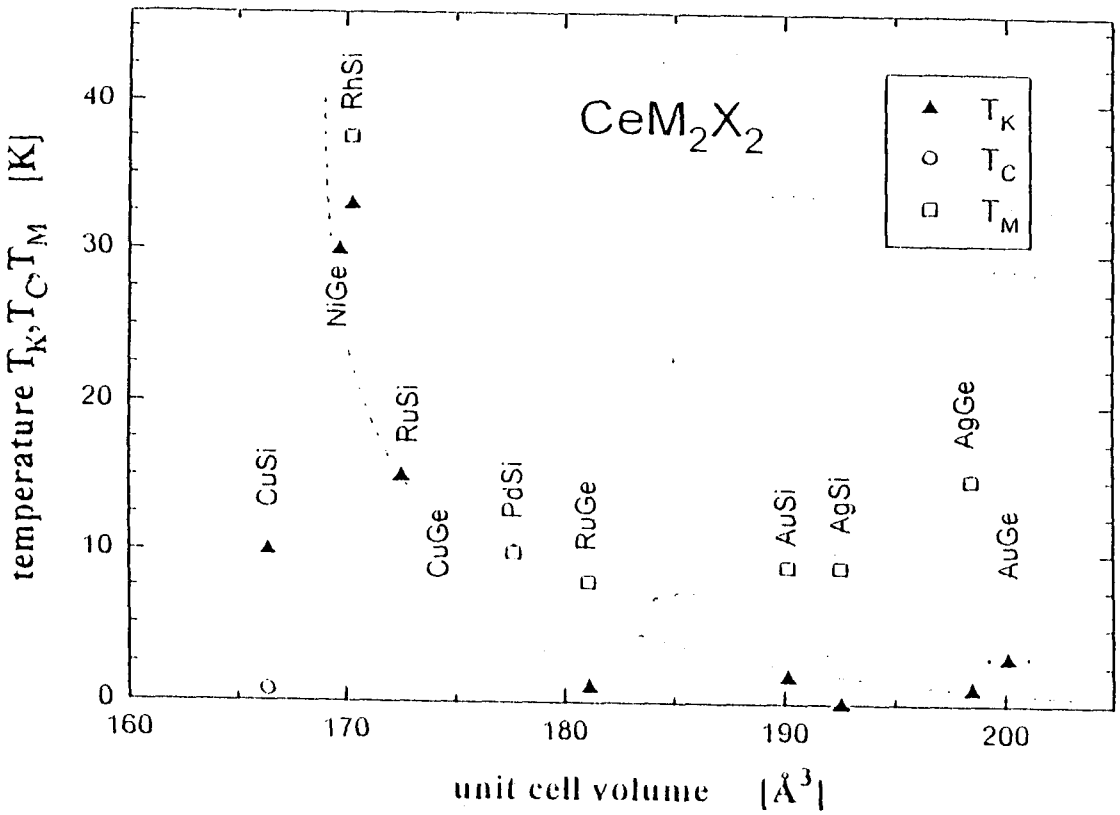


A. Loidl *et al.*

Fig. 41 Kondo temperature $T_K$ (▲) and magnetic ordering temperature $T_M$ (□) versus unit cell volume in $CeM_2X_2$.

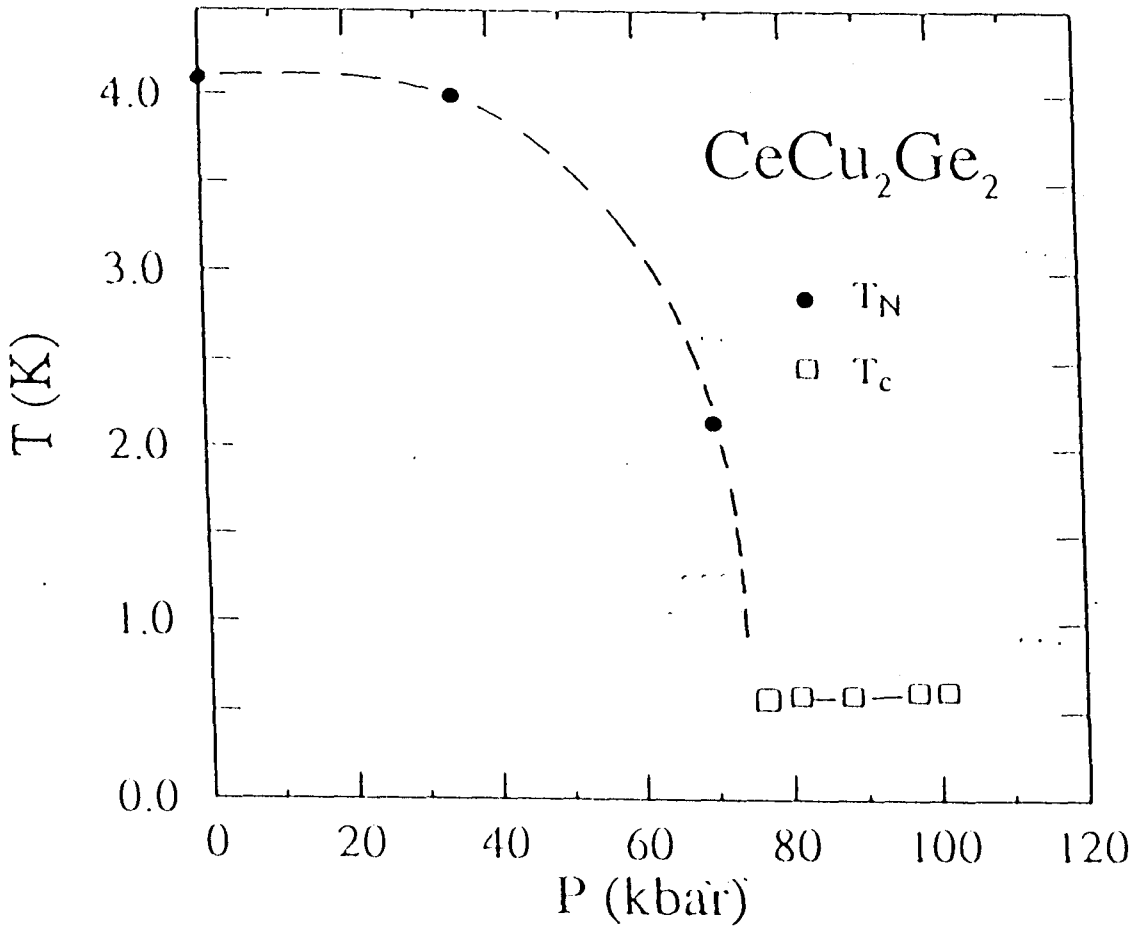


(10kbar=1GPa)

D. Jaccard *et al.*

Fig. 42 The phase diagram of $CeCu_2Ge_2$ under high pressure.

role of pairing interaction in a heavy-electron superconductor. So, it is understandable that superconductivity is observed in a certain critical region with respect to the application of pressure which suppress the magnetic order.

We measured the electrical resistance and the magnetization under high pressure down to cryogenic temperatures to observe the behaviors of these fascinating superconductivities. We chose $CeCu_2Ge_2$, $CePd_2Si_2$ and $CeRh_2Si_2$ as specimens which may show unconventional superconductivities only under high pressures.

## 2.$CeCu_2Ge_2$

### Motivations

The first pressure- induced superconductivity in a heavy- electron system was discovered at 7.5GPa in $CeCu_2Ge_2$[18] which is an antiferromagnet at ambient pressure. Interestingly, the onset of the superconducting transition is observed at the same temperature of $T_c$=0.7K with that of isostructural $CeCu_2Si_2$, which is the first heavy- electron superconductor.[16] Furthermore, $CeCu_2Si_2$ itself undergoes a large enhancement[19] of $T_c$ in a pressure range of 2-3GPa.(Fig.43) Recent NQR experiment on the two compounds[20] has revealed that the physical properties at 7.6GPa in $CeCu_2Ge_2$ are related to that of $CeCu_2Si_2$ at ambient pressure. In $CeM_2X_2$ family, the superconductivity may occur commonly in an optimum range of pressure, or in an appropriate extent of strength of the hybridization.

We performed the electrical resistance and the magnetization measurements, expecting the appearance of the enhancement of $T_c$ similarly in $CeCu_2Ge_2$ at further applying pressure.

### Results

At first we measured the electrical resistance of $CeCu_2Ge_2$. Fig.44 shows the electrical resistance of $CeCu_2Ge_2$ at high pressures. There is decrease of resistance around $T$=4.2K at $P$=0.5GPa. This decrease may be caused by antiferromagnetic order. Then we applied pressure and measured the resistance up to $P$=17GPa. At 7.5GPa, a sudden drop of resistance appeared at around $T$=0.7K. This anomalous drop is considered to be a superconducting transition because its temperature and pressure value are in agreement with previous result. We have increased pressure up to $P$=17GPa in the subsequent runs. But there was no efficient enhancement of transition temperature.

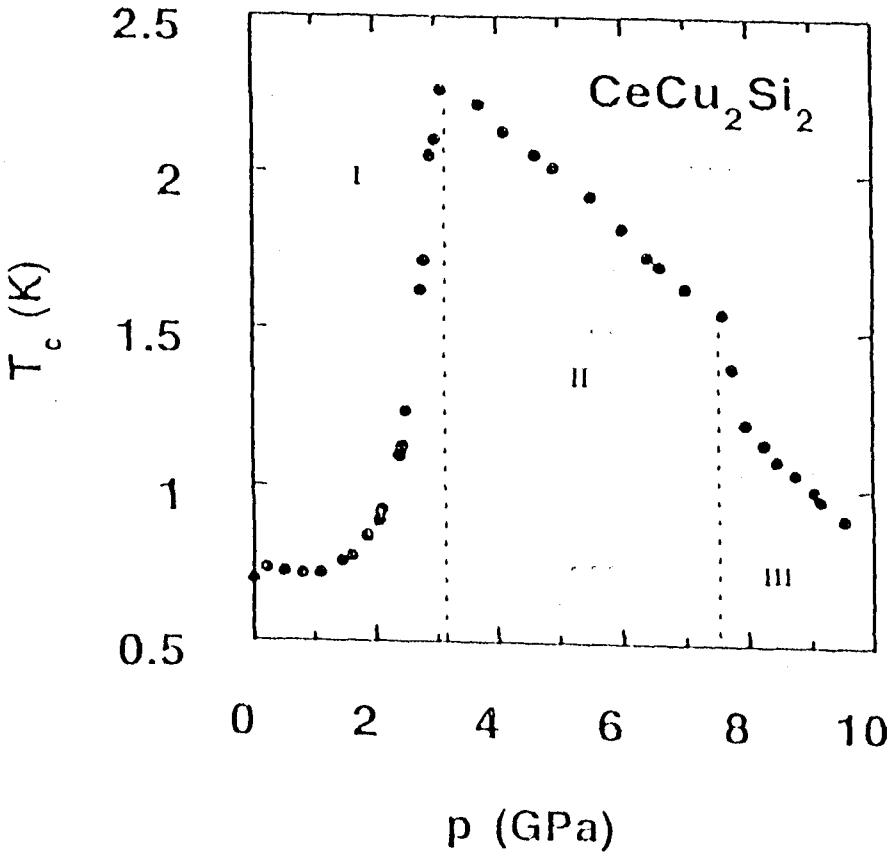


F. Thomas *et al.*

Fig. 43 Change of the superconducting transition temperature $T_c$ of $CeCu_2Si_2$ with pressure.

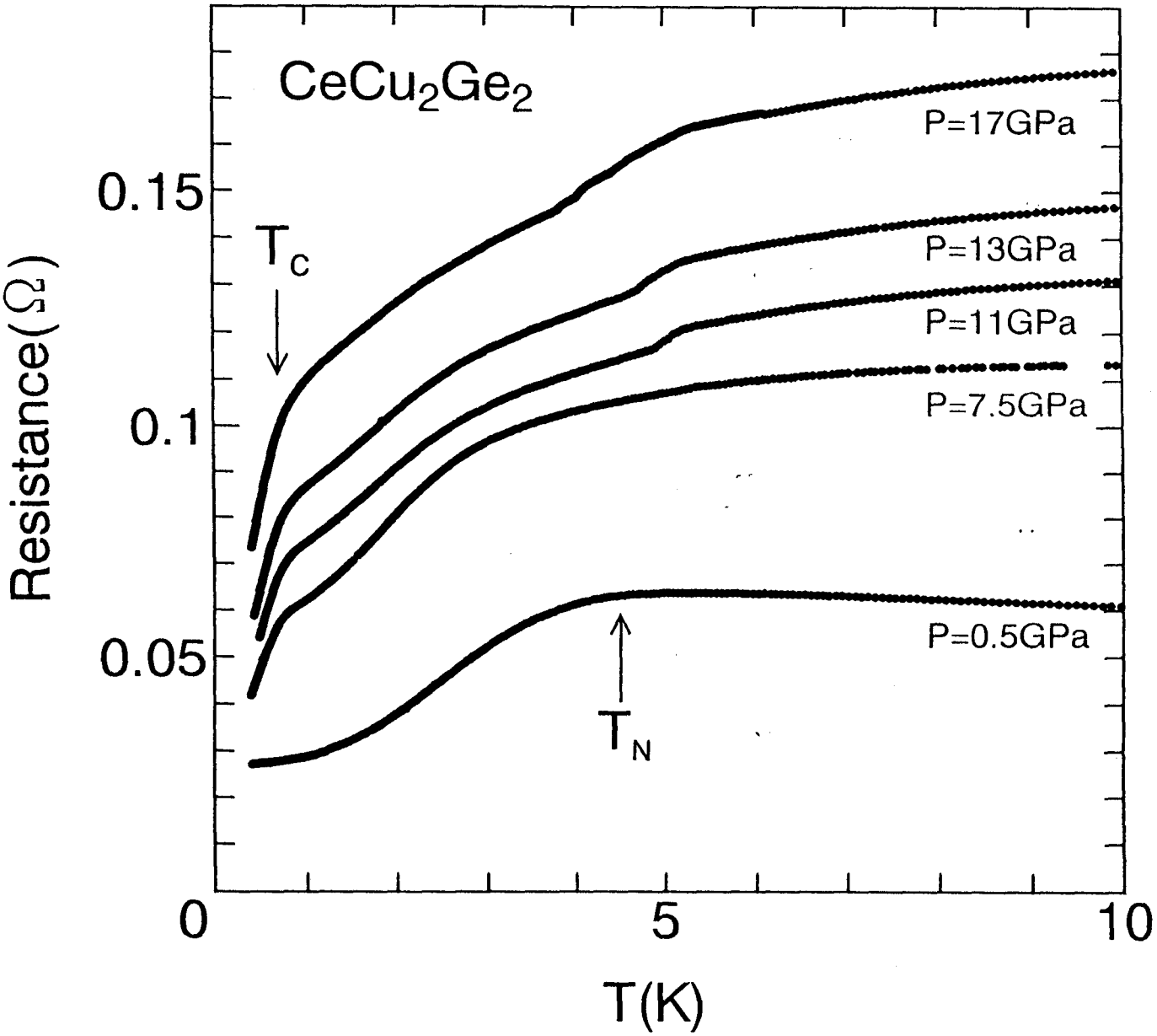


Fig. 44 Electrical resistance of $CeCu_2Ge_2$ under high pressure.

Then we tried sampling again and measured the electrical resistance. Figure 45 shows the resistance at pressure $P$=11,18 and 24GPa. At pressure $P$=18 and 24GPa, the onset of $T_c$ obviously change above 1K. This enhancement of the transition is expected, as it is observed in $CeCu_2Si_2$.

To make the enhancement of the transition clear, we measured the magnetization of the $CeCu_2Ge_2$ under high pressure to detect a Meissner signal at the superconducting transition. Figure 46 shows the temperature dependence of the magnetization at $P$=11.5GPa. At around $T$=0.6K, there is decrease of magnetization which is the Meissner signal from the specimen. Though we can confirm the Meissner signal below $P$=11.5GPa, no obvious signal was observed above this pressure.

**Discussion**

We have claimed that the decrease of the electrical resistance at around $T$=0.7K above 7.5GPa is caused by superconducting transition, but there remain some problems. All the resistance curves don't reach to zero in spite of expectation of superconducting transition. By the way, the uniaxial pressure is generated by a DAC in which we measure the electrical resistance. Superconductivity in heavy- electron system is considered to be very sensitive to impurity or inhomogeneity in the lattice, so it is possible that an incomplete superconducting transition takes place in our experiments because of structural distortion caused by inhomogeneous pressure.

We can use a pressure medium in a sample space when we perform a magnetization measurement. We use a mixture of water and alcohol as a pressure medium in our magnetization measurement. The mixture is effective as a pressure medium to produce hydrostatic pressure up to around 10GPa. Axial pressure may develop above 10GPa. Probably, this is the reason why we can not observe a Meissner signal above 11.5GPa. We observe a sign of the enhancement in repeated experiments, but the resistance values do not reach to

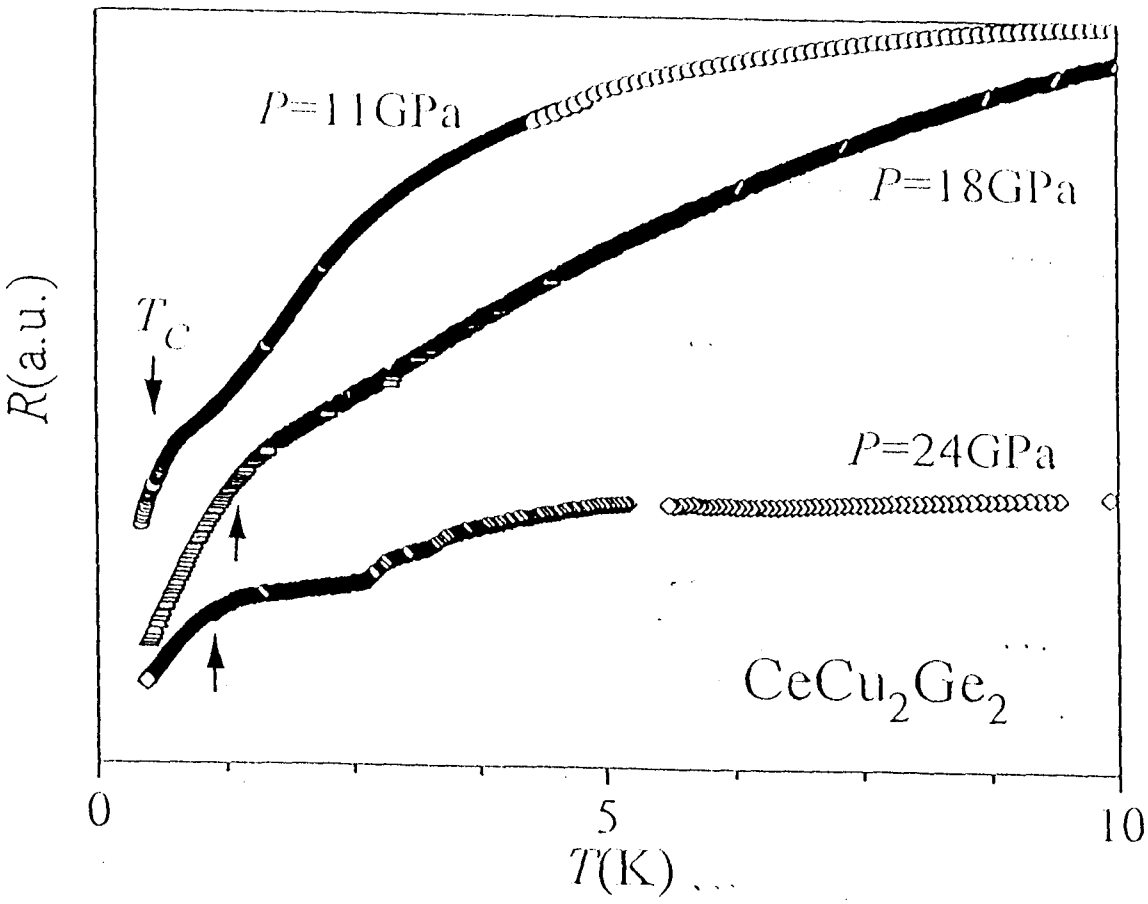


Fig. 45 Electrical resistance of $CeCu_2Ge_2$ under high pressure in different sampling.

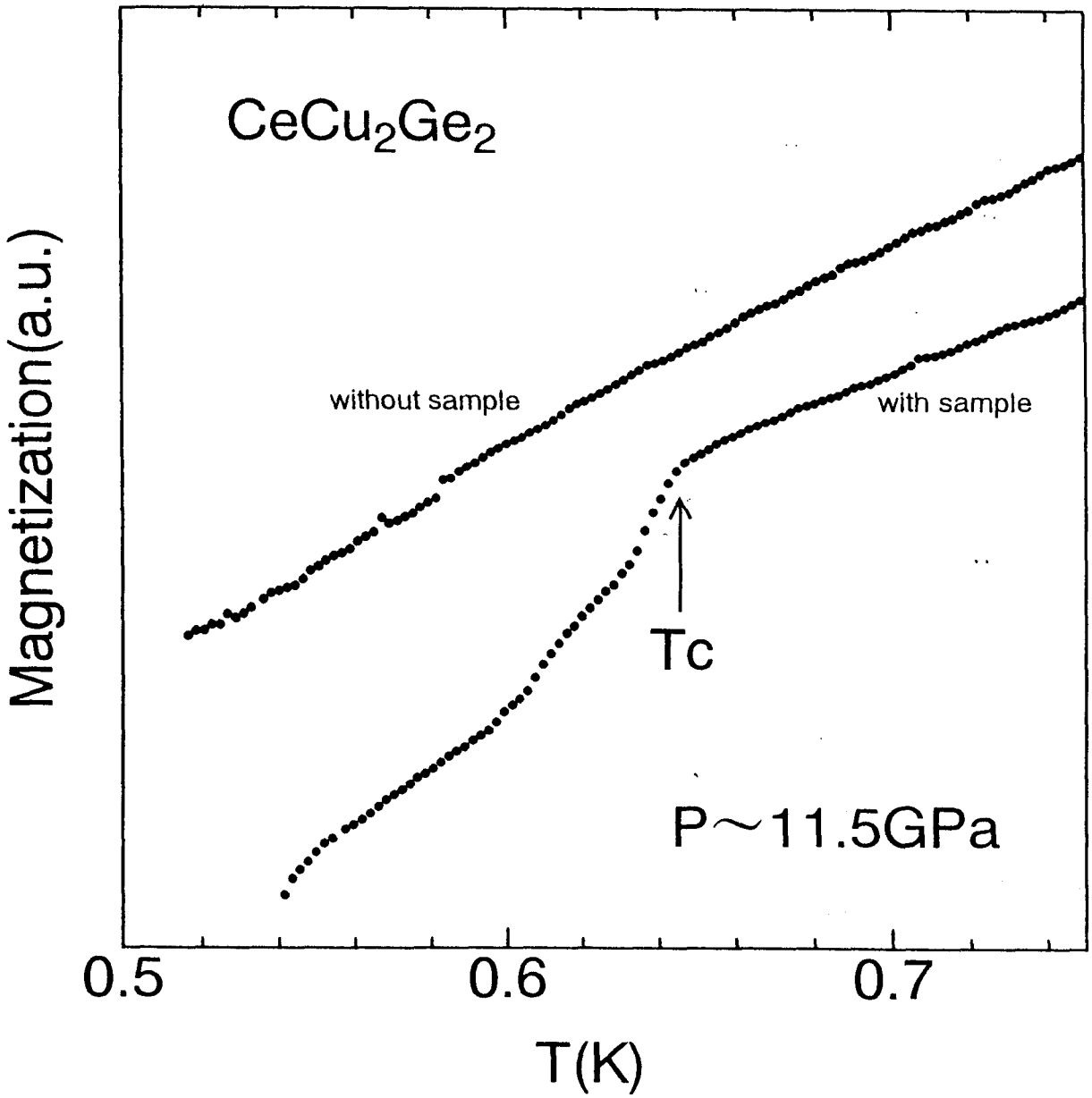


Fig. 46 The magnetization of $CeCu_2Ge_2$ at 11.5GPa. There is a clear decrease of magnetization by superconducting transition of $CeCu_2Ge_2$.

zero because of inevitable pressure inhomogeneity.

We expect that this enhancement of $T_c$ is essential. To confirm the enhancement of $T_c$ further, magnetization measurements at further pressures using more effective pressure medium are required.

## 3.$CePd_2Si_2$, $CeRh_2Si_2$

### Motivations

Since the discovery of pressure- induced heavy- fermion superconductor $CeCu_2Ge_2$ in 1992, there are only two compounds, $CeCu_2Si_2$ and $CeCu_2Ge_2$, showing superconductivity in a $CeM_2X_2$ family. However, Julian *et al.* recently discovered a pressure induced superconductivity in $CePd_2Si_2$[21] and also Rauchschwalbe *et al.* discovered it in $CeRh_2Si_2$.[22]

$CePd_2Si_2$ shows an antiferromagnetic ordering at around 10K. Julian *et al.* measured the electrical resistance and discovered the pressure- induced superconductivity. The phase diagram of $CePd_2Si_2$ is shown in Fig.47. The magnetic ordering is suppressed by applying pressure, then superconductivity appears above 2.2GPa with transition temperature $T_c$=0.2K. This phase diagram is very similar to that of $CeCu_2Ge_2$.

$CeRh_2Si_2$ is also antiferromagnet at ambient pressure with $T_N$=37K. Such high ordering temperature is suppressed very fast by applying pressure, then no magnetic order is observed at around $P$=1GPa. Rauchschwalbe *et al.* discovered a superconductivity with transition temperature of $T_c$=0.4K.

These two superconductivity is characterized by small critical pressure $P_c$. The difficulty of our experiments has been caused by the high pressure value, so we would have big advantages in experiments on these two compounds, large volume of specimen, homogeneous pressure generating and so on.

We are interested in the phase diagram of $CePd_2Si_2$ and $CeRh_2Si_2$. It seems to be important to see whether there is an enhancement of $T_c$ at higher pressures or not. There may be some universality about appearance of superconducting transition among $CeM_2X_2$ compounds and this would be a key for making clear the mechanism of this unconventional superconductivity.

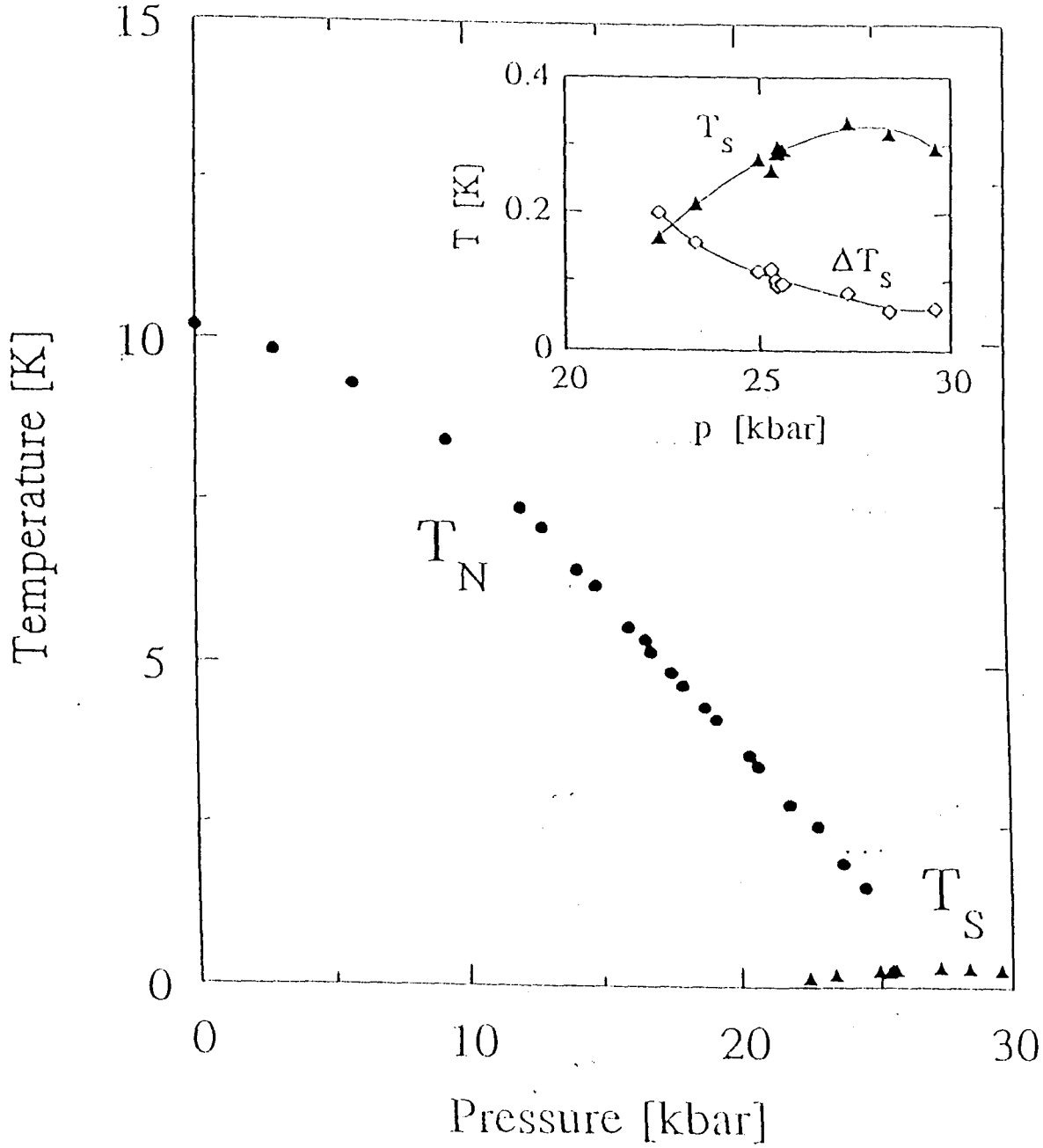


(10kbar=1GPa)

S.R.Julian *et al.*

Fig. 47 The phase diagram of $CePd_2Si_2$ under pressure.

**Result and Discussions**

We measured the resistance of $CePd_2Si_2$ at $P$=3.2GPa. A small drop of resistance is observed with onset at $T$=0.2K. This drop is suppressed by magnetic fields as shown in Fig.48. This decrease of the resistance is considered to be due to a superconducting transition because of its temperature and pressure range and the behavior in magnetic fields, but we couldn't observe a zero resistance like the case in $CeCu_2Ge_2$.

After that we increased pressure up to $P$=5.0GPa. We observed the drop again but it became very small. Then we decrease pressure value back to $P$=3.0GPa, but the decrease of resistance became smaller. It is hard to distinguish the drop of resistance in the third run ($P$=3.0GPa) as shown in Fig.49. The stress in specimen caused by inhomogeneous pressure would be stored by repetition of applying pressure.

We can also observe a drop of the resistance with non-zero resistance in $CeRh_2Si_2$. Figure 50 shows the electrical resistance of $CeRh_2Si_2$ at $P$=1.3GPa. An anomalous drop of the resistance is seen at $T$=0.4K. This drop is also considered to be a superconducting transition because its temperature and pressure range is consistent with the previous work and the drop is suppressed by the magnetic field.

It is very characteristic in every heavy electron superconductor that the temperature dependence of the electrical resistance above transition temperature $T_c$ is extraordinary. Figure 51 shows the temperature dependence of the resistance of $CeCu_2Ge_2$ below 6K. We can see the $T$-linear dependence in every resistance curve above $T_c$. Prof. Moriya suggests in his theory that the behavior of the temperature dependence of the resistance is non-fermi liquid like because of the spin fluctuation in magnetically unstable region. Our results suggest that this superconductivity occurs in this region and the source of the pairing interaction would be antiferromagnetic spin fluctuation.

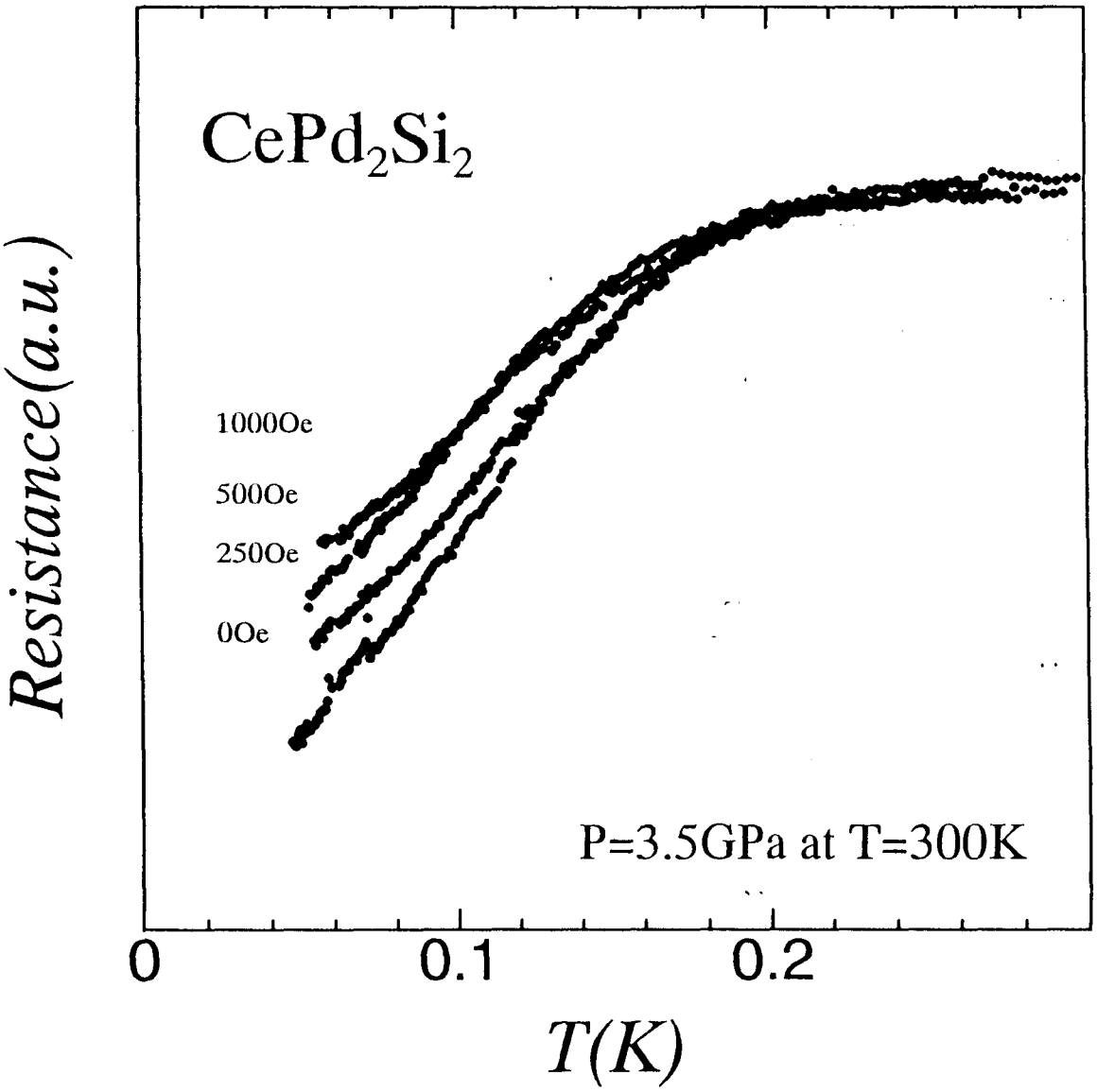


Fig. 48 Superconducting transition of $CePd_2Si_2$ under magnetic fields.

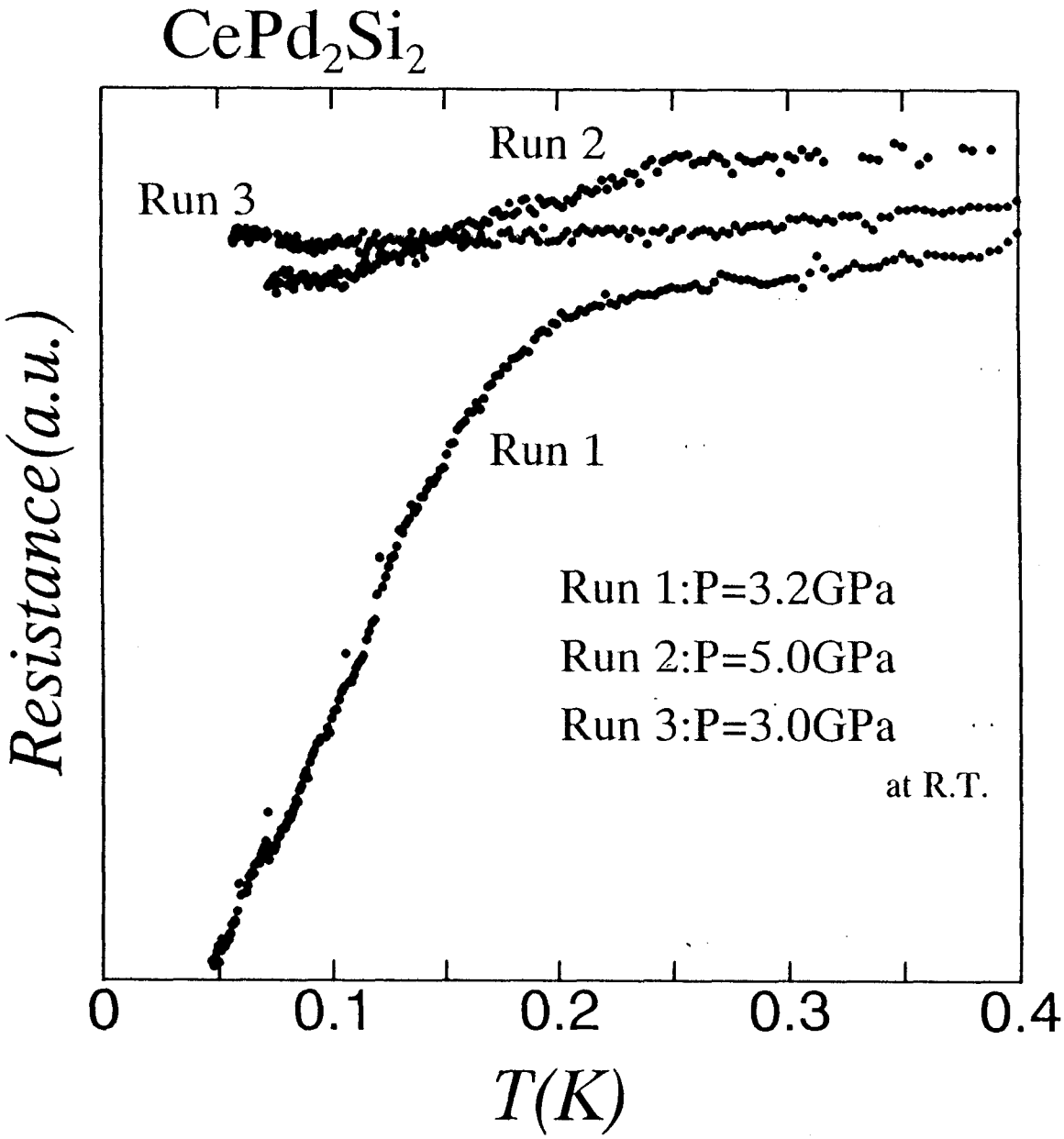


Fig. 49 Superconducting transition of $CePd_2Si_2$ at different runs. The transition is suppressed as adjusting pressure value.

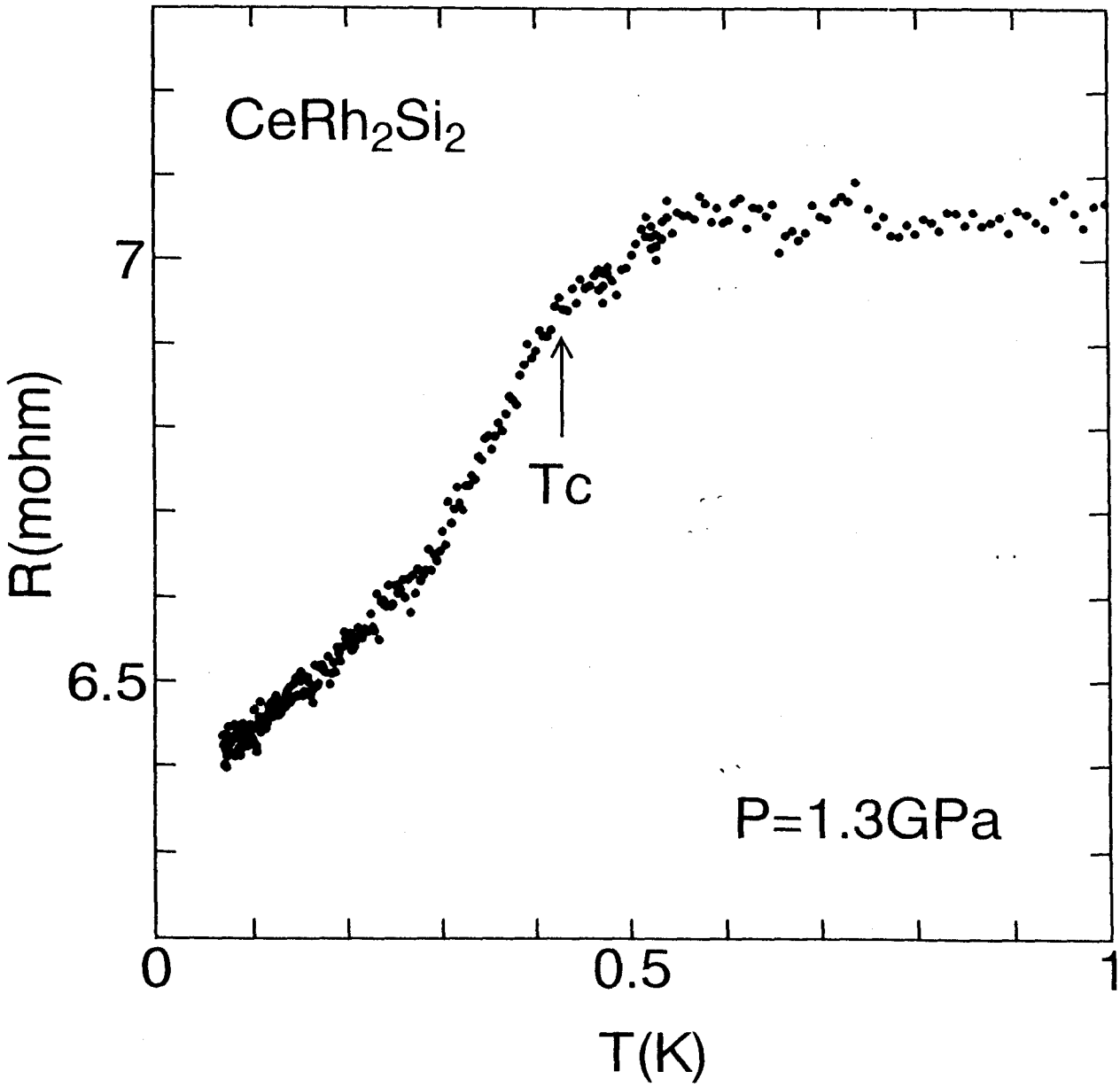


Fig. 50 Superconducting transition of $CeRh_2Si_2$ at 1.3GPa.

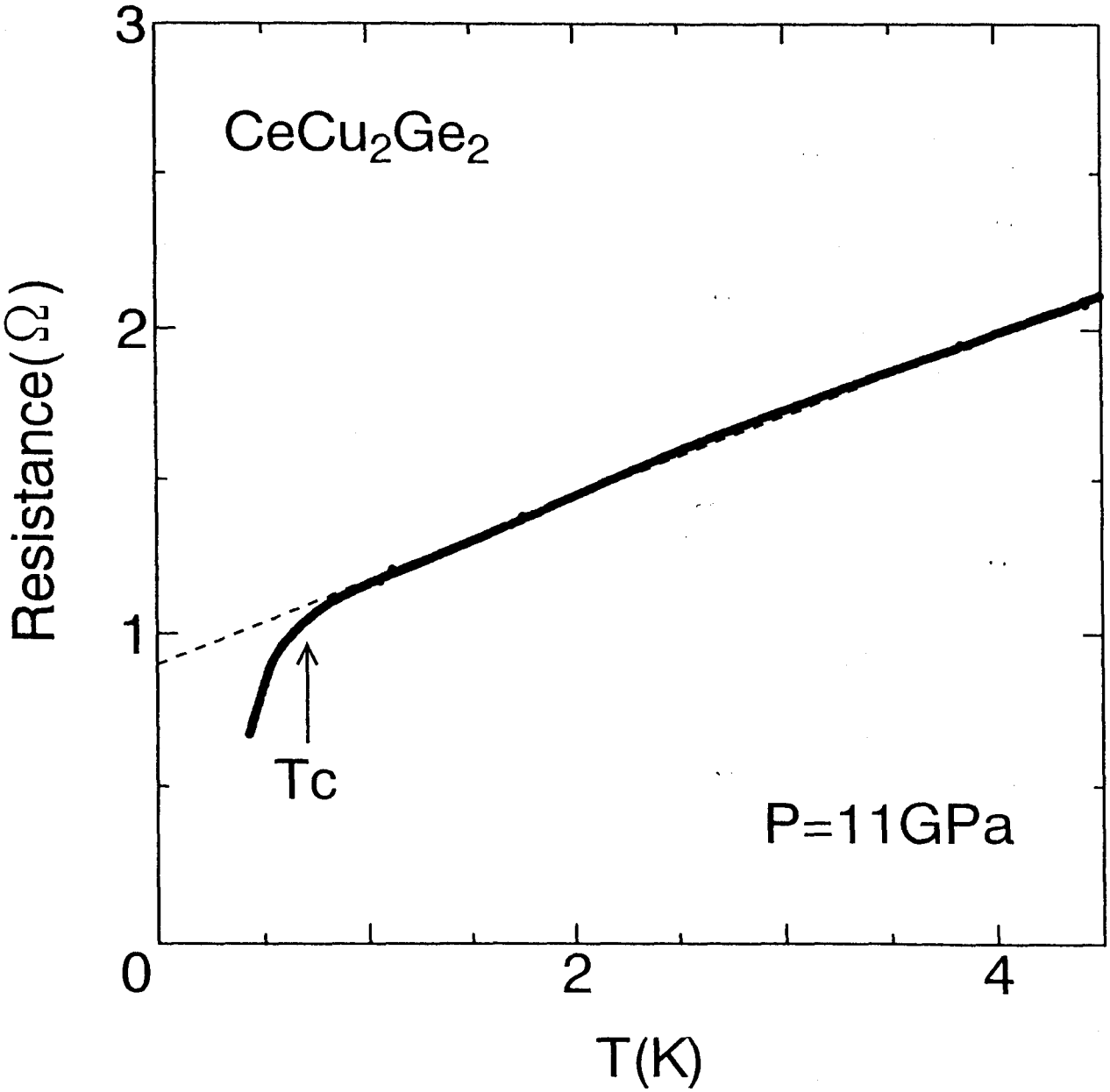


Fig. 51 Non-fermi liquid like $T$- linear dependence of resistance in $CeCu_2Ge_2$ above superconducting transition temperature.

## 4.Conclusion

From resistance and magnetization measurements under high pressure, we have investigated the change of physical properties in heavy-electron antiferromagnets, $CeCu_2Ge_2$, $CePd_2Si_2$ and $CeRh_2Si_2$. In $CeCu_2Ge_2$, it has been confirmed that pressure-induced superconductivity still remains up to $P$=17GPa, keeping nearly the same $T_c$ of around 0.7K. Above this pressure, we confirmed the sign of enhancement of $T_c$ by the electrical resistance measurements but could not observe the Meissner signal by the magnetization measurements. In $CePd_2Si_2$ and $CeRh_2Si_2$, we confirmed the drop of the resistance which is consistent with the previous reports, supposing it is due to a superconducting transition. The temperature dependence of the resistance in these three compounds above critical temperature shows non-fermi liquid like $T$-linear dependence. This suggests that spin fluctuation plays a role of pairing interaction of the superconductivity in these heavy-electron compounds.

# Acknowledgement

The author would like to express his sincere gratitude to Professor Kiichi Amaya for pertinent guidance, continuous encouragement and enlightening discussions throughout this work.

The author also would like to express his thanks to Mr. Shoji Kometani for his devoted cooperation in experiments and to Dr. Katsuya Shimizu for useful advices and valuable suggestions through this work.

The author is indebted to Professor Nozomu Hamaya of Ochanomizu Women University for supplying high quality specimen and for enlightening discussions on the crystal structure of $SnI_4$.

The author is grateful to Dr. Tatsuo Kobayashi for useful comments and for enlightening discussions throughout this work.

The author wish to thank Dr. M.Eremets for his support in experiment by which the appearance of superconductivity became definite.

Thanks are also due to colleagues of Amaya Laboratory for their cooperations and encouragement through this work.

Finally, the author would like to thank my family for their understanding and support over a long period.

# References


[1]F.Meller and I.Faukuchen, Acta Crystallog., **8**(1955)343.

[2]R.W.Lynch and H.G.Drickamer, J.Chem.Phys., **45**(1966)1020.

[3]Y.Fujii, M.Kowaka and A.Onodera, J.Phys.C:Solid State Phys, **18**(1985)789.

[4]B.M.Riggleman and H.G.Drickamer, J.CHem.Phys., **38**(1963)2721.

[5]A.L.Chen, P.Y.Yu and M.P.Pasternak, Phys.Rev.B:Condenced Matter, **44**(1991)2883.

[6]N.Hamaya, K.Sato, K.U.Watanabe, K.Fuchizaki, Y.Fujii and Y.Ohishi, to be published.

[7]Y.Fujii, K.Hase, N.Hamaya, Y.Ohishi, A.Onodera, O.Shimomura and K.Takemura, Phy.Rev.Lett., **58**(1987)796.

[8]A.S.Balchan and H.G.Drickamer, J.Chem.Phys., **34**(1961)1948.

[9]N.Sakai, K.Takemura and K.Tsuji, J.Phys.Soc.Jpn., **51**(1982)1811.

[10]K.Shimizu, T.Yamauchi, N.Tamitani, N.Takeshita, M.Ishizuka, K.Amaya and S.Endo, J.Superconductivity, **7**(1994)921.

[11]S.Sugai, J.Phys.C:Solid State Phys., **18**(1985)799.

[12]M.P.Pasternak and R.D.Taylor, Phys.Rev., **B37**(1988)8130.

[13]F.Wang and R.Ingalls, *High Pressure Science and Technology*, edited by W.A.Trzeciakowski (World Science, Singapore; 1996), p.289.

[14]R.Reichlin, A.K.McMahan, M.Ross, S.Martin, J.Hu, R.J.Hemley H.K.Mao and Y.Wu, Phys.Rev. **B49**(1994)3725.

[15]H.Sakamoto, T.Oda, M.Shirai and N.Suzuki, J.Phys.Soc.Jpn., **65**(1996)489.

[16]F.Steglich, J.Aarts, C.D.Bredl, W.Leike, D.Meschede, W.Franz and H.Sch臓er, Phys.Rev.Lett., **43**(1979)1892.

[17]A.Loidl, G.Knopp, H.Spille, F.Steglich and A.P.Murani, Physica B, **156&157**(1989)794.

[18]D.Jaccard, K.Behnia and J.Sierro, Physics Lett. A, **163**(1992)475.

[19]B.Bellarbi, A.Benoit, D.Jaccard, J.M.Mignot and H.F.Braun, Phys.Rev.B,

**30**(1984)1182.

[20]Y.Kitaoka, H.Tou, G.-q.Zheng, K.Ishida, K.Asayama, T.C.Kobayashi, A.Kohda, N.Takeshita, K.Amaya, Y.Onuki, C.Geibel, C.Schank and F.Steglich, Physyca B, **206&207**(1995)55.

[21]F.M.Grosche, S.R.Julian, N.D.Mathur and G.G.Lonzarich, Physica B, **223&224**(1996)50.

[22]R.Movshovich, T.Graf, D.Mandrus, J.D.Thompson, J.L.Smith and Z.Fisk, Phys.Rev.B, **53**(1996)8241.